FINAL REPORT

New Approaches to Evaluate the Biological Degradation of RDX in Groundwater

SERDP Project ER-1607

August 2014

Paul Hatzinger
Mark Fuller
CB&I Federal Services

SERDP
DOD ▪ EPA ▪ DOE

TABLE OF CONTENTS

LIST OF TABLES

LIST OF FIGURES

ACRONYM LIST

‰	parts-per-thousand
bgs	below ground surface
bp	base pair
BRI	National Research Council of Canada, Biotechnology Research Institute
BSM	basal salts medium
C	carbon
°C	degree Celsius
cm	centimeter
CsCl	cesium chloride
CSIA	compound specific stable isotope analysis
δ	delta
d	day
DNA	deoxyribonucleic acid
DNX	hexahydro-1,3-dinitroso-5-nitro-1,3,5-triazine
DO	dissolved oxygen
DoD	Department of Defence
ε	epsilon
EPA	Environmental Protection Agency
ES^-	electrospray ionization
ESTCP	Environmental Security Technology Certification Program
EtBr	ethidium bromide
ft	foot or feet
g	gram
g	gravity
GC	gas chromatography
GC-FID	gas chromatography - flame ionization detector
GC-IRMS	gas chromatography - isotope ratio mass spectrometry
GC-MS	gas chromatography - mass spectrometry
GMF	glass microfiber
h	hour
H	hydrogen
HAAP	Holston Army Ammunition Plant
HCHO	formaldehyde
HDPE	high density polyethylene
He	helium
HMX	octahydro-1,3,5,7-tetranitro-1,3,5,7-tetrazocine
HPLC	high performance liquid chromatography
IAAP	Iowa Army Ammunition Plant
ICP-MS	inductively coupled plasma - mass spectrometry
IRMS	isotope ratio mass spectrometry
k	kilo
L	liter
LC-MS	liquid chromatography-mass spectrometry
µ	micro
m	milli or meter
M	molar

m/z	mass to charge ratio
MEDINA	methylene dinitramine
MeOH, CH_3OH	methanol
min	minute
mm	millimeter
MNA	monitored natural attenuation
MNX	hexahydro-1-nitroso-3,5-dinitro-1,3,5-triazine
mol	mole
MS	mass spectrometry
mV	millivolt
N	nitrogen
n	nano
N_2O	nitrous oxide
NAVAIR	Naval Air Warfare Weapons Division, China Lake, CA
NDAB	4-nitro-2,4-diazabutanal
NSWC	Naval Surface Warfare Center
NTA	nitriloacetic acid
NXs	combined nitroso metabolites of RDX
ORP	oxidation-reduction potential
P	phosphorus
P450	cytochrome P450 oxygenase enzyme
PCR	polymerase chain reaction
PDA	photodiode array
pK_a	acid dissociation constant
Q-FAST	quantitative function and structure
RDX	hexahydro-1,3,5-trinitro-1,3,5-triazine
rpm	revolutions per minute
rRNA	ribosomal ribonucleic acid
S	sulfur
SERDP	Strategic Environmental Research and Development Program
SIP	stable isotope probing
SPE	solid phase extraction
SPME	solid phase micro extraction
SS	sea salts
TE	Tris-EDTA buffer
TFA	trifluoroacetic acid
TNX	hexahydro-1,3,5-trinitroso-1,3,5-triazine
TOC	total organic carbon
t-RFLP	terminal restriction fragment length polymorphism
UIC	University of Illinois at Chicago
USGS	United States Geological Survey
UV	ultraviolet
VOC	volatile organic compound
VPDB	Vienna Pee Dee Belemnite
wt	weight
XenA, XenB	xenobiotic reductase enzyme A and B

ACKNOWLEDGEMENTS

This SERDP Project was a collaborative effort among Dr. Bella Chu at Texas A&M University, Dr. Neil C. Sturchio at the University of Illinois at Chicago, Dr. Jalal Hawari at the National Research Council of Canada, Biotechnology Research Institute, Dr. Steve Fallis at the Naval Air Warfare Center Weapons Division, China Lake and Dr. Mark E. Fuller and Dr. Paul B. Hatzinger of CB&I Federal Services, LLC. We wish to acknowledge all of the collaborators for their significant contributions to the success of this research project. We also wish to acknowledge Linnea Heraty, Louise Paquet, Fanny Monteil-Rivera, Christina Andaya, Charles Condee, Hyungkeun Roh, Kun-Ching Cho, and Do Gyun Lee for their important technical contributions to this project. We gratefully acknowledge SERDP for their financial support, and Dr. Andrea Leeson, the Environmental Restoration Program Manager at SERDP, for her guidance. Finally, we wish to acknowledge the DoD facilities and program managers that provided site access and samples for the research conducted herein.

REPORT DOCUMENTATION PAGE

Form Approved
OMB No. 0704-0188

PLEASE DO NOT RETURN YOUR FORM TO THE ABOVE ORGANIZATION.

1. REPORT DATE *(DD-MM-YYYY)*	2. REPORT TYPE	3. DATES COVERED *(From - To)*
8-27-2014	Final	May 2008 - August 2014

4. TITLE AND SUBTITLE
NEW APPROACHES TO EVALUATE THE BIOLOGICAL DEGRADATION OF RDX IN GROUNDWATER

5a. CONTRACT NUMBER
W912-HQ-08-C-0031

5b. GRANT NUMBER
NA

5c. PROGRAM ELEMENT NUMBER
NA

6. AUTHOR(S)
Hatzinger, Paul B., Ph.D.
Fuller, Mark E., Ph.D.

5d. PROJECT NUMBER
ER-1607

5e. TASK NUMBER
NA

5f. WORK UNIT NUMBER
NA

7. PERFORMING ORGANIZATION NAME(S) AND ADDRESS(ES)
CB&I Federal Services. LLC
17 Princess Road
Lawrenceville, NJ 08648

8. PERFORMING ORGANIZATION REPORT NUMBER
NA

9. SPONSORING/MONITORING AGENCY NAME(S) AND ADDRESS(ES)
Strategic Environmental Research and Development Program
4800 Mark Center Drive, Suite 17D08
Alexandria, VA 22350-3600

10. SPONSOR/MONITOR'S ACRONYM(S)
SERDP

11. SPONSOR/MONITOR'S REPORT NUMBER(S)
NA

12. DISTRIBUTION/AVAILABILITY STATEMENT
Distribution Statement A: Approved for Public Release, Distribution is Unlimited

13. SUPPLEMENTARY NOTES
None

14. ABSTRACT

The primary goal of this SERDP project was to combine state-of-the art analytical techniques, molecular approaches, and biogeochemical studies to enhance our understanding of the biodegradation of hexahydro-1,3,5-trinitro-1,3,5-triazine (RDX) in groundwater. New methods were developed and tested to preserve key RDX metabolites, and the presence of these metabolites was examined at several DoD sites. Microcosm and mesocosm studies with aquifer samples were conducted to assess pathways and rates of RDX degradation under differing geochemical conditions. The microbial communities involved in degradation under these conditions were then characterized using stable isotope probing (SIP) with both 13C-labeled and 15N-labeled RDX. A wide array of organisms, many of which have not previously been associated with RDX degradation, were detected using SIP. Finally, a compound specific stable isotope (CSIA) method was developed and validated to quantify fractionation of C and N isotopes during RDX biodegradation. The SIP and CSIA techniques provide new insights into RDX biodegradation in groundwater.

15. SUBJECT TERMS
RDX, hexahydro-1,3,5-trinitro-1,3,5-triazine, bioremediation, biodegradation, groundwater, stable isotope probing, SIP, compound specific isotope analysis, CSIA, preservation, metabolites, microcosm, electron accepting

16. SECURITY CLASSIFICATION OF:			17. LIMITATION OF ABSTRACT	18. NUMBER OF PAGES	19a. NAME OF RESPONSIBLE PERSON
a. REPORT	b. ABSTRACT	c. THIS PAGE			Dr Paul B. Hatzinger
U	U	U	UU	127	19b. TELEPHONE NUMBER *(Include area code)* 609-895-5356

Reset

Standard Form 298 (Rev. 8/98)
Prescribed by ANSI Std. Z39.18

ABSTRACT

Objectives:
The primary objective of this project was to combine state-of-the art analytical techniques, molecular approaches, and biogeochemical studies to enhance our understanding of the biodegradation of hexahydro-1,3,5-trinitro-1,3,5-triazine (RDX) in groundwater aquifers.

Technical Approach:
The following research was conducted:

1. Key indicator metabolites of aerobic and anaerobic RDX biodegradation were analyzed in groundwater from multiple contaminated sites using specialized analytical approaches. New preservation methods were developed and evaluated to ensure that the analyte concentrations detected in the laboratory accurately represent those in the site groundwater;

2. Laboratory microcosm and mesocosm studies were conducted to better understand the influence of important geochemical variables on the rates, extents, and pathways of RDX biodegradation;

3. Stable isotope probing (SIP) methods were developed and employed using ^{13}C- and ^{15}N-labeled RDX to better understand the microbial communities involved in RDX biodegradation in groundwater environments; and

4. Compound-specific stable isotope analysis (CSIA) methods were developed and tested to quantify fractionation factors for C and N in RDX during biodegradation via aerobic and anaerobic pathways using pure cultures.

Results:
During the initial task in this project, the stability of RDX indicator metabolites, including methylenedinitramine (MEDINA), 4-nitro-2,4-diazabutanal (NDAB), formaldehyde (HCHO) and RDX-nitroso derivatives (hexahydro-1-nitroso-3,5-dinitro-1,3,5-triazine (MNX), hexahydro-1,3-dinitroso-5-nitro-1,3,5-triazine (DNX), and hexahydro-1,3,5-trinitroso-1,3,5-triazine (TNX) were tested under various conditions in aerobic and anoxic groundwater. MEDINA was found to be the most labile compound. Among the various conditions tested, adding 10% sea salts to the groundwater and storing samples at 4°C was the most effective method for preserving MEDINA. The other compounds tested, (NDAB, MNX, DNX, TNX, RDX, HCHO) appeared to be stable in the presence of sea salts with less than 2% loss occurring during the first 2 weeks of storage. Thus, the data suggest that the addition of 10% sea salts and storage at 4°C is an effective preservation method for most of the key intermediates from both the aerobic and anaerobic biodegradation of RDX.

Using the preservation techniques developed during the first phase of the project, more than 30 wells with differing groundwater geochemistry were sampled at seven different RDX contaminated sites. Some wells were sampled on multiple occasions. The key indicator

metabolites for anaerobic biodegradation of RDX, including MNX, DNX, TNX, and MEDINA were measured. Among all of the sites tested, MNX was detected in two wells at Picatinny Arsenal, NJ (at a location previously amended with carbon substrate) at trace concentrations, and MNX, DNX and/or TNX were detected in multiple wells at the Pantex Plant, TX. The presence of these metabolites indicates that anaerobic biodegradation of RDX previously occurred or was occurring at these sites. At the Pantex Plant, the corresponding nitroso-derivatives for HMX were also detected. MEDINA was not detected in any of the wells that were sampled, which may reflect the transient nature of this compound in the groundwater even with appropriate preservation during sampling. Interestingly, NDAB, which is a key intermediate of aerobic RDX degradation, was observed at trace concentrations in two of the Pantex Plant wells, but not at any of the other locations. This compound has only rarely been detected in soils or groundwater in the past, suggesting that either aerobic degradation of RDX in groundwater aquifers is not a common process or that NDAB derived from this process does not generally persist under prevailing aquifer conditions.

Several of the smaller intermediates of RDX degradation, including nitrous oxide, formaldehyde, and methanol were found in groundwater at many of the sites, with the latter two compounds being highest in anaerobic groundwater that was previously amended with soluble organic carbon (Picatinny Arsenal) or passed through a mulch barrier wall (Pueblo Chemical Depot, CO). The accumulation of formaldehyde and methanol under anaerobic conditions is not unexpected, and these compounds are not necessarily related to RDX degradation, although they are potential intermediates. More interesting, however, was the general occurrence of N_2O in aerobic wells that were also contaminated with RDX at various sites. As with formaldehyde and methanol, N_2O has potential sources in groundwater that are unrelated to RDX metabolism, including both nitrification and denitrification. However, there was a significant positive correlation between RDX concentrations and N_2O concentrations for several of the sites with predominantly aerobic wells. This relationship warrants further study using more sensitive stable isotope methods.

A mesocosm study was conducted in samples from Dahlgren, VA to evaluate the degradation of RDX under different electron-accepting conditions and to evaluate the responsible organisms using SIP with ^{13}C-RDX and ^{15}N-RDX. Mesocosms were amended with succinate as a carbon source and NO_3^-, SO_4^{2-}, Mn(IV) or Fe(III) as terminal electron acceptors. One mesocosm received no additional electron acceptor to promote methanogenesis. RDX degradation was not observed under NO_3^--reducing conditions (or aerobic conditions in a preliminary study with site samples). RDX degradation with high accumulation (and slow degradation) of nitroso-metabolites was observed with Mn(IV) and Fe(III) as the predominant electron acceptors. Conversely, much more rapid RDX degradation was documented in microcosms under both sulfate-reducing and methanogenic conditions, with low and transient accumulation of nitroso metabolites (10% and 40% of the added RDX at a maximum, respectively), and with MNX as the primary metabolite. The data indicate that sequential nitro group reduction was the major RDX degradation pathway under Mn(IV)- and Fe(III)-reducing conditions, whereas, a pathway involving denitration or ring cleavage likely dominated under sulfate-reducing and methanogenic conditions.

Microcosms were prepared from each of the electron acceptor mesocosms and incubated with either ^{13}C-labeled RDX or ring-, nitro- or fully-labeled ^{15}N-RDX. RDX degradation was monitored in each microcosm, and SIP was conducted when degradation of RDX and intermediates was complete or nearing completion. Using the ^{13}C-DNA fractions from the microcosms that had received ^{13}C-labeled RDX as templates for cloning and sequencing, identities of active bacteria capable of using RDX and/or RDX intermediates as a carbon source were determined. A total of fifteen 16S rRNA sequences, clustering in α-*Proteobacteria* (unclassified *Rhizobiales*) γ-*Proteobacteria (Pseudomonas)*, *Clostridia (Desulfosporosinus*), and *Actinobacteria (Eggerthella)* were detected in the ^{13}C-DNA fractions. A total of twenty seven sequences were derived from different ^{15}N-DNA fractions, with the sequences also clustered in α- and γ-*Proteobacteria*, and *Clostridia*. These results indicate that active RDX-degraders are phylogenetically diverse and that their occurrences vary somewhat under different electron-accepting regimens, although some of the same genera were observed to utilize RDX under different geochemical conditions. For example, a number of clones clustered in the genus of *Desulfosporosinus* under each of the different electron-accepting conditions where RDX degradation was observed. *Desulfosporosinus* species are known for their adaptable metabolism, including their ability to use not only sulfate, but also nitrate, Fe(III), or As(V) as terminal electron acceptors. Similarly, the frequent detection of sequences identified as *Pseudomonas* likely reflects the unique ability of this genus to use many different electron acceptors. The detection of sequences identified as *Pseudomonas* sp. from highly anaerobic enrichments (e.g., sulfate reducing and methanogenic conditions) has been reported previously. The detection of *Pseudomonas* sp. during this study under differing geochemical conditions, and with both C and N SIP, highlights the wide diversity of this genus, and their importance in many environmental processes.

Our data suggest that, from a remediation perspective, sulfate-reducing or methanogenic conditions are desirable for RDX treatment in order to avoid the long-term accumulation of nitroso-intermediates. The selection of carbon substrate added during biostimulation may be one means of driving the degradative processes in a favorable direction. Use of emulsified vegetable oils has been shown to generate good sulfate-reducing and methanogenic conditions, and also serves as a long-term source of short chain organic acid that may favor the growth of preferred degradative genera. The data also suggest, surprisingly, that some groups of bacteria, such as *Desulfosporosinus,* can play an important role in RDX degradation under a variety of different dominant electron–accepting conditions. One area for future study is better understanding of the roles of *Desulfosporosinus* and *Pseudomonas* (and closely-related species) during *in situ* RDX degradation.

SIP experiments were also conducted using both ^{13}C-labeled and ^{15}N-labeled RDX in groundwater samples from a location at Picatinny Arsenal that had been previously amended with cheese whey to promote *in situ* anaerobic biodegradation of RDX. One set of samples received additional cheese whey to evaluate its effect on the RDX-degrading microbial communities. As observed in the Dahlgren SIP studies, a variety of different bacteria incorporated ^{13}C- and ^{15}N-label from RDX into DNA. For ^{15}N-labeled RDX, a total of fifteen 16S rRNA gene sequences were derived by using the ^{15}N-DNA fractions. These sequences were clustered in *Clostridia*, β-*Proteobacteria*, and *Spirochaetes*. Interestingly, *Desulfosporosinus* (in *Clostridia*) was among the different strains detected using ^{15}N-SIP.

Sixteen different 16S rRNA gene sequences were derived from microcosms receiving ^{13}C-labeled RDX, and they resided in the *Bacteroidia*, *Clostridia,* α-, β- and δ-*Proteobacteria*, and *Spirochaetes*. For both ^{15}N and ^{13}C SIP, the organisms isolated differed from previously isolated RDX degraders. Cheese whey stimulated RDX biotransformation, altered the types of RDX-degrading bacteria, and decreased microbial community diversity.

The SIP analyses conducted during this project reveal that the organisms capable of using C and/or N from RDX or its degradation intermediates under anoxic conditions are much more diverse than previously thought based on studies with pure cultures. Moreover, the studies show that bacteria can degrade the nitramine under a variety of different geochemical conditions and that the organisms involved as well as the dominant pathways utilized may vary depending on those conditions. Interestingly, despite a wealth of research on aerobic RDX biodegradation, we were unable to stimulate aerobic degradation at the sites evaluated for SIP analysis. More detailed studies are required to better understand the relationships among the RDX-degrading organisms and whether microbial community analysis can be used to predict optimal conditions for stimulating RDX degradation at a site.

During the final task in this project, gas-chromatography isotope-ratio mass spectrometry (GC-IRMS) methods were developed to quantify stable isotope ratios stable isotope ratios of both nitrogen ($\delta^{15}N$) and carbon ($\delta^{13}C$) in RDX. Unlike the SIP approach, RDX enriched in ^{15}N or ^{13}C was not required for this task; rather, this approach is applicable for RDX as it is found in the environment (i.e., with isotopes at natural abundance). These CSIA methods were subsequently used to assess stable isotope enrichment during aerobic and anaerobic degradation of RDX by eleven different pure cultures that degrade the nitramine through the known aerobic pathway and multiple anaerobic pathways. There were clear distinctions in the stable isotope fractionation which occurred via aerobic and anaerobic RDX degradation pathways. Among four aerobic RDX degrading strains that were tested, fractionation of N but not C was observed. The mean $\varepsilon^{15}N$ for the four strains was -2.4 ± 0.5 ‰, and the $\varepsilon^{13}C$ was -0.3 ± 1.0 ‰ (not different from zero). A more significant N than C kinetic isotope effect would be expected for this reaction based on the fact that a N-N bond is broken when the initial nitro group is cleaved from the RDX molecule as the first proposed step in the degradation pathway mediated by the XplA/B cytochrome P450 system. A large N fractionation ($\varepsilon^{15}N$ between -6.8‰ and -13.2 ‰ for different strains) was observed for seven different pure cultures degrading RDX through various anaerobic pathways. This large N fractionation is consistent with various proposed mechanisms of initial enzymatic attack on the RDX molecule, most of which involve a N-N bond. The largest N fractionation was observed for two strains that degrade RDX using the XenA/B enzyme system.

Interestingly, fractionation of C in RDX under anaerobic conditions also was observed ($\varepsilon^{13}C$ between -2.1‰ and -7.1‰ for different strains). This is somewhat unexpected in that many proposed mechanisms of initial enzymatic attack do not involve C-H or C-N bond. As such, this observed C fractionation may be a secondary isotope effect or, in some instances, a carbon bond may be involved in the reaction. Carbon stable isotope data were not obtained for any strains that exclusively degraded RDX through nitro-reduction to MNX. The observed variability in $\varepsilon^{13}C$ most likely reflects the fact that (1) strains appear to degrade RDX by multiple pathways in many instances; and, (2) the initial degradative step for RDX as it

breaks down to MEDINA (which may be a multi-step process) may vary by strain, and reflect attack by different enzymes. Further work is required to better understand fractionation of C and N in RDX at an enzymatic and mechanistic level. Additional studies are also necessary to evaluate fractionation of C and N in RDX in natural systems and under differing geochemical conditions.

Benefits:

Overall, the results of this SERDP project provide new insights into the biodegradation of RDX in groundwater, including the detection of new groups of organisms involved in this process under varying geochemical conditions and quantification of stable isotope fractionation of both C and N during both aerobic and anaerobic degradation. The SIP and CSIA techniques developed during this project are expected to have application at DoD sites for documenting *in situ* RDX biodegradation as a natural attenuation process or during bioremediation efforts. Moreover, the CSIA data for RDX indicate that N stable isotope ratio analysis can be useful for documenting both aerobic and anaerobic biodegradation of RDX in field samples, and potentially for discerning the two processes. In addition, C stable isotope analysis can be useful for documenting anaerobic RDX biodegradation. Finally, a new technique was developed that provides effective preservation for most of the key intermediates from both the aerobic and anaerobic biodegradation of RDX in groundwater. This method can be applied at DoD and other sites to ensure that labile degradation products of RDX are preserved in groundwater samples between collection and laboratory analysis.

1.0 PROJECT BACKGROUND and OBJECTIVES

Methods to remove nitramine and nitroaromatic explosives from surface soils, including enhanced bioremediation, are well documented but there are presently few proven techniques to effectively treat explosives, particularly nitramine explosives, in groundwater. In large part, an inadequate understanding of the microbiology, relevant biogeochemistry, and metabolic pathways of explosives degradation *in situ* account for the absence of consistently effective bioremediation approaches. Significant progress has been made during the past few years in the isolation and characterization of pure cultures that utilize RDX as a nitrogen source under both aerobic (e.g.; *Rhodococcus* sp.) and anaerobic (e.g.; *Clostridium*, *Shewanella*, *Desulfovibrio*) conditions (7, 20, 79, 80). Most recently, Thompson et al. reported the first two aerobic isolates (*Gordonia* and *Williamsia* sp.) that are capable of using RDX as a source of carbon, nitrogen, and energy (69). However, despite recent success in pure culture studies, the key organisms involved in the biodegradation of this nitramine in natural environments, as well as the metabolic pathways they utilize, remain largely speculative. Some significant questions remain concerning the microbial transformation of this compound, including the following:

1. *Which organisms are responsible for nitramine degradation in situ?*
2. *What are the key pathways of biodegradation and can we effectively measure "indicator" metabolites to differentiate these pathways?*
3. *What environmental and geochemical factors determine the kinetics and pathway(s) of RDX metabolism?*
4. *How can we effectively quantify nitramine biodegradation in natural systems?*
5. *How can we enhance degradative rates or promote specific types of metabolism in nature?*

This SERDP project assembled a team of academic, government, DoD, and industry researchers with capabilities to examine these key questions. The objective of SERDP Project ER-1435 was to combine state-of-the art analytical techniques, molecular approaches, and biogeochemical studies to enhance our understanding of the biodegradation of the nitramine explosive hexahydro-1,3,5-trinitro-1,3,5-triazine (RDX) in subsurface environments. A new understanding of such biodegradation processes will contribute to the ability of the DoD to predict the fate of nitramine explosives in contaminated groundwater environments, and to more consistently enhance their rates and extents of biodegradation through active remedial approaches.

The following research was conducted during this project:

5. Key indicator metabolites of aerobic and anaerobic RDX biodegradation (including MEDINA, NDAB, nitroso-derivatives, nitrous oxide and others) were analyzed in groundwater from multiple contaminated sites using specialized analytical approaches. In addition, new preservation methods were developed and evaluated to ensure that the analytes detected in the laboratory accurately represent those in the site groundwater;

6. Laboratory microcosm and mesocosm studies were conducted to understand the influence of important geochemical and environmental variables on the rates, extents, and pathways of RDX biodegradation;

7. Stable isotope probing (SIP) methods were developed and employed using ^{13}C- and ^{15}N-labeled RDX to better understand the microbial communities involved in RDX biodegradation in groundwater environments; and

8. Compound-specific stable isotope analysis (CSIA) methods were developed and tested to identify fractionation "signatures" for the known RDX degradative pathways using pure cultures under laboratory conditions.

2.0 PROJECT TASKS

2.1 Task 1 – Analysis of Indicator Metabolites of RDX Degradation at Contaminated Sites

The results summarized in this section here have been previously published:

Paquet, L., F. Monteil-Rivera, P.B. Hatzinger, M. Fuller and J. Hawari. (2011) Analysis of the key intermediates of RDX (hexahydro-1,3,5-trinitro-1,3,5-triazine) in groundwater: Occurrence, stability and preservation. *Journal of Environmental Monitoring* 13(8):2304-2311.

2.1.1 Goal

During this task, we developed necessary field collection and preservation techniques for labile RDX metabolites, and conducted a survey of nitramine-contaminated groundwater for various indicator metabolites. Groundwater samples were collected from nitramine contaminated sites across the United States (7 locations). We selected multiple wells along the flow path of plumes when possible, and locations with differing geochemistries (i.e., pH, dissolved oxygen, reduction potential, anion levels, etc). In addition, we obtained a subset of samples from sites at which active bioremediation approaches for RDX were ongoing or had been performed recently.

2.1.2 Introduction

Over the last decade, the Analytical & Environmental Chemistry Group at the National Research Council of Canada, Biotechnology Research Institute (BRI) identified several key metabolites of RDX that provided insight on potential degradation pathways of the nitramine under various environmental conditions **(Figure 2.1.2-1)**. Recently, the group detected NDAB ($NHNO_2CH_2NHCHO$) in groundwater at a former army ammunition plant. As NDAB is a known metabolite of RDX generated by either aerobic biodegradation by pure cultures (**Figure 2.1.2-1**) or abiotic processes, its detection in the environment is clear evidence for (1) the current or past presence of RDX, and (2) the potential presence of microorganisms that are capable of degrading this nitramine aerobically, or (3) the potential presence of a chemical agent capable of degrading RDX. Other products such as the nitroso derivatives (hexahydro-3,5-dinitro-1-nitroso-1,3,5-triazine (MNX), hexahydro-5-nitro-1,3-dinitroso-1,3,5-triazine (DNX), hexahydro-1,3,5-trinitroso-1,3,5-triazine (TNX)), and MEDINA ($NHNO_2CH_2NHNO_2$) are indicative of an anaerobic degradation pathway. Detecting these indicator metabolites on site would thus be helpful to understand the biological processes taking place in the field. Until now, however analysis for RDX degradation products including NDAB, MEDINA, nitroso derivatives, nitrous oxide (N_2O), methanol (CH_3OH), and formaldehyde (HCHO) has not been performed routinely at explosives-contaminated

sites. Thus, the extent to which indicator metabolites occur and persist in aquifers contaminated with RDX is presently unknown. This lack of knowledge is partly due to the fact that a widespread survey has not been performed, as well as to the lack of appropriate sampling and preservation techniques.

Analytical methods to quantify RDX metabolites are relatively well established (20, 21, 34, 45), but as previously noted, knowledge on the stability and preservation of these metabolites in real field samples is lacking. One of the main objectives of this task was therefore to determine appropriate preservation techniques for some of the more unique metabolites of RDX, such as NDAB, MEDINA, the three nitroso derivatives (MNX, DNX, TNX) and HCHO (**Figure 2.1.2-2**). Stability of these compounds was studied under various conditions in order to propose appropriate modes of preservation.

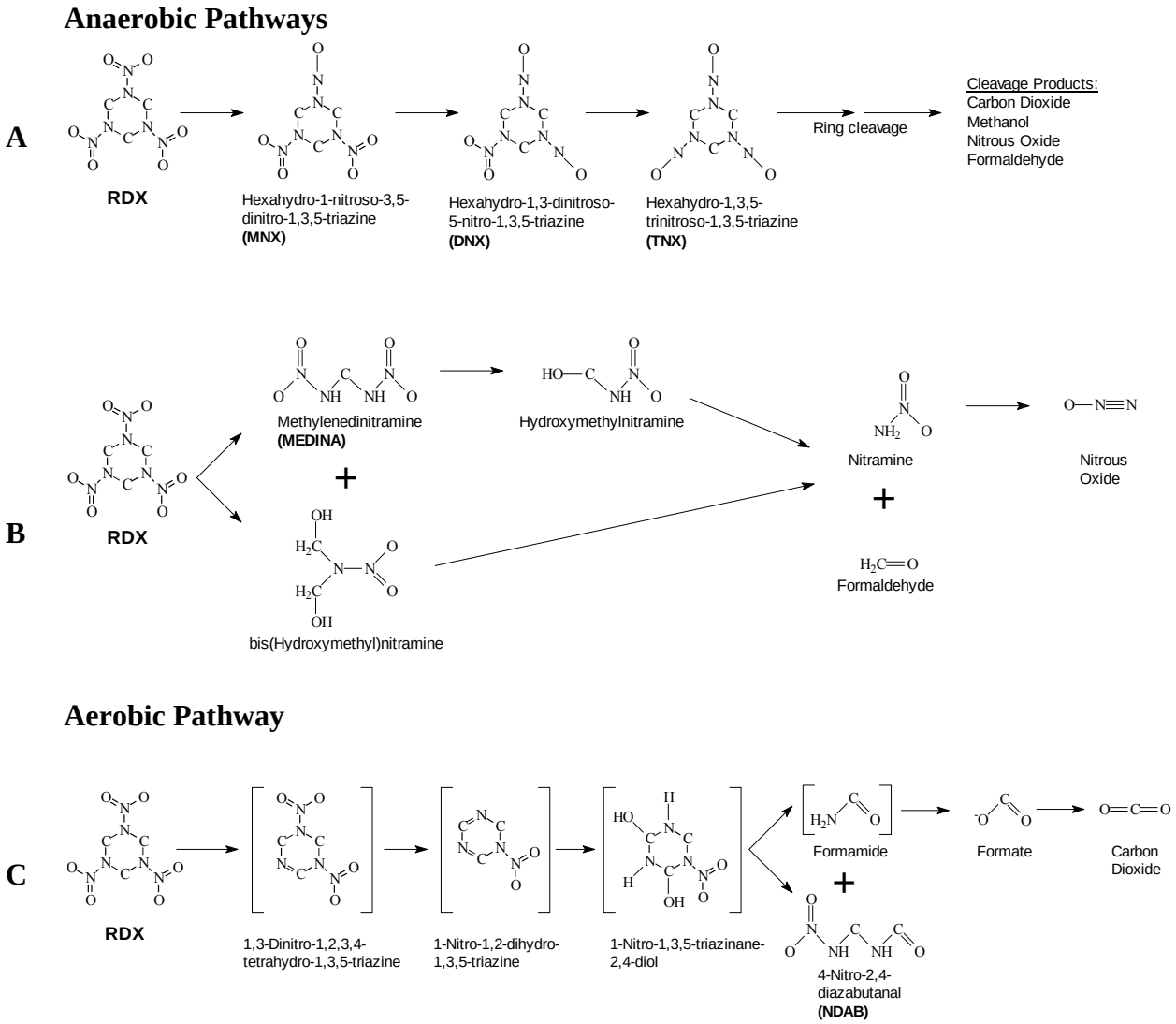

Figure 2.1.2-1. Pathways of RDX metabolism under anaerobic and aerobic conditions.

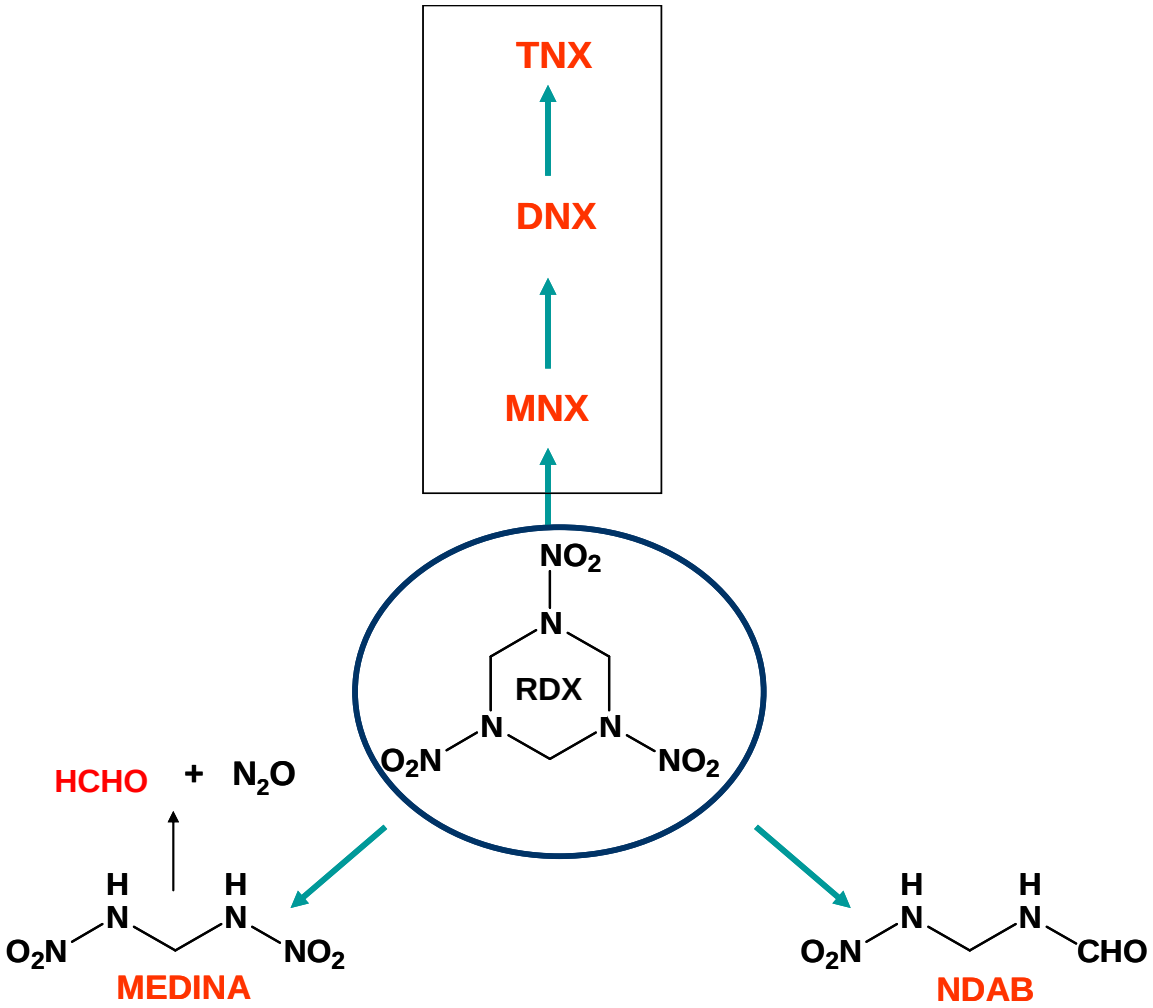

Figure 2.1.2-2. Key "indicator" metabolites of RDX (in red) being investigated during this project.

2.1.3 Preservation Methods Development and Testing

2.1.3.1 Sample Preservation - Materials and Methods

Chemicals

1,3,5-trinitro-1,3,5-triazine (RDX), methylene dinitramine (MEDINA), and hexahydro-1,3,5-trinitroso-1,3,5-triazine (TNX) were provided by Defense Research and Development Canada (Valcartier, QC). 4-Nitro-2,4-diazabutanal (NDAB), hexahydro-3,5-dinitro-1-nitroso-1,3,5-triazine (MNX), and hexahydro-5-nitro-1,3-dinitroso-1,3,5-triazine (DNX) were purchased from SRI (Menlo Park, CA). Formaldehyde (HCHO) was purchased from Sigma-Aldrich (Oakville, ON). Deionized water was obtained with a Milli-Q^{UV} plus (Millipore) system. Other chemicals were of reagent grade.

Groundwater sampling

Groundwater from two wells in Area 157 of the Picatinny Arsenal, Dover NJ was provided to BRI for stability testing of MEDINA, NDAB, and formaldehyde (HCHO) as detailed below. Water was collected from wells 157MW-2 and 157MW-5 for this purpose. At the time of sample collection, groundwater from 157MW-2 was aerobic with a high ORP (+450 mV) and that from 157MW-5 was anaerobic with an ORP of -145 mV (due to previous addition of cheese whey in the vicinity of the well). Various preservation methods for MEDINA were examined in the field, including salt preservation and rapid freezing with dry ice.

Stability experiments

Solutions of either MEDINA (30 mg/L), HCHO (4 mg/L), NDAB (2 mg/L) or nitroso derivatives (MNX: 2.3 mg/L, DNX: 5.5 mg/L, TNX: 1.9 mg/L) were prepared in deionized water or in Picatinny groundwater and left static and away from light at the indicated temperature (4°C: refrigerator, 23°C: room temperature, 40°C: incubator). At specific times, samples were collected and analyzed by HPLC as described below. For groundwater, sterile controls were obtained by filtering the water through a 0.22 μm membrane before adding the chemical to be monitored.

Chemical analyses

RDX and nitroso derivatives. RDX and its nitroso derivatives, MNX, DNX, and TNX, were analyzed by reverse phase HPLC using a Supelcosil LC-CN column (Supelco, Oakville, ON) maintained at 35°C. The mobile phase consisted of a methanol/water gradient at a flow rate of 1.5 mL/min. The initial solvent composition was 30% methanol and 70% water, which was held for 8 min. A linear gradient was run from 30% to 65% methanol over 12 min. This solvent ratio was changed to the initial conditions over 5 min. These initial conditions were then held for 5 additional min. Detection was performed using a photodiode array (PDA) detector set at 230 nm.

NDAB and MEDINA. The ring-cleavage compounds, NDAB and MEDINA, were analyzed by HPLC using an AnionSep Ice-Ion-310 Fast organic acids column 6.5 × 150 mm (Cobert Associates Chromatography Products, St-Louis, MO) kept at 40°C. The mobile phase was composed of 1.73 mM sulfuric acid with a flow rate of 0.6 mL/min. The detection was conducted at a wavelength of 225 nm.

Formaldehyde, Methanol, Nitrous Oxide. Formaldehyde (HCHO) was analyzed as described by Summers (1990) with a few modifications. Samples were derivatized with 2,4-pentanedione in the presence of ammonium acetate and glacial acetic acid for 1 h at 40°C. The derivatives were then analyzed by HPLC using a Supelcosil LC-8 column (25 cm, 4.6 mm i.d., 5 μm) (Supelco, Oakville, ON) maintained at 40°C. The mobile phase consisted of

an acetonitrile gradient of 15 to 27 %, at a flow rate of 1.5 mL/min for 6 min. Detection and quantification were carried out using a fluorescence detector (excitation at 430 nm and emission at 520 nm). MeOH and N_2O were analyzed by GC-FID.

2.1.3.2 Sample Preservation - Results and Discussion

MEDINA. Although MEDINA has been observed in several studies involving RDX degradation by pure or mixed cultures (31, 78), it has never been detected in field samples. The reason for this is likely related to its high instability in aqueous media. The present study was thus conducted to find stabilizing agents for MEDINA in aqueous solution.

The stability of MEDINA was first studied in deionized water under various pH conditions (pH 3: H_3PO_4; pH 5.5: H_2O alone; pH 12: NaOH) **(Figure 2.1.3-1)**. When shaken (150 rpm) at 40°C and in the dark, MEDINA (30 mg/L) appeared to degrade quickly in pure deionized water (100% loss after 1 d). While acid conditions slightly stabilized the dinitramine (99% loss after 14 d), alkaline conditions led to more pronounced chemical stability, with only 40% loss of MEDINA after 22 d. These results are in agreement with Urbanski (1967) (70), who noted that MEDINA readily decomposes when the pH ranges between 3 and 8 but is fairly stable under either acidic (pH 1.0) or basic (pH 10.0) conditions.

Acidification is commonly used to stabilize field samples containing organic compounds including explosives and VOCs because low pH effectively inhibits most microbial activity. In the present case, however, acidification was not effective for MEDINA preservation in aqueous samples. Similarly, although alkaline conditions partially stabilized MEDINA in the laboratory studies, these conditions are likely to result in the abiotic degradation of RDX and other RDX metabolites via alkaline hydrolysis. Thus, our data suggest that modification of groundwater pH is not a particularly effective way to preserve MEDINA in water.

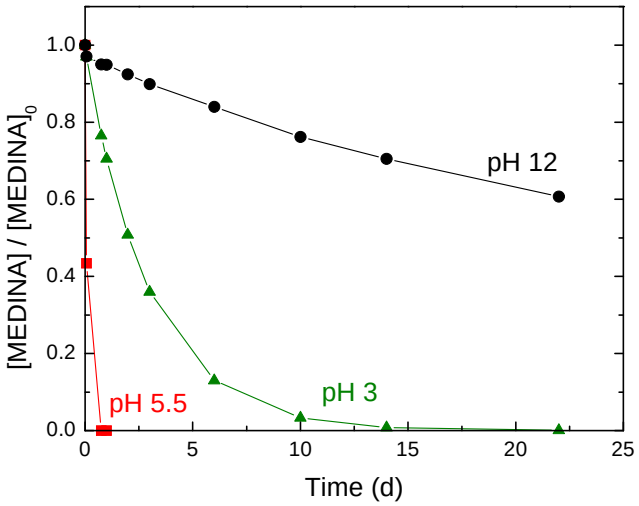

Figure 2.1.3-1. Effect of pH on MEDINA degradation in water.

Temperature is another factor that can be used to limit the loss of organic compounds in samples. The stability of an aqueous solution of MEDINA (30 mg/L) was investigated at various temperatures **(Figure 2.1.3-2)**. Decreasing temperature from 40 to 4°C significantly increased the stability of MEDINA in water, but did not completely prevent its degradation. Considering three days as a general minimum time necessary between sampling and analysis, one would expect a loss of at least 15% MEDINA to take place before analysis. Although storing and shipping samples at 4°C will increase the chances of detecting MEDINA if it is being produced in an aquifer, storage at 4°C alone is unlikely to sufficiently preserve field samples.

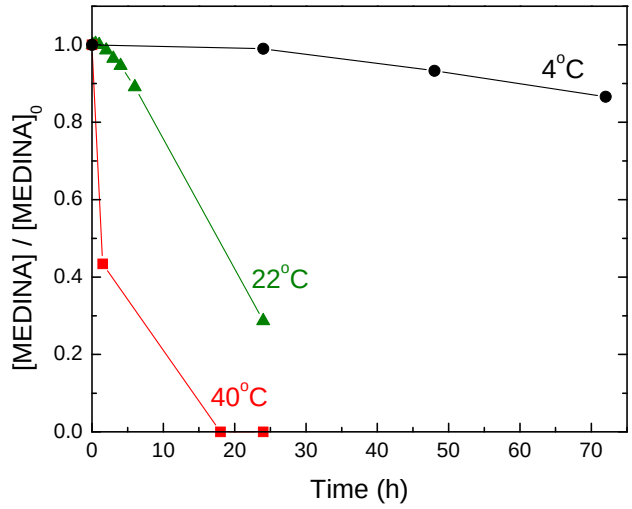

Figure 2.1.3-2. Effect of temperature on MEDINA degradation in water.

Previously, while studying the degradation of RDX and HMX by zero-valent iron in marine media (SERDP Project ER-1431), scientists at BRI noticed an enhanced detection of MEDINA. Based on this earlier observation, we tested the effect of sea salts on the stability of MEDINA for this project. Adding sea salts to deionized water was found to significantly increase the stability of MEDINA at either 4°C or room temperature **(Figure 2.1.3-3)**. After 6 d at 4ºC, for instance, a loss of only 5, 2 and 0.5% was observed for 3, 5 and 10% sea salts (w:v), respectively, compared to 34% loss without salts. Interestingly, when sodium chloride (3%) was added instead of sea salts, MEDINA was lost at a rate similar to unamended water (data not shown), suggesting that this common salt (or salinity alone) is not responsible for the observed stabilization. The improved stability of MEDINA in sea water may thus be partially due to the slight alkalinity of marine water (pH 7.9), or to the presence of other components (metals, sulfates, carbonates). Experiments were subsequently conducted to better understand the role of sea salts in MEDINA stabilization (**Section 2.1.3.4**).

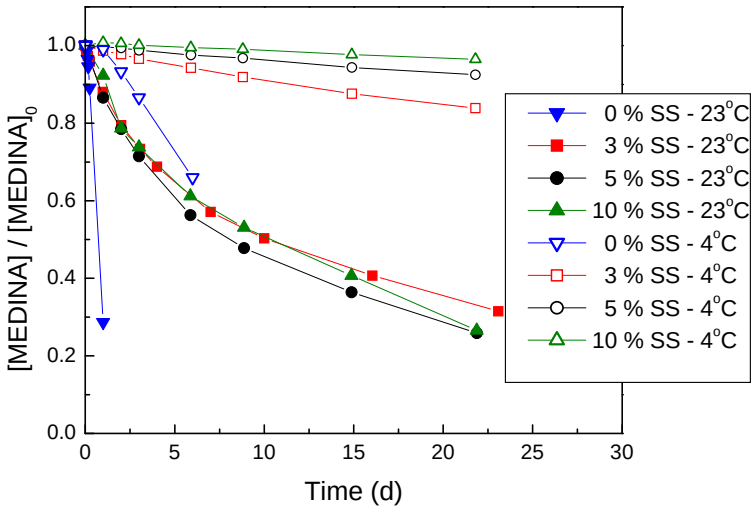

Figure 2.1.3-3. Effect of sea salts (SS) addition on MEDINA stability in deionized water.

Given the positive results obtained using sea salts in deionized water, we investigated the potential use of sea salts to stabilize MEDINA in actual groundwater samples. Groundwater collected from well 157MW-2 at Picatinny Arsenal in May 2008 was used for these studies. The water was aerobic with a positive ORP (~ + 450 mV). Aliquots of groundwater, both filtered through a 0.22 µm filter and unfiltered, were amended with MEDINA. Sea salts were added to both amended samples. The addition of sea salts (10%, pH 7.9) resulted in the preservation of MEDINA, with only about 8% loss after 28 d at 4°C in both the sterile and non-sterile samples **(Figure 2.1.3-4)**. The similarity of the disappearance curves suggests that biodegradation of MEDINA was not occurring in either sample, and that filtration was not necessary if sea salts were added. In summary, our data suggest that the addition of 10% sea salts to groundwater samples combined with storage at 4°C is an effective technique for preservation of MEDINA.

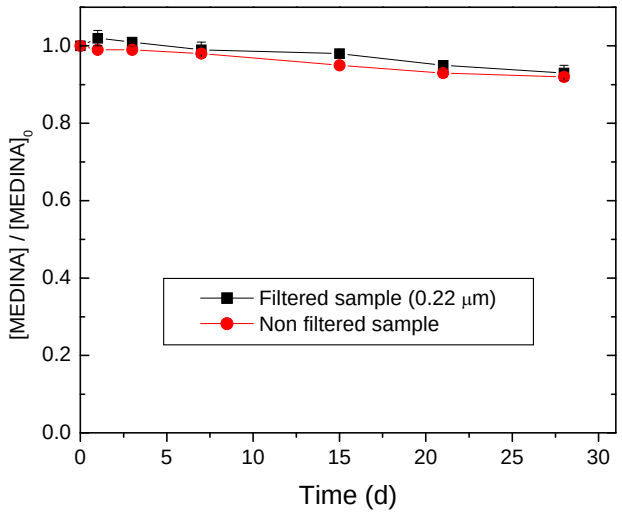

Figure 2.1.3-4. MEDINA stability in groundwater with 10% sea salts at 4°C.

***Formaldehyde (HCHO)*:** The stability of formaldehyde (HCHO) was investigated in filtered and non-filtered groundwater from well 157MW-2 at Picatinny Arsenal. Three sets of conditions were tested: HCHO (4 mg/L) was monitored at 4°C after adding 10% sea salts, 20% methanol, or 20% ethanol. Methanol was selected because it is a common preservation agent used by manufacturers to stabilize formaldehyde solutions, and ethanol was investigated as a potential replacement for methanol, which is more toxic than ethanol. Formaldehyde was found to be stable in the filter-sterile groundwater samples with or without sea salts, methanol, or ethanol as preservatives (**Figure 2.1.3-5**). It should be noted that the HCHO used for the study was introduced from a commercial solution of 37% HCHO, which also contains 10 to 15% methanol. Methanol was thus present at a concentration of approximately 1.0-1.5 mg/L in all samples. The stability observed under sterile conditions may have thus been partially caused by the presence of methanol.

In the non-sterile sample without preservatives, HCHO began to degrade after 10 d and was completely gone after 30 d **(Figure 2.1.3-5)**. However, no loss of HCHO was observed over 30 d in unfiltered samples that were amended with methanol, ethanol, or sea salts. Thus, as observed with MEDINA, sea salts can be used for preservation of formaldehyde in filtered or unfiltered groundwater.

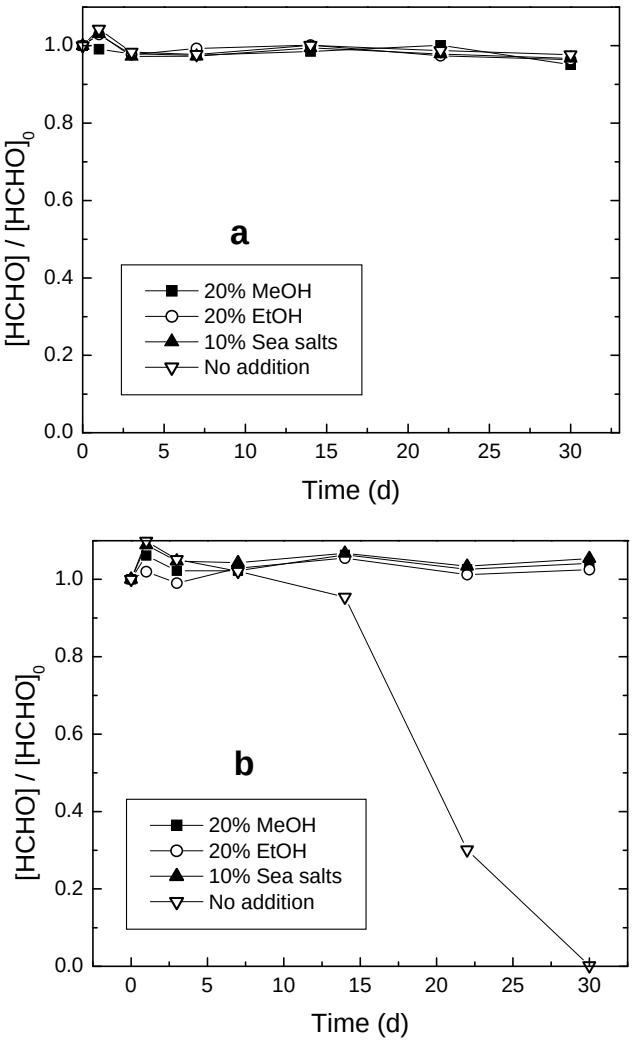

Figure 2.1.3-5. Stability of HCHO in sterile (a) or nonsterile (b) groundwater at 4°C with various preservation agents.

NDAB: NDAB is a metabolite of the aerobic catabolism of RDX by bacteria (see **Figure 2.1.2-1, Pathway C**). NDAB was previously detected it in soil samples collected from the Iowa Army Ammunition Plant (IAAP) (22), and it has also been detected in plant tissues following phytotransformation of RDX (35). NDAB was initially added to deionized water, and the pH was adjusted to 3.0, 5.5, or 12.0. The concentration of NDAB at the various pH values was then followed with time at 40°C. In direct contrast with MEDINA, NDAB was stable in neutral deionized water (i.e., pH 5.5), but degraded under alkaline (pH 12) or acidic (pH 3) conditions (**Figure 2.1.3-6**). NDAB also remained stable in groundwater from well 157MW-2 at the Picatinny Arsenal incubated at 4°C both with or without 10% sea salts. Filtration did not have any effect on the persistence of NDAB, thus demonstrating that neither

chemical nor biological NDAB degradation processes were active in the groundwater (**Figure 2.1.3-7**).

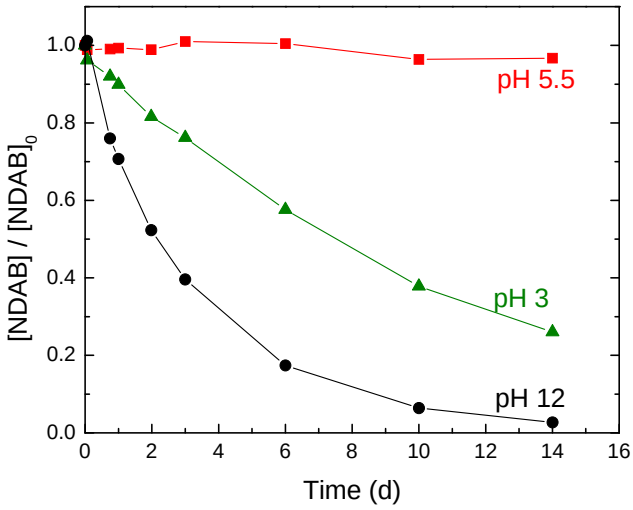

Figure 2.1.3-6. Effect of pH on NDAB degradation in water (150 rpm, 40°C).

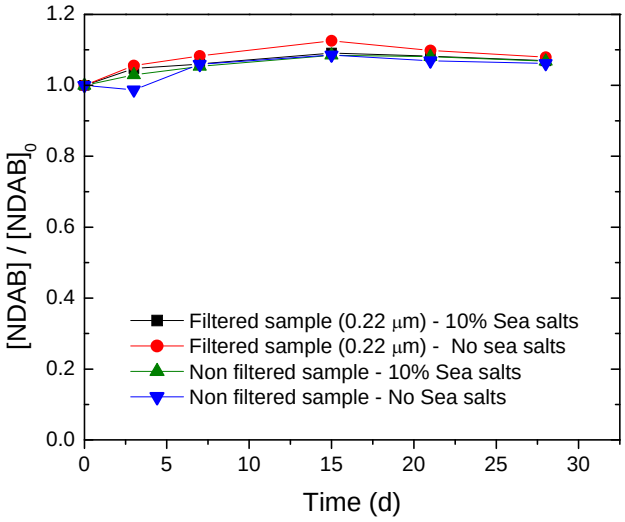

Figure 2.1.3-7. Stability of NDAB in groundwater at 4°C.

Nitroso derivatives: MNX and TNX, but not DNX, are frequently detected in groundwater samples contaminated with RDX. For instance, both MNX and TNX (but not DNX) were detected in environmental samples from IAAP (*Hawari, unpublished data*). The stability of these compounds has not been extensively studied. During this project, the influence of sea salts on the stability of the three nitroso derivatives was evaluated in filtered and non-filtered groundwater from Picatinny well 157MW-2. A standard mix of the nitroso-derivatives (56%

DNX, 24% MNX, 20% TNX; SRI, Menlo Park, CA, USA) was used to amend the groundwater. RDX, which was present in traces in the groundwater, was also monitored. The parent nitramine and its three derivatives were all stable in the groundwater for 21 d, whether the salts were added or not, and irrespective of filtration **(Figure 2.1.3-8)**. The conditions that have been observed to limit MEDINA and formaldehyde degradation (i.e., preservation with 10% sea salts at 4°C) are therefore compatible with the preservation of RDX and nitroso-compounds in groundwater.

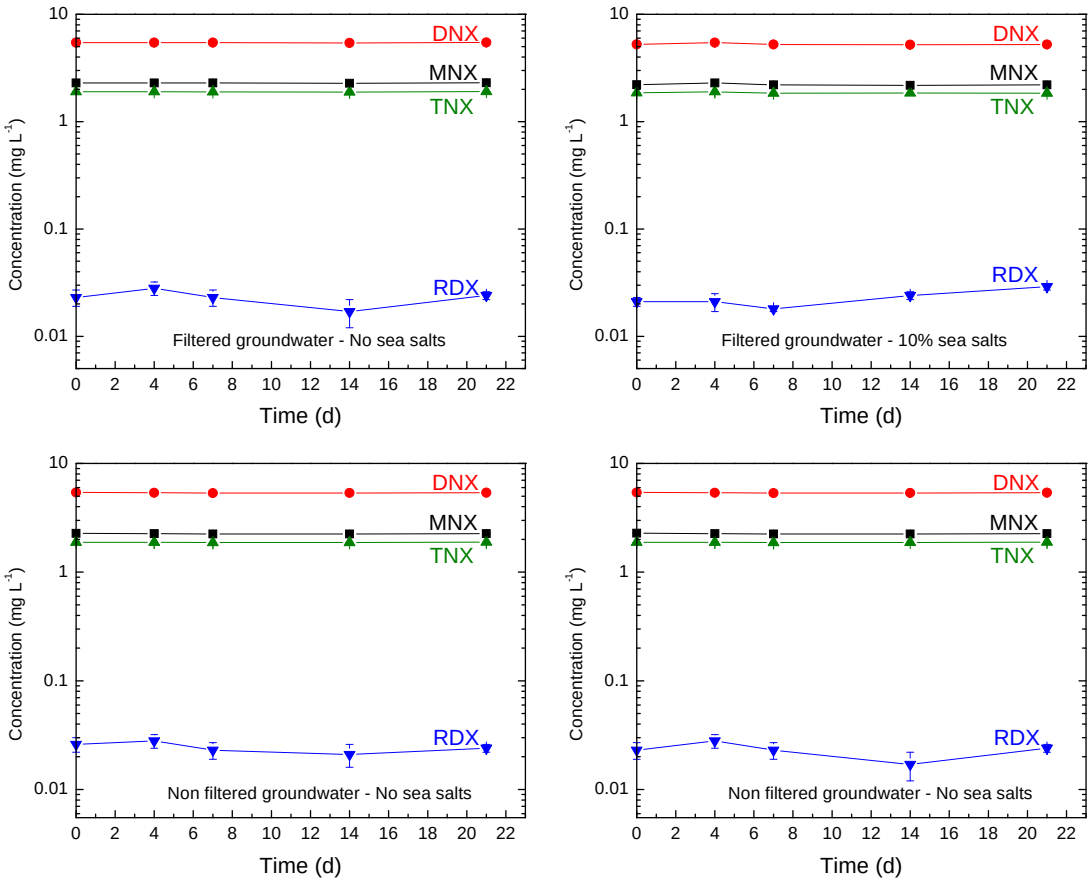

Figure 2.1.3-8. Stability of RDX and its nitroso derivatives in groundwater at 4°C.

2.1.3.3. Mechanistic Studies on Sea Salt Stabilization of Indicator RDX Metabolites

We previously showed a significant positive effect of sea salts on the stability of methylenedinitramine (MEDINA) in both deionized water and field groundwater (**Figure 2.1.3-3**). Thus, the addition of 10% sea salts (SS, Sigma) to all samples as a preservative for MEDINA appears to be a viable preservation method. However, the cause of the increased stability of MEDINA in the presence of sea salts was not readily apparent, particularly since an equal concentration of NaCl was not an effective preservative. These studies were undertaken to determine why the sea salts acted to promote MEDINA stability.

The first mechanism tested was that anions from the sea salts might complex with the acid protons of MEDINA, thereby decreasing the reactivity of the dinitramine in water. The potential effect of anions in the sea salts was assessed by monitoring MEDINA concentration in aqueous samples containing either SO_4^{2-} (7 g/L) or HCO_3^- (0.5 g/L), at concentrations similar to those expected when 10% sea salts are added to water.

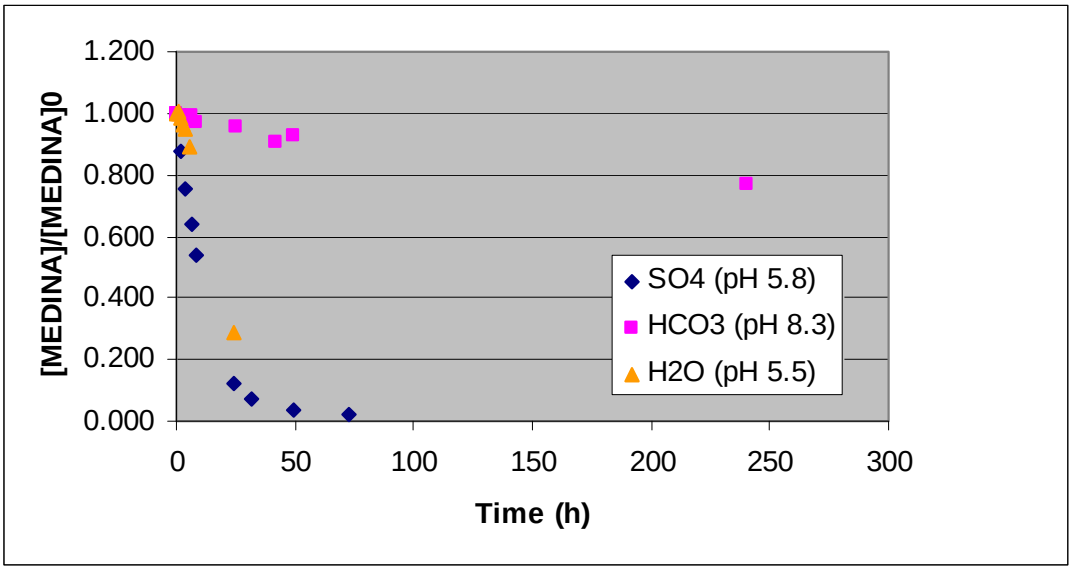

Figure 2.1.3-9. Stability of MEDINA in deionized water in the presence of sulfate or bicarbonate ions and at room temperature.

As shown in **Figure 2.1.3-9**, sulfate ions did not prevent decomposition of MEDINA in deionized water. However, bicarbonate ions did appear to stabilize MEDINA based on the much higher recoveries observed after 24 h (96% compared to 29% in deionized water). The bicarbonate solution had a pH of 8.3, and the high pH may have also been partially responsible for the stability of MEDINA over the timeframe tested.

The potential effectiveness of anion complexation versus elevation in pH was then evaluated by comparing the stability of MEDINA in aqueous bicarbonate solutions adjusted to pH values ranging between 4.3 and 9 ($[HCO_3^-] = 9 \times 10^{-3}$ mol/L, except for the solution at pH 4.3 which is deionized water). The results shown in **Figure 2.1.3-10** suggest that pH plays an important role in the stability of MEDINA. While MEDINA is stable at pH 9, it rapidly decomposes at pH 6, even though the initial bicarbonate concentration was the same. It should be noted, however, that the pK_a of bicarbonate is ~6.4 (pK_a between bicarbonate and free carbon dioxide), so it is possible that the conversion of much of the bicarbonate to carbon dioxide at the lower pH also played a role in the decreased stability of MEDINA. Decomposition of MEDINA was accompanied by the formation of one equivalent of formaldehyde and two equivalents of nitrous oxide. The findings suggest that the positive

effect of sea salts on the stability of MEDINA is attributed to the fact that it buffers the pH to ~8, but additional studies with other buffering systems may be necessary to conclusively distinguish the pH effect from that of the bicarbonate ion alone.

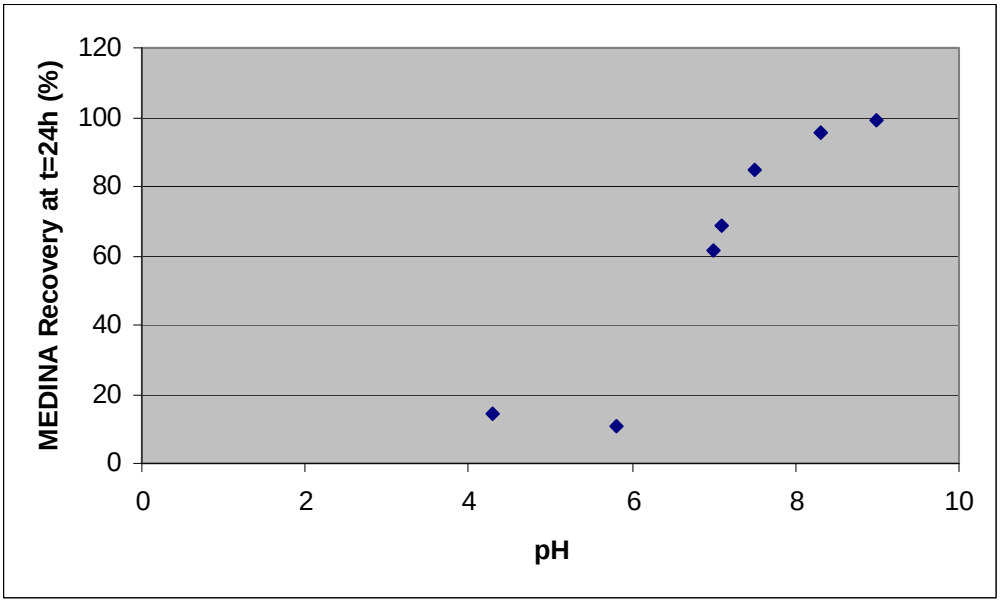

Figure 2.1.3-10. Recovery of MEDINA in aqueous bicarbonate solutions adjusted at various pH values.

2.1.3.4. Preservation of Indicator RDX Metabolites in Anaerobic Groundwater

Another series of studies were performed using anaerobic groundwater samples from Picatinny Arsenal, NJ. These samples consisted of anaerobic water from a location that had previously received cheese whey during ESTCP Project ER-200425, and water that had received fresh cheese whey in the laboratory to stimulate biodegradation of explosives (157MW-5 with nutrients). The objective was to evaluate preservation of MEDINA and NDAB in samples where active anaerobic biodegradation was occurring.

The groundwater was handled in a glove box under anaerobic conditions. Each sample was spiked with MEDINA and 4-nitro-2,4-diazabutanal (NDAB), and either filtered through a 0.22 μm filter to remove bacteria or left unfiltered. Aliquots of the filtered and unfiltered samples were then amended with 10% sea salts; control samples that did not receive sea salts were also included. Groundwater was incubated at 4°C, and both MEDINA and NDAB were then monitored. RDX and nitroso-derivatives, which were present in the groundwater samples, also were monitored during the study.

NDAB was generally stable in all samples, irrespective of filtration or sea salt addition (**Figure 2.1.3-11**). Thus, if present in an anaerobic aquifer, NDAB should be detectable

irrespective of preservation status. This could reflect the inherent stability of NDAB under anaerobic conditions.

For MEDINA, filtration was not protective under anaerobic conditions, suggesting that its degradation in these groundwater samples was primarily abiotic rather than biological (**Figure 2.1.3-12**). In both unamended and nutrient amended groundwater, sea salts appreciably slowed (but did not completely inhibit) MEDINA degradation. In the samples without additional cheese whey, ~20% of the added MEDINA degraded over 6 weeks of incubation in sea salt-amended samples, compared to 100% degradation in less than 4 weeks in samples without the salts. In the samples with freshly added cheese whey, ~40% of the MEDINA degraded in groundwater with sea salts, whereas 100% degraded in <2 weeks without the sea salt amendment. The lower pH (~6.0) in the cheese whey-amended samples was probably responsible for a faster abiotic degradation rate given that losses were similar in both the filtered and unfiltered treatments. However, even under highly anaerobic conditions, sea salts were observed to act as a reasonably good preservative for MEDINA. In all cases, <20% loss of MEDINA was observed during more than a week of incubation in the presence of sea salts.

RDX and its three nitroso derivatives (hexahydro-1-nitroso-3,5-dinitro-1,3,5-triazine (MNX), hexahydro-1,3-dinitroso-5-nitro-1,3,5-triazine (DNX), and hexahydro-1,3,5-trinitroso-1,3,5-triazine (TNX)), were also monitored at 4ºC in each of the water samples under anaerobic conditions. RDX started to degrade slowly after 30 days in the unfiltered, cheese whey-amended groundwater, whereas the three nitroso compounds remained stable in all samples (results not shown).

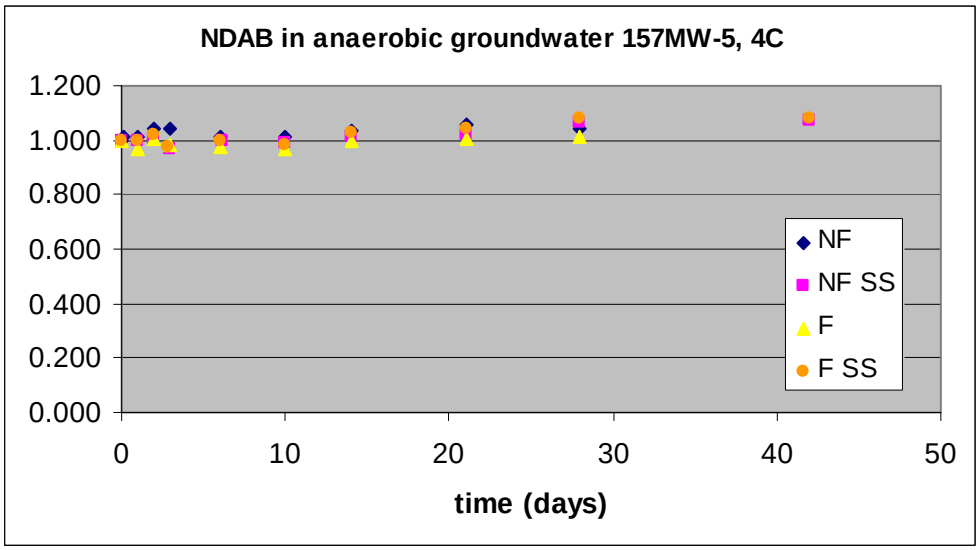

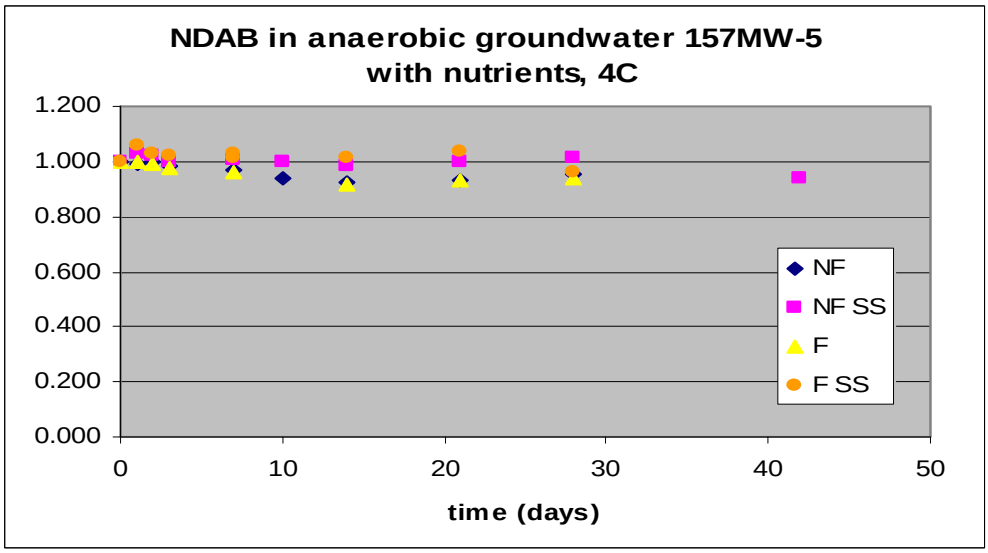

NF: Non filtered; F: Filtered; SS: with sea salts. Initial pH: 6.9 (no nutrients) or 6.0 (with nutrients) with SS.

Figure 2.1.3-11. Stability of NDAB in anaerobic groundwater 157MW-5 with and without added nutrients.

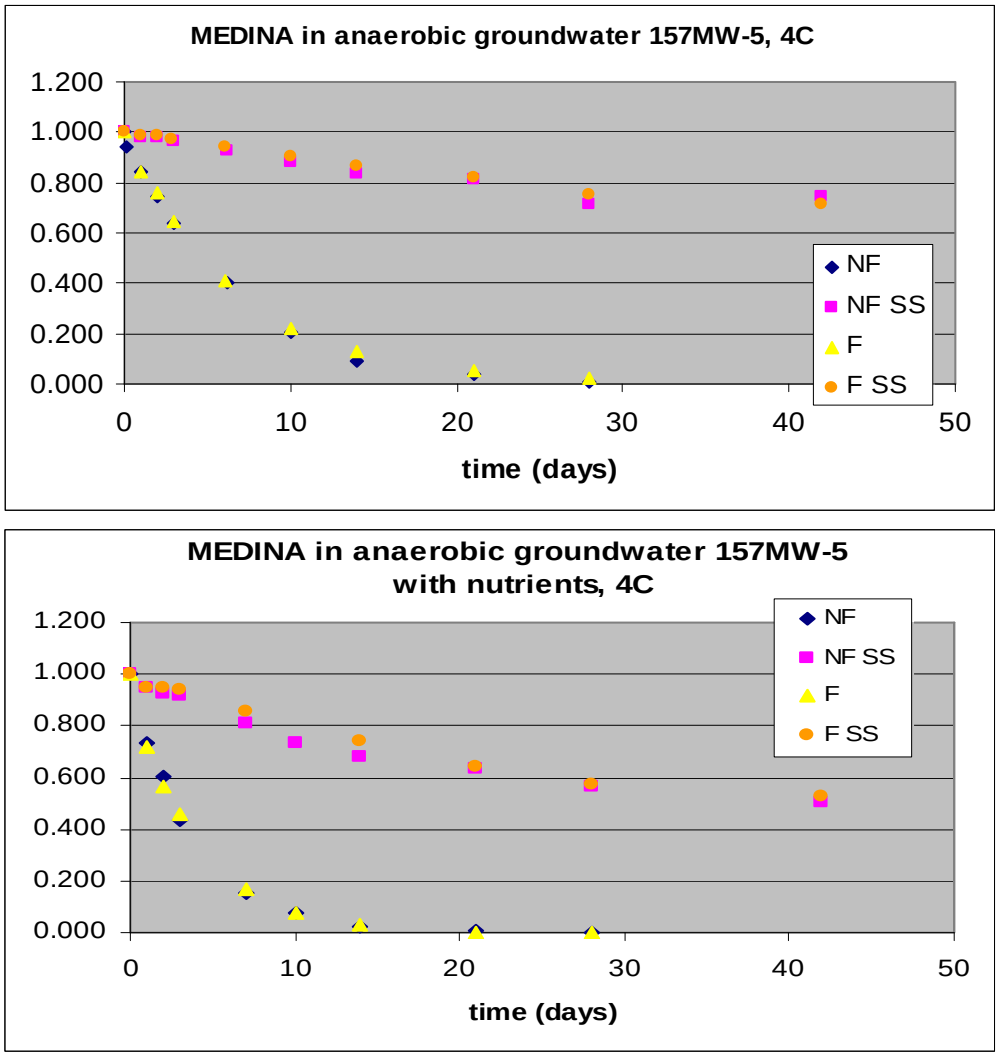

NF: Non filtered; F: Filtered; SS: with sea salts. Initial pH: 6.9 (no nutrients) or 6.0 (with nutrients) with SS.

Figure 2.1.3-12. Stability of MEDINA in anaerobic groundwater 157MW-5 with and without added nutrients.

2.1.3.5 Preservation of Metabolites - Conclusions

The stability of RDX indicator metabolites, including methylenedinitramine (MEDINA), 4-nitro-2,4-diazabutanal (NDAB), formaldehyde (HCHO) and RDX-nitroso derivatives (hexahydro-1-nitroso-3,5-dinitro-1,3,5-triazine (MNX), hexahydro-1,3-dinitroso-5-nitro-1,3,5-triazine (DNX), and hexahydro-1,3,5-trinitroso-1,3,5-triazine (TNX) were tested under various preservation conditions in field groundwater. MEDINA was found to be the most labile compound. Among the various conditions tested, adding 10% sea salts to the groundwater and storing samples at 4°C appeared to be the most effective method for preserving MEDINA. The other compounds tested, (NDAB, MNX, DNX, TNX, RDX,

HCHO) appeared to be stable in the presence of sea salts with less than 2% loss occurred during the first 2 weeks. Thus, our data suggest that the addition of 10% sea salts and storage at 4°C is an effective preservation method for most of the key intermediates from both the aerobic and anaerobic catabolism of RDX.

2.1.4 Field Sampling for RDX and Key Metabolites

2.1.4.1 Site Selection and Sampling

Sampling was performed at numerous field sites to evaluate whether *in situ* degradation of RDX could be documented under aerobic or anoxic conditions. A total of seven sites were sampled for RDX and metabolites during the project, with multiple wells sampled at each site (44 wells total; 3 sampled on two separate occasions). Two sites were sampled on multiple occasions. Compiled data from all of the sites are presented. The sites sampled are as follows: Dahlgren NSWC, VA (4 aerobic wells), sampled on 24 November 2008; Indian Head NSWC, MD (3 anaerobic wells) sampled on 25 November 2008; Picatinny Arsenal, NJ (4 aerobic and 4 suboxic/anaerobic wells), sampled on 15 December 2008 and (3 aerobic and 1 suboxic/anaerobic wells) sampled on 09 October 2009; Massachusetts Military Reservation (MMR), MA (5 aerobic wells) sampled on 21 April 2009; Pueblo Chemical Depot, NM (2 anaerobic and 2 aerobic wells) sampled on 14 May 2009 and (5 aerobic wells) sampled on 27 October, 2009; the Pantex Plant, TX (4 aerobic wells) sampled on 14 May, 2009; Umatilla Chemical Depot (6 aerobic wells) on 25 January 2010.

Samples were collected from each well using low-flow techniques and preserved according to the analyte/preservative matrix presented in **Table 2.1.4-1**. The preservation techniques developed during the initial phase of this project were implemented during sample collection. For each well, the following general procedure was used by CB&I project personnel or other on-site environmental staff as given below:

- Identify well, and in field notebook, note well ID numbers. Photograph location if possible.
- Calibrate YSI or equivalent field meter for basic geochemical parameters (conductivity, dissolved oxygen, pH, temperature, ORP) according to manufacturer guidelines.
- Take water level and leave tape in well.
- Place a Grundfos, peristaltic, or bladder pump to mid-screen depth within the well. Use dedicated pump in well if available (e.g., Picatinny ER-0435 demonstration).
- Attach pump discharge line to YSI flow cell.
- Begin groundwater flow at ~100 to 500 mL/min.
- Measure groundwater field parameters and water elevation every 5 min. Record data on field sheet for each well.

- When parameters stabilize according to guidelines listed on the field sheet, remove the follow cell from the pump and take samples for parameters in **Table 2.1.4-1**.

The sample bottles were filled according to the following guidelines.

- RDX and Metabolites: Fill 2 1-L amber glass bottles with water for analysis of RDX, MNX, DNX, TNX. Tape lids shut, and place on ice.
- MEDINA: Add 4 g of sea salt (Sigma-Aldrich, product number S9883) to a 40- mL VOA vial (in laboratory). Add 40 mL of water to the vial. Shake and place on ice.
- NDAB, MeOH, Formate: Place a sterile (autoclaved) 0.45 µm glass microfiber syringe filter (Fisher P/N: 09-914-34) on a 60 mL disposable syringe. Fill syringe. Filter ~10 mL on to the ground, then collect 10-13 mL into each of 2 sterile 15-mL polypropylene tubes. Screw on cap, and place on ice.
- Formaldehyde: Add 7.5 mL methanol to 50-mL polypropylene tube. Fill with GW to 50 mL mark, shake, place on ice.
- Anions: Add ~240 mL to a 250-mL HDPE bottle for anions.
- Nitrous Oxide: Fill a 120-mL glass serum bottle, then seal with teflon-lined butyl rubber septum (no headspace) and aluminum crimp.
- ICP-MS METALS: Place an in-line 0.45 µm filter on the discharge line from the pump. Allow water to pass filter for 30 to 60 seconds. Filter ~250 mL of water into a 250-mL HDPE bottle for metals analysis. Add few drops of HNO3 as preservative.
- VOCs: Fill 2 40-mL amber glass vials, no headspace. Add few drops of HCl.
- SPME: Fill 1 x 1-L amber glass bottle and secure screw-cap tightly.

Table 2.1.4-1. Groundwater analytes, analytical laboratory, sample volume, and preservation method(s).

Chemical	Preservation	Analytical Lab	Bottle	Volume
Field parameters	NA	CB&I	Field Meter	--
8330 Analysis	Ice	CB&I	1 L glass amber bottle	1 L
ICP-MS Metals	Filter (in line), HNO_3, ice	CB&I (external)	250 or 500 mL HDPE bottle	250-500 mL
Anions (NO_2, NO_3, etc.)	Ice	CB&I	100 or 250 mL HDPE bottle	100-250 mL
RDX, MNX, DNX, TNX	Ice	BRI	1 L glass amber bottle	1 L
MEDINA	Sea salt/ice	BRI	40 mL glass VOA	2 x 40 mL
NDAB	(1) 0.45 µm GMF filter/ice; and (2) sea salt/ice	BRI	15 mL polypropylene tube (sterile)	10-12 mL
MeOH + Formate	(1) 0.45 µm GMF filter /ice and (2) sea salt/ice	BRI	15 mL polypropylene tube (sterile)	10-12 mL
HCHO	7.5 mL MeOH/ice	BRI	50 mL polypropylene tube (sterile)	50 mL
N_2O	Ice	BRI	2 x 40 mL clear vials - no headspace	2 x 40 mL
RDX-SPME	Ice	UIC	1 L glass amber bottle	1 L

2.1.4.2 Results of Groundwater Sampling

A summary of the field parameters recorded during sample collection are presented in **Table 2.1.4-2**. The groundwater samples (n = 44 wells; 7 sites) ranged from highly aerobic to moderately anoxic/anaerobic, as indicated by the range of DO and ORP values. Most of the groundwater was neutral in pH (pH = 7.13 ± 0.55 S.U.). A summary of the compiled groundwater chemistry data is presented in **Table 2.1.4-3**. The groundwater from all seven sites sampled were relatively low in inorganic nutrients (N, P) and organic carbon, with the exception of some of the wells at Picatinny Arsenal. However, groundwater at this location was previously amended with cheese whey as a co-substrate (ESTCP Project ER-200425).

RDX was detected in 25 of the 44 wells sampled at the seven sites at concentrations ranging from 0.3 to 708 µg/L and HMX was detected in 21 of the 44 wells at concentrations from 0.2 to 85 µg/L (**Table 2.1.4-4**). It should be noted that, at most sites, we attempted to select a subset of wells that were not impacted by explosives in order to assess background levels of some of the degradation products of interest that have multiple origins (e.g., N_2O, HCHO, etc.).

Picatinny Arsenal: Picatinny Arsenal was sampled on two occasions. The samples showed the presence of RDX (6.8 to 59 µg/L), and HMX (1.8 to 187 µg/L) in 8 of the 12 samples collected. All HMX nitroso derivatives were detected in one of the anoxic samples, while MNX was detected in four other samples. All of these wells were anoxic, and cheese whey had previously been added to promote RDX biodegradation (ESTCP ER-0435). Neither MEDINA nor NDAB was found in the samples from Picatinny Arsenal. Formaldehyde (HCHO) and nitrous oxide (N_2O) were detected in a majority of the Picatinny Arsenal samples. Formaldehyde was present in larger amounts when MeOH was used as a stabilizer, compared to sea salts. We therefore recommend using distilled MeOH (15%) rather than sea salts to enhance the detection of HCHO, if the latter is of interest.

It is worthwhile noting that although HCHO and N_2O are common products of RDX degradation, they may not serve as definite markers of RDX degradation because they are often present in the environment. We therefore also recommend that control samples be collected from nearby, uncontaminated well(s) in the vicinity of the sampled sites to verify the origin of the measured compounds. In addition, HCHO and N_2O are end products of RDX degradation that do not provide information on the initial pathway(s) and on the biochemical processes involved in RDX on site degradation.

Pantex Plant: Four wells were sampled from the Pantex Plant in TX (Pantex), three of which were contaminated with RDX and one of which was an upgradient control well (PTX06-1076). The highest concentrations of nitramine explosives observed to date during this project were detected in the 3 wells from Pantex, with concentrations ranging from 178 to 708 µg/L. In addition, the nitroso-intermediate TNX was detected in all three of the wells, DNX was detected in two, and MNX was detected in one. None of these intermediates, which are indicative of reductive degradation of RDX (Pathway A in **Figure 2.1.2-1**), were observed in the control well. MEDINA, which would indicate reductive degradation of RDX via pathway B (**Figure 2.1.2-1**) was not detected at Pantex, but NDAB, which is thought to be formed primarily via aerobic RDX biodegradation was detected at low concentrations (5.9 and 15 µg/L) in two of the wells. This was the only site where NDAB was detected during this project, and there are only a few other instances in which this compound has been reportedly detected in natural environments with RDX. Enrichments with Pantex groundwater were initiated upon detection of NDAB, but cultures capable of aerobically degrading RDX were

not isolated. Nitrous oxide (N_2O) was also detected in the three Pantex wells with high RDX concentrations at levels ranging from 27 to 39 µg/L, which are among the highest concentrations observed to date. In the well from Pantex without RDX, (PTX06-1076), N_2O was detected at only 4 µg/L.

Although the focus of this project is RDX, HMX was also detected in three of the Pantex wells at concentrations ranging from 4 to 85 µg/L. Moreover, nitroso derivatives of HMX (nitroso-HMX or NO-HMX) were detected in the two samples that contained the highest concentrations of HMX (**Table 2.1.4-5**). Because no standards are commercially available for NO-HMX, their concentrations could not be quantified. However, their presence was confirmed by HPLC-MS, and 4-NO-HMX was shown to be the major product. The occurrence of these intermediates supports reductive degradation of HMX in these wells, although whether the process is biotic or abiotic could not be confirmed.

MMR and Pueblo Chemical Depot: RDX was detected in two of the five wells sampled at MMR and in one of the three wells at the Pueblo Chemical Depot, but the concentration was <10 µg/L in all wells sampled at these sites. Higher concentrations were expected in some of these wells based on historical data and discussions with site personnel. The degradation intermediates MNX, DNX, TNX, MEDINA and NDAB were not detected in wells at either location. It should be noted, however, that three of the wells at the Pueblo Site were downgradient of an existing mulch barrier wall that was installed through an ESTCP Project for RDX treatment (ER-200426). Nitrous oxide (N_2O) was detected at low concentrations in a few of the wells with RDX.

Because of the low initial concentrations, a second round of sampling was conducted at Pueblo Chemical Depot in a different area of the site. RDX was detected in 3 of the 6 wells sampled and RDX was detected in 1 of the 6 wells. The degradation intermediates MNX, DNX, TNX, MEDINA and NDAB again were not detected.

Dahlgren, VA and Indian Head, MD: RDX (14 to 99 µg/L) and HMX (3 to 72 µg/L) were detected in some of the Dahlgren and Indian Head groundwater samples, but nitroso compounds (MNX, DNX, TNX), MEDINA or NDAB were not detected.

Table 2.1.4-2. Summary of the field parameters recorded during sample collection.

			GW Field Parameters (at time of sampling)							
			DTW	Flow Rate	Temp	pH	DO	ORP	Sp. Cond.	Tubid.
LOCATION	WELL ID	DATE	Ft-btoc	ml/min	°C	S.U.	mg/L	mV	µs/cm	NTU
Dahlgren NSWC	GWOBOD02	11/24/08	8.55	500	17.36	5.20	1.47	288.9	0.079	-
	GWOBOD03	11/24/08	9.55	500	17.54	5.45	3.70	236.3	0.073	-
	CMOBOD02	11/24/08	8.15	500	16.89	4.76	4.12	425.3	0.052	-
	EEA-S17 (BG)	11/24/08	11.50	500	15.51	5.02	1.88	293.2	0.039	-
Indian Head NSWC	MW-01	11/25/08	3.67	250	17.02	5.91	0.30	-14.2	0.647	-
	MW-03	11/25/08	4.05	250	17.81	6.70	0.33	-102.3	0.735	-
	MW-04	11/25/08	5.95	250	19.22	6.32	0.41	-36.8	1.285	-
Picatinny Arsenal	157MW-1	12/15/08	7.80	200	12.74	4.87	2.13	265.8	0.149	-3.0
	157MW-2	12/15/08	6.35	250	10.92	5.23	1.84	250.8	0.172	-2.5
	157MW-4	12/15/08	5.90	250	10.34	6.73	0.21	-128.3	0.437	0.7
	157MW-5	12/15/08	4.20	200	11.09	6.31	0.19	-120.4	0.358	6.1
	157MW-6D	12/15/08	7.05	200	11.01	5.56	1.02	26.8	0.145	24.7
	157MW-7S	12/15/08	7.88	250	10.56	6.40	0.27	-103.5	0.427	32.6
	157MW-7D	12/15/08	6.78	200	10.67	6.71	0.22	-143.1	0.679	1.8
	157MW-8D	12/15/08	5.87	200	10.06	5.65	3.45	209.8	0.081	-2.1
Massachusetts Military Reservation	MW-114 M2	04/21/09	80.08	420	9.94	6.01	12.58	181.6	67.000	1.7
	MW-129 M2	04/22/09	69.55	410	9.69	5.73	12.54	185.7	65.000	1.1
	MW-129 M3	04/22/09	69.48	420	9.83	5.60	12.17	207.7	64.000	1.5
	MW-77 M1	04/21/09	83.83	410	9.77	5.90	12.25	182.3	63.000	1.7
	MW-77 M2	04/21/09	83.81	420	9.75	5.54	12.19	213.4	71.000	1.2
Pueblo Chemical Depot	R1A-1	05/14/09	14.90	300	14.44	7.60	7.32	-60.3	0.636	1.5
	R1B-1	05/14/09	15.25	500	15.10	6.79	2.97	-237.8	0.653	3.4
	R3A-1	05/14/09	16.80	333	14.43	7.61	2.44	45.4	0.706	2.1
	TNTMW-11 (BG)	05/14/09	24.65	300	16.14	7.78	5.85	5.2	0.709	2.3
Pantex	PTX06-1039A	05/14/09	265.31	350	15.88	8.08	6.31	74.0	0.666	1.3
	PTX06-1047A	05/13/09	277.42	150	18.40	7.64	7.03	99.0	0.465	0.5
	PTX06-1050	05/14/09	255.37	350	16.39	7.61	6.18	98.0	0.551	1.6
	PTX06-1076 (BG)	05/13/09	348.90	150	18.37	7.90	5.99	107.0	0.475	0.5
Picatinny Arsenal #2	157MW-3	10/09/09	9.10	200	11.36	5.76	1.13	144.5	0.185	-
	157MW-5	10/09/09	6.20	200	11.25	6.87	0.40	-134.7	0.368	-
	157MW-6D	10/09/09	8.82	200	11.49	5.85	0.92	42.6	0.182	-
	157MW-8D	10/09/09	7.80	200	11.35	5.57	3.56	143.9	0.115	-
Pueblo Chemical Depot #2	TNTMW38	10/26/09	17.97	500	14.84	7.39	6.62	91.9	0.716	18.9
	AOI3BMW5 (BG)	10/26/09	9.39	155	15.50	7.89	8.12	156.0	0.611	9.3
	AOI2AMW4	10/27/09	36.64	500	14.34	7.15	1.33	88.0	0.818	1000.0
	AOIMW6 (BG)	10/27/09	13.90	150	14.48	7.64	6.28	139.5	0.835	5.8
	AOI3BMW15 (BG)	10/27/09	8.97	150	14.62	7.52	4.62	58.0	0.759	7.3
	TNTMW04	10/28/09	12.76	100	8.81	7.53	4.77	150.0	16.320	12.0
Umatilla Chemical Depot	MW4-3	01/25/10	53.10	375	14.60	7.90	9.89	132.7	459.000	0.0
	MW4-112	01/25/10	58.20	375	15.01	7.99	9.21	132.4	444.000	0.0
	MW4-116 (BG)	01/25/10	106.25	75	7.27	7.82	10.00	160.2	494.000	0.0
	MW4-111	01/25/10	54.87	300	12.42	8.04	9.52	138.2	531.000	5.1
	MW47-2	01/25/10	127.14	150	12.11	8.03	10.13	131.9	505.000	10.0
	MW-WO-21	01/25/10	121.23	300	14.27	7.91	9.95	157.7	485.000	14.3
	-. Not determined - no reading or no sample collected									

Table 2.1.4-3. Summary of groundwater chemistry results.

		GW Chemical Parameters [U defined as <PQL]										
		NO2	NO3	SO4	PO4	Cl	Br	F	TOC	NH3 (TKN)	CLO4	Chlorate
LOCATION	WELL ID	mg/L	mg/L	mg/L	mg/L	mg/L	mg/L	mg/L	mg/L	mg/L	µg/L	mg/L
Dahlgren NSWC	GWOBOD02	<0.1	1.2	9.5	<0.1	8.4	ND	ND	5.0	1.3	258.0	<0.1
	GWOBOD03	<0.1	0.9	6.4	<0.1	6.7	ND	ND	3.4	0.4	586.0	<0.1
	CMOBOD02	<0.1	<0.1	4.3	<0.1	3.8	ND	ND	3.6	0.5	52.2	<0.1
	EEA-S17 (BG)	<0.1	0.3	8.5	<0.1	2.2	ND	ND	2.8	0.3	2.1	<0.1
Indian Head NSWC	MW-01	<0.1	<0.1	1.7	<0.1	77.4	-	-	20.3	6.6	18400.0	<0.1
	MW-03	<0.1	<0.1	0.4	<0.1	85.4	-	-	8.0	4.7	1.8	<0.1
	MW-04	<0.1	1.6	13.5	<0.1	193.0	-	-	12.6	6.4	14700.0	<0.1
Picatinny Arsenal	157MW-1	<0.1	0.3	17.5	<0.1	24.2	<0.1	<0.1	3.5	0.1	<0.5	<0.1
	157MW-2	<0.1	0.4	13.5	<0.1	35.3	<0.1	<0.1	3.8	0.3	<0.5	<0.1
	157MW-4	<0.1	<0.1	1.7	<0.1	52.1	<0.1	<0.1	5.9	0.3	<0.5	<0.1
	157MW-5	<0.1	<0.1	9.2	<0.1	44.9	<0.1	<0.1	4.2	0.5	<0.5	<0.1
	157MW-6D	<0.1	<0.1	11.9	<0.1	19.7	<0.1	<0.1	<1	0.3	<0.5	<0.1
	157MW-7S	<0.1	<0.1	0.2	<0.1	18.2	<0.1	<0.1	29.7	10.8	<0.5	<0.1
	157MW-7D	<0.1	<0.1	<0.1	<0.1	51.2	<0.1	<0.1	14.9	4.9	<0.5	<0.1
	157MW-8D	<0.1	<0.1	13.1	<0.1	7.8	<0.1	<0.1	2.6	0.3	<0.5	<0.1
Massachusetts Military Reservation	MW-114 M2	<0.1	0.02	7.1	<0.1	8.4	-	-	-	-	-	-
	MW-129 M2	<0.1	0.03	6.8	<0.1	7.4	-	-	-	-	-	-
	MW-129 M3	<0.1	0.3	6.5	<0.1	8.0	-	-	-	-	-	-
	MW-77 M1	<0.1	<0.1	5.6	<0.1	8.5	-	-	-	-	-	-
	MW-77 M2	<0.1	0.2	8.0	<0.1	5.8	-	-	-	-	-	-
Pueblo Chemical Depot	R1A-1	<0.1	3.8	99.6	<0.1	23.0	0.3	0.9	3.4	0.1	<0.5	<0.1
	R1B-1	<0.1	<0.1	29.3	<0.1	18.2	0.2	0.9	5.1	0.3	<0.5	<0.1
	R3A-1	<0.1	<0.1	50.6	<0.1	18.9	0.3	0.8	4.2	0.4	<0.5	<0.1
	TNTMW-11 (BG)	<0.1	0.8	115.0	<0.1	19.1	0.3	0.7	2.8	0.5	<0.5	<0.1
Pantex	PTX06-1039A	<0.1	0.9	39.1	<0.1	69.8	0.3	0.5	2.3	0.5	<0.5	<0.1
	PTX06-1047A	<0.1	2.2	14.6	<0.1	31.7	0.3	1.9	2.6	0.7	1.0	<0.1
	PTX06-1050	<0.1	1.2	10.7	<0.1	54.0	0.2	0.5	2.2	0.5	<0.5	<0.1
	PTX06-1076 (BG)	<0.1	1.2	18.9	<0.1	13.2	0.2	2.2	1.9	0.3	0.3	<0.1
Picatinny Arsenal #2	157MW-3	<0.1	0.1	10.5	<0.1	29.0	<0.1	<0.1	3.4	-	-	-
	157MW-5	<0.1	<0.1	8.6	<0.1	48.0	<0.1	<0.1	3.1	-	-	-
	157MW-6D	<0.1	0.1	9.4	<0.1	32.4	<0.1	<0.1	2.5	-	-	-
	157MW-8D	<0.1	0.1	9.4	<0.1	17.3	0.2	<0.1	2.5	-	-	-
Pueblo Chemical Depot #2	TNTMW38	<0.1	8.8	94.8	<0.1	23.8	0.2	1.5	4.8	0.1	ND	ND
	AOI3BMW5 (BG)	<0.1	2.9	101.0	<0.1	2.7	<0.1	0.8	5.1	<0.5	ND	ND
	AOI2AMW4	0.2	20.9	118.0	<0.1	22.2	0.3	1.0	3.4	6.6	ND	ND
	AOIMW6 (BG)	<0.1	3.0	185.0	<0.1	25.2	0.3	0.6	1.8	<0.5	ND	ND
	AOI3BMW15 (BG)	<0.1	0.5	124.0	<0.1	21.2	0.3	0.9	1.4	<0.5	ND	ND
	TNTMW04	<0.1	1.2	248.0	<0.1	103.0	1.0	1.9	13.4	1.3	ND	ND
Umatilla Chemical Depot	MW4-3	<0.1	8.1	25.7	<0.1	15.8	0.0	0.5	2.3	0.4	ND	<0.1
	MW4-112	<0.1	2.8	23.8	<0.1	24.6	0.1	0.5	1.7	<0.5	ND	<0.1
	MW4-116 (BG)	<0.1	7.3	24.4	<0.1	16.1	0.1	0.3	2.7	<0.5	ND	<0.1
	MW4-111	<0.1	1.4	42.7	<0.1	33.4	0.2	0.4	2.6	<0.5	ND	<0.1
	MW47-2	<0.1	8.2	33.0	<0.1	18.1	0.1	0.6	2.1	<0.5	ND	<0.1
	MW-WO-21	<0.1	7.9	25.1	<0.1	16.1	0.1	0.5	2.2	<0.5	ND	<0.1
	-. Not determined - no reading or no sample collected											

Table 2.1.4-4. Summary of analytical results for HMX, RDX, and metabolites.

		Explosives & Metabolites (BRI), µg/L [U defined as <PQL]								15% MeOH	10% SS	Filtered		
		HMX	MNX	DNX	TNX	RDX	MEDINA	NDAB	MeOH	HCHO	HCHO	HCHO	N2O	Formate
LOCATION	WELL ID	µg/L	µg/L	µg/L	µg/L	µg/L	µg/L	µg/L	µg/L	µg/L	µg/L	µg/L	µg/L	µg/L
Dahlgren NSWC	GWOBOD02	28.1	<0.2	<0.2	<0.2	18.8	<10	<10	<300	210	<20	212	31	-
	GWOBOD03	3.5	<0.2	<0.2	<0.2	31.6	<10	<10	<300	64	<20	35	15	-
	CMOBOD02	37.0	<0.2	<0.2	<0.2	98.6	<10	<10	100	<20	<20	<20	21	-
	EEA-S17 (BG)	<0.1	<0.2	<0.2	<0.2	<0.2	<10	<10	600	42	<20	33	4	-
Indian Head NSWC	MW-01	4.3	<0.2	<0.2	<0.2	<0.2	<10	<10	2800	2051	207	377	<2	-
	MW-03	<0.1	<0.2	<0.2	<0.2	<0.2	<10	<10	9000	844	23	42	<2	-
	MW-04	71.6	<0.2	<0.2	<0.2	14.4	<10	<10	1000	1329	24	136	17	-
Picatinny Arsenal	157MW-1	22.4	0.5	<0.2	<0.2	35.3	<10	<10	<300	<20	<20	<20	28	-
	157MW-2	2.2	<0.2	<0.2	<0.2	6.8	<10	<10	<300	<20	<20	<20	27	-
	157MW-4	<0.1	<0.2	<0.2	<0.2	<0.2	<10	<10	400	3081	182	174	6	-
	157MW-5	6.2	<0.2	<0.2	<0.2	<0.2	<10	<10	<300	2171	<20	<20	4	-
	157MW-6D	1.8	<0.2	<0.2	<0.2	12.2	<10	<10	<300	825	<20	<20	3	-
	157MW-7S	<0.1	<0.2	<0.2	<0.2	<0.2	<10	<10	<300	3427	2144	198	<2	-
	157MW-7D	<0.1	<0.2	<0.2	<0.2	<0.2	<10	<10	<300	4068	1969	193	<2	-
	157MW-8D	24.7	0.5	<0.2	<0.2	24.0	<10	<10	<300	<20	<20	<20	<2	-
Massachusetts Military Reservation	MW-114 M2	5.8	<0.2	<0.2	<0.2	4.4	<10	<10	1556	38	-	-	2	-
	MW-129 M2	<0.1	<0.2	<0.2	<0.2	<0.2	<10	<10	<300	43	-	-	1	-
	MW-129 M3	<0.1	<0.2	<0.2	<0.2	<0.2	<10	<10	<300	43	-	-	1	-
	MW-77 M1	<0.1	<0.2	<0.2	<0.2	<0.2	<10	<10	369	36	-	-	1	-
	MW-77 M2	5.5	0.1	<0.2	<0.2	10.5	<10	<10	294	38	-	-	8	-
Pueblo Chemical Depot	R1A-1	0.1	<0.1	<0.1	<0.1	2.5	<10	<10	6000	224	-	-	3	-
	R1B-1	<0.1	<0.1	<0.1	<0.1	<0.2	<10	<10	2700	1565	-	-	<2	-
	R3A-1	<0.1	<0.1	<0.1	<0.1	<0.2	<10	<10	2800	165	-	-	<2	-
	TNTMW-11 (BG)	<0.1	<0.1	<0.1	<0.1	<0.2	<10	<10	7100	39	-	-	2	-
Pantex	PTX06-1039A	85.0	3.4	6.1	45.4	708.0	<10	59	500	43	-	-	39	-
	PTX06-1047A	4.1	<0.1	<0.1	48.1	684.0	<10	150	500	39	-	-	27	-
	PTX06-1050	23.9	<0.1	2.1	10.6	177.5	<10	<10	500	42	-	-	28	-
	PTX06-1076 (BG)	<0.1	<0.1	<0.1	<0.1	<0.2	<10	<10	300	43	-	-	4	-
Picatinny Arsenal #2	157MW-3	16.8	3.9	<0.1	<0.1	86.0	<10	<10	<200	41	-	-	7	-
	157MW-5	<0.1	<0.1	<0.1	<0.1	<0.2	<10	<10	<200	1691	-	-	3	-
	157MW-6D	2.6	<0.1	<0.1	<0.1	8.3	<10	<10	<200	984	-	-	7	-
	157MW-8D	20.8	1.4	<0.1	<0.1	28.0	<10	<10	<200	<20	-	-	5	-
Pueblo Chemical Depot #2	TNTMW38	<0.1	<0.1	<0.1	<0.1	13.3	<10	<10	347	40	-	-	5	-
	AOI3BMW5 (BG)	<0.1	<0.1	<0.1	<0.1	<0.2	<10	<10	201	45	-	-	4	-
	AOI2AMW4	0.2	<0.1	<0.1	<0.1	21.8	<10	<10	351	75	-	-	134	-
	AOIMW6 (BG)	<0.1	<0.1	<0.1	<0.1	<0.2	<10	<10	2738	40	-	-	7	-
	AOI3BMW15 (BG)	<0.1	<0.1	<0.1	<0.1	0.3	<10	<10	10584	89	-	-	5	-
	TNTMW04	<0.1	<0.1	<0.1	<0.1		<10	<10	7045	33	-	-	12	-
Umatilla Chemical Depot	MW4-3	<0.1	<0.1	<0.1	<0.1	7.8	<10	<10	165	28	-	-	9	-
	MW4-112	3.8	<0.1	<0.1	<0.1	15.4	<10	<10	781	28	-	-	10	-
	MW4-116 (BG)	<0.1	<0.1	<0.1	<0.1	<0.2	<10	<10	<200	23	-	-	8	-
	MW4-111	0.1	<0.1	<0.1	<0.1	7.6	<10	<10	<200	28	-	-	7	-
	MW47-2	<0.1	<0.1	<0.1	<0.1	18.1	<10	<10	18751	35	-	-	5	-
	MW-WO-21	0.5	<0.1	<0.1	<0.1	54.9	<10	<10	41932	40	-	-	15	-

-. Not determined - no reading or no sample collected

Table 2.1.4-5. Summary of analytical results for HMX and NO-HMX metabolites.

WELL ID	HMX (µg/L)	NO-HMX	2-NO-HMX	3-NO-HMX	4-NO-HMX
Pantex Plant					
PTX06-1039A	85.0	Yes	Yes	Yes	Yes
PTX06-1047A	4.1	No	No	No	Yes
PTX06-1050	23.9	Yes	Yes	Yes	Yes
PTX06-1076	< 0.1	ND	ND	ND	ND

ND – not determined
Yes – detected but not quantifiable because standards are not available.
No – not detected.

2.1.5 Conclusions from Site Sampling

The key degradation intermediates for anaerobic catabolism of RDX include the nitroso-derivatives MNX, DNX, and TNX, and the ring cleavage product MEDINA. Small metabolites, such as nitrous oxide, formaldehyde and methanol also occur during anaerobic catabolism of RDX, although these intermediates are not necessarily specific for RDX metabolism (**Figure 2.1.2-2**). Using the preservation techniques developed during the first six months of this project, we detected MNX, DNX, and TNX in wells from the Pantex Plant in TX. The corresponding nitroso-derivatives for HMX (NO-HMX) were also detected. MEDINA was not detected. Even though sample preservation with sea salts would stabilize any MEDINA present, the lack of detection of MEDINA may reflect the very transient half-life of this compound in the groundwater.

The results indicated that reductive degradation of both RDX and HMX was likely occurring at the Pantex Plant. Interestingly, NDAB, which is an intermediate of aerobic RDX degradation by some *Rhodococcus* sp., was also detected at trace concentrations in two of the Pantex Plant wells. This was the first site for which we have observed NDAB in groundwater, although it should be noted that concentrations were exceedingly low.

Several of the smaller intermediates of RDX degradation, including nitrous oxide, formaldehyde, and methanol were found in groundwater at the other sites (**Table 2.1.4-4**), with the latter two compounds being highest in anaerobic groundwater that was previously amended with soluble organic carbon (Picatinny Arsenal) or passed through a mulch barrier wall (Pueblo Chemical Depot). The accumulation of formaldehyde and methanol under anaerobic conditions is not unexpected. More interesting, however, is the general occurrence of N_2O in aerobic wells that are also contaminated with RDX at various sites. We do not currently know if the N_2O is actually a product of aerobic RDX degradation or whether this reflects the geochemical conditions at the sites, as there are various sources of N_2O in groundwater (e.g., nitrification, denitrification, etc.) that are unrelated to RDX metabolism. However, when RDX concentrations are plotted vs. N_2O concentrations for several of the sites with predominantly aerobic wells (MMR, Pantex, Dahlgren), a general correlation is apparent (**Figure 2.1.5-1**). This relationship is interesting and deserves further study using more sensitive stable isotope methods.

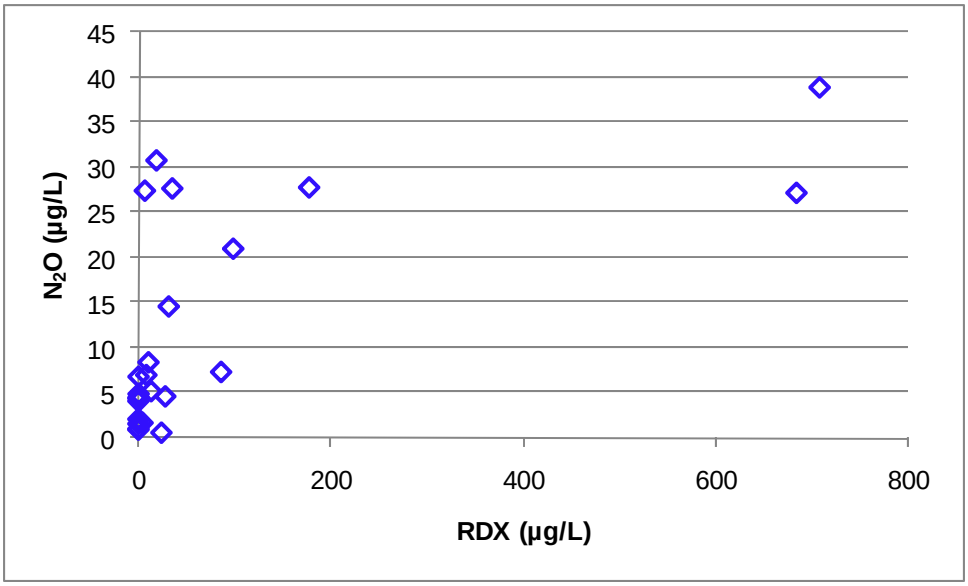

Figure 2.1.5-1. Concentrations of RDX vs. N_2O in groundwater from the Pantex Plant (TX), MMR (MA). and Dahlgren (VA).

NDAB has been observed to be a terminal degradation intermediate of RDX by some *Rhodococcus* sp. (20) and other aerobic RDX degraders (69), but it has rarely been measured in environmental samples. However, because NDAB is reasonably stable in groundwater at neutral pH, this metabolite may be an ideal indicator of natural aerobic biodegradation of RDX. During this project, >30 wells that had aerobic, oxidizing groundwater were sampled. NDAB was detected in two wells from the Pantex Plant in TX, but not in wells from any of the other sites. Interestingly, however, typical anaerobic degradation products of RDX (MNX, DNX, TNX) and HMX (NO-HMX) were detected in the same Pantex wells. The data suggest either that both aerobic and anaerobic degradation of RDX may be occurring at the Pantex site. However, in recent studies in our laboratory, *Rhodococcus* sp. were observed to biodegrade RDX and to produce NDAB under microaerophilic conditions (<0.05 mg/L dissolved oxygen) (24). Thus, perhaps both pathways A and C in **Figure 2.1.2-1** can occur concurrently under appropriate geochemical conditions.

2.2 Task 2 – Geochemical and Environmental Conditions Affecting RDX Biodegradation

2.2.1 Objective

During this task, we conducted laboratory microcosm and mesocosm studies designed to better understand the influence of geochemical and environmental conditions on the rates, extents, and pathways of RDX biodegradation. Initial screening experiments were performed in laboratory microcosms composed of site solids and groundwater. The variables examined during the microcosm studies include the influence of cosubstrate type and the presence of available nitrogen on RDX metabolism. Follow-on mesocosm studies examined the effects of terminal electron-accepting conditions on RDX degradation in aquifer slurry enrichments.

2.2.2 Dahlgren Microcosms - Nutrient Screening

2.2.2.1 Methods

The initial site selected for study was the Naval Surface Warfare Center in Dahlgren, VA. An initial collection of groundwater and hand-augered sediments was conducted in November, 2008 followed by Geoprobe sample collection in January, 2009 (see **Section 2.2.3**).

A screening level study was established to determine which nutrient sources and general redox conditions (aerobic vs. anoxic/anaerobic) were conducive to RDX degradation in the Dahlgren groundwater. Sediments were homogenized and distributed to 160 mL serum bottles (10 g per bottle, wet wt). The native groundwater contained a very low concentration of RDX (<50 μg/L), so the groundwater was amended with technical grade RDX to achieve a final concentration of 0.5 mg/L. The groundwater also contained approximately 0.6 mg/L perchlorate. Perchlorate was not the focus of this project, but its presence did add to the nutrient addition requirement in terms of amount of electron donor equivalents required. Groundwater and nutrients were added to an initial volume of 100 mL. The treatments in **Table 2.2.2-1** were included in the screening study.

Killed controls were amended with 1% (v:v) formaldehyde. Simple carbon sources (glucose, succinate, lactate, ethanol) were added at concentrations of 1 mg/L. Complex carbon sources (cheese whey, molasses, vegetable oil) were added at a concentration of 1 mg/L of TOC. Groundwater for anaerobic treatments was pre-purged with nitrogen, then allowed to degas and equilibrate in a glove bag overnight before use. All sampling of anaerobic bottles was performed in an H_2-free glove bag. Groundwater for aerobic treatment was purged with air prior to use. Bottles were amended with pure oxygen every week to maintain aerobic conditions (10 mL per bottle).

Table 2.2.2-1. Treatments in screening-level microcosm study conducted with Dahlgren aquifer samples.

Bottle #	Treatment	Replicates
1,2,3	Aerobic Killed Control	3
4,5,6	Aerobic	3
7,8,9	Aerobic SG	3
10,11,12	Anaerobic Killed Control	3
13,14,15	Anaerobic	3
16,17,18	Anaerobic S1-cheese whey	3
19,20,21	Anaerobic S2-molasses	3
22,23,24	Anaerobic S3-edible oil substrate	3
25,26,27	Anaerobic S4-glucose	3
28,29,30	Anaerobic S5-succinate (sodium salt)	3
31,32,33	Anaerobic S6-lactate (sodium salt)	3
34,35,36	Anaerobic S7-ethanol	3

For sampling, 7 mL of homogenized slurry was removed from each bottle using a sterile pipet. The sample was placed in a 15 mL blue cap centrifuge tube and spun for 5 min at 3400 rpm at room temperature (25°C). The cleared supernatant was passed through a 0.45 μm glass microfiber filter, collecting ~2 mL into two separate vials, one for RDX and one for perchlorate analyses. RDX and metabolites was measured using HPLC (modified EPA Method 8330). Perchlorate was measured using IC (EPA Method 314).

2.2.2.2 Dahlgren Microcosms - Results

No degradation of RDX was observed in any of the aerobic bottles regardless of whether a nutrient source (succinate plus glucose) was added or not (data not shown). After nearly 200 days under anoxic/anaerobic conditions, RDX biodegradation occurred in all the carbon source amended bottles (**Figure 2.2.2-1**). The most rapid RDX degradation was observed in succinate-amended bottles, while the slowest was in the ethanol-amended bottles. Both complex and simple carbon sources stimulated RDX degradation in these microcosms. Some RDX degradation was also observed in one of the three unamended anaerobic bottles after 200 days.

2.2.2.3 Dahlgren Microcosm Study - Conclusions

Groundwater and sediment at the Dahlgren site harbored a robust RDX-degrading microbial community. A range of carbon sources stimulated degradation of RDX under anaerobic, but not aerobic conditions. Based on the results, succinate was chosen for follow-on studies examining the degradation of RDX under a range of electron acceptor conditions in large-scale microcosms (see section 2.2.3).

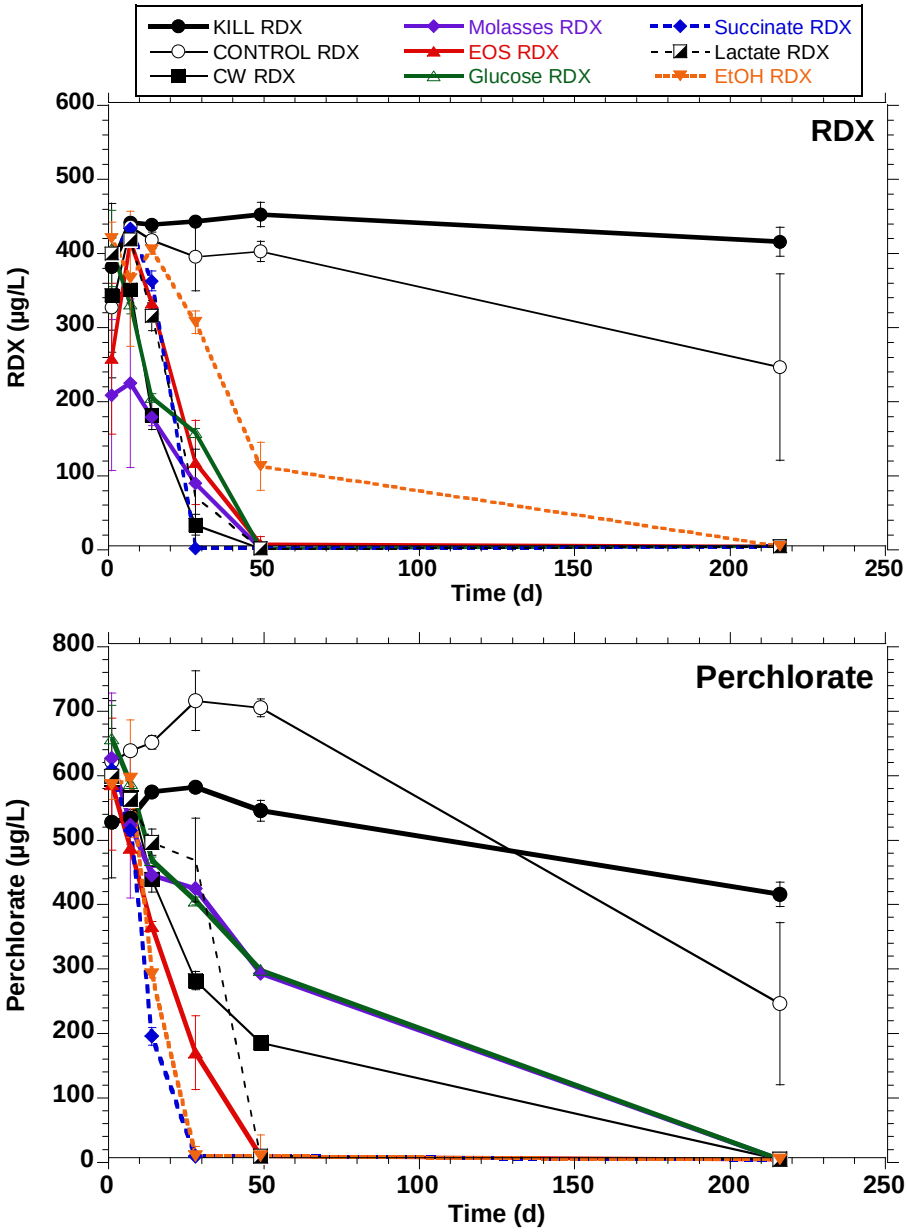

Data points represent the average of 3 replicate bottles with error bars showing 1 standard deviation about the average.

Figure 2.2.2-1. Degradation of RDX (top) and perchlorate (bottom) in anaerobic microcosm bottles prepared with materials from Dahlgren NSWC and treated with various carbon sources or no addition.

2.2.3 Establishment of RDX Degradation under Various Electron Acceptor Conditions

2.2.3.1 Methods

Sample Collection: The initial site selected for further study was the Churchill Range at the Naval Surface Warfare Center (NSWC) in Dahlgren, VA. An initial collection of groundwater and hand-augered aquifer materials was conducted on 24 November 2008. Because hand-augering to depth proved difficult, additional samples were obtained using a Geoprobe rig on 15 January 2009 (**Figure 2.2.3-1; top panel**). Additional groundwater for laboratory microcosm studies was also collected from Well GWOBOD-03 during this sampling event (**Figure 2.2.3-1; bottom panel**).

Aquifer core materials were collected from ~10 to 20 ft below ground surface (bgs) from 10 locations in the vicinity of groundwater well GWOBOD03. The water table was encountered at ~8 ft bgs. The core samples were extruded in the field from 4 ft acetate sleeves, and material from each boring was combined in a single large Zip-Loc style bag. The samples were then placed into a second bag and placed on ice. One core sample was left intact and brought to the CB&I Laboratory in Lawrenceville, NJ for examination of site lithology and for contaminant analysis (see next section). The other samples were placed at 4°C for use in microcosm and column studies.

Core Sample Analysis: The intact core collected from Dahlgren NSWC was sectioned in the laboratory, and the sediment lithology was determined by a senior geologist at CB&I. A core log was prepared from this information. In addition, samples were collected approximately every 0.5 ft from 5 ft to 20 ft bgs and analyzed for total organic carbon (TOC), explosives by EPA Method 8330, and perchlorate by EPA Method 314.0. A photograph of the extracted core undergoing sampling and geological evaluation is shown in **Figure 2.2.3-2** and results from the TOC and perchlorate analyses are provided in **Figures 2.2.3-3 & 2.2.3-4**, respectively. All 8330 explosives were below detection (<50 to 130 µg/L depending on analyte) in all depth-dependent core samples. Perchlorate, however, was detected in surface soils at low concentrations (~130 µg/kg), but the oxidant declined in concentration with depth, and was below detection in saturated aquifer materials deeper than 12 ft bgs. TOC was high at various depths, exceeding 3,000 mg/kg at 8 and 12.5 ft bgs. Organic material was observed by eye (root matter, black organic mat) in the cores at various depths throughout the core, accounting for the high TOC. It is possible that the TOC may serve as a natural electron donor to support biodegradation of explosives at this site.

Figure 2.2.3-1. Collection of site aquifer solids (top panel) and groundwater (bottom panel) from Dahlgren NSWC.

Figure 2.2.3-2. Sample collection from intact Geoprobe core taken form Dahlgren NSWC.

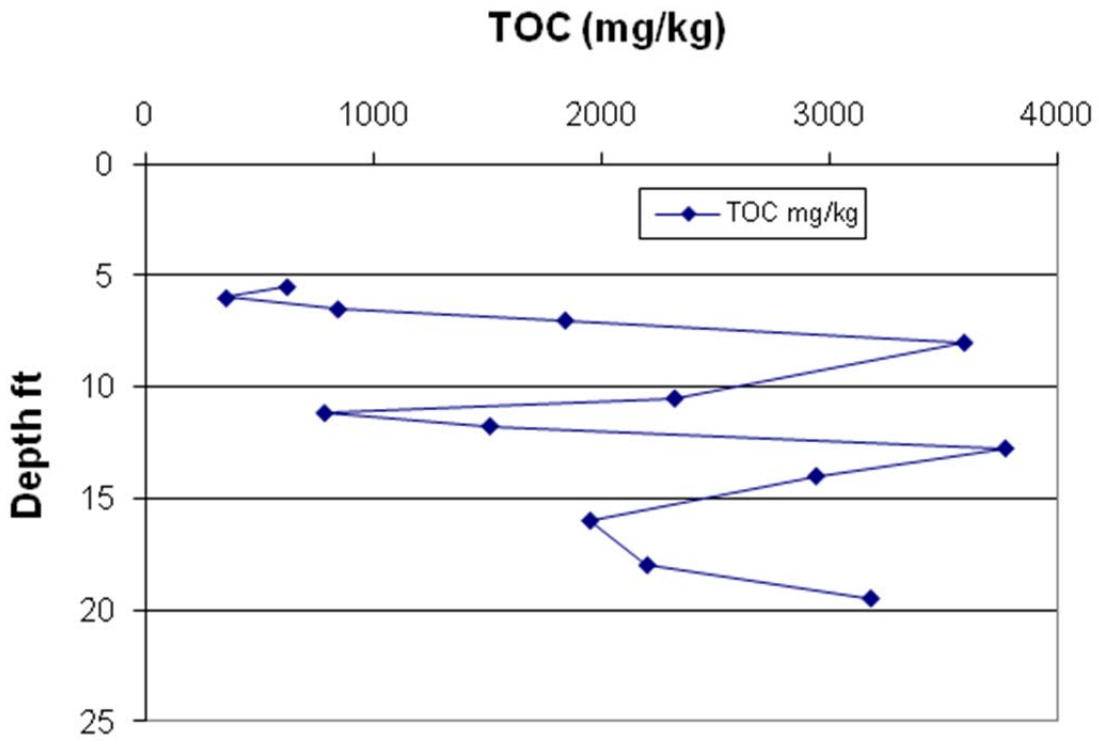

Figure 2.2.3-3. Depth-dependent TOC concentrations in core material from Dahlgren NSWC.

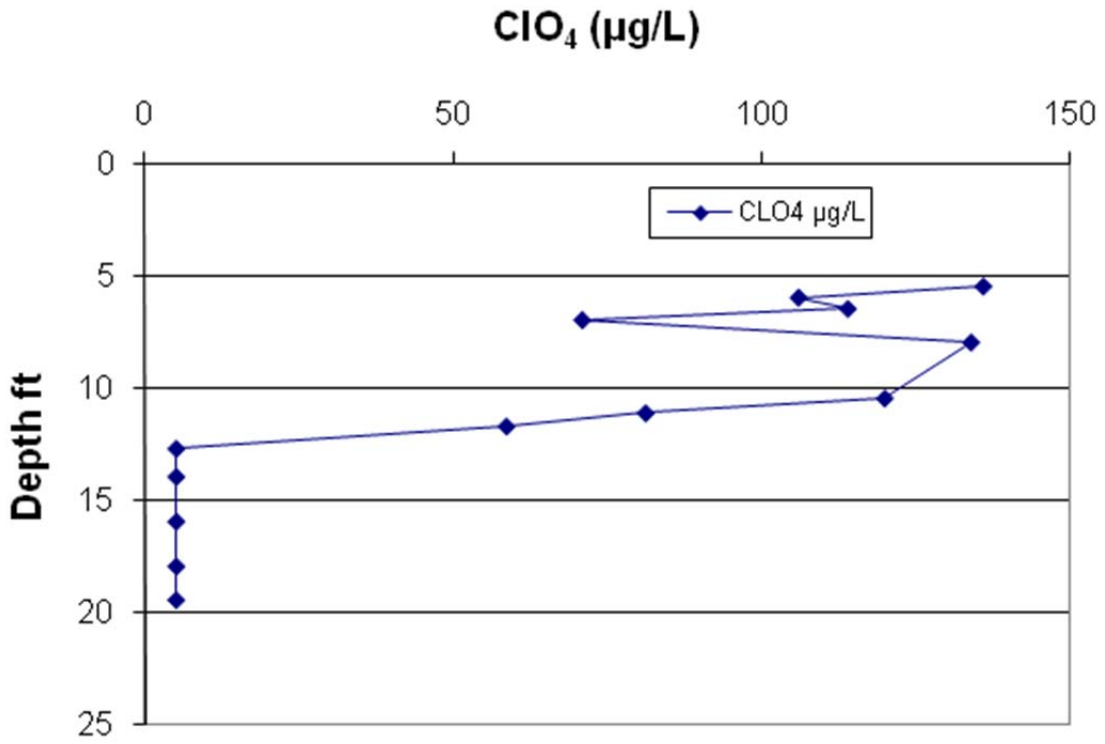

Figure 2.2.3-4. Depth-dependent perchlorate concentrations in core material from Dahlgren NSWC.

Mesocosm Design and Set-up: Large mesocosms were prepared using Dahlgren site groundwater and saturated sediments to study the effects of different electron acceptor conditions on RDX degradation and on the characteristics of microbial communities conducting RDX degradation via SIP. The aquifer solids collected during the January, 2009 sampling event were placed on ice, driven to the laboratory in Lawrenceville, NJ, and thoroughly homogenized. Groundwater was pumped directly into bleached and sterilized 20 L soda kegs. Sediment (0.5 kg wet wt) and groundwater (8 L) were placed into five 10 L mini-kegs (also bleached and sterilized) (**Figure 2.2.3-5**), and the kegs were purged with nitrogen for 3 h to remove residual oxygen.

Figure 2.2.3-5. Mini-keg system being used to examine RDX degradation under selected electron acceptor conditions.

The groundwater plus sediment contained RDX at ~0.05 mg/L, perchlorate at ~0.6 mg/L, as well as 150 mg/L sulfate and 1 mg/L nitrate-N. All kegs were amended with sodium succinate and RDX to achieve initial concentrations of 40 mg/L and 0.150 mg/L, respectively. Each keg was then amended with a different electron acceptor in order to stimulate a variety of different organisms potentially capable of degrading RDX, and to discern the prevalent electron-accepting regimen whereby RDX is biodegraded in the Dahlgren samples. The kegs were amended with 1 mM of electron acceptor as shown in **Table 2.2.3-1**. Kegs were pressurized to 30 psi and incubated at 15°C, and were shaken day for two minutes each weekday for the first two weeks. Thereafter, shaking was reduced to the time when sampling was performed or when amendments were being added.

Table 2.2.3-1. Treatments used in Dahlgren mesocosm study to assess RDX biodegradation under different electron-accepting conditions.

Keg	Condition	Electron acceptor added
A	None	None
B	Nitrate reducing	KNO_3
C	Iron reducing	$FeCl_3$-$6H_2O$
D	Manganese reducing	MnO_2
E	Sulfate reducing	K_2SO_4

Samples were removed from the kegs periodically as follows: 2 mL was passed through a 0.45 µm glass microfiber (GMF) filter for RDX and breakdown products (EPA Method 8330); 25 mL was passed through a 0.22 µm nylon filter into a vial acidified with nitric acid for soluble iron (HACH kit, 0.5 mg/L detection limit); 5 mL was passed through a 0.22 µm nylon filter into a vial acidified with nitric acid for soluble manganese (HACH kit, 0.5 mg/L detection limit); 10-15 mL was passed through a 0.22 µm nylon filter into a sterile polypropylene tube for perchlorate (EPA Method 314, 0.01 mg/L detection limit), succinate (EPA Method 300m, 0.5 mg/L detection limit), nitrate (EPA Method 300, 0.5 mg/L detection limit), and sulfate (EPA Method 300, 0.5 mg/L detection limit). Samples were also collected to measure the dissolved oxygen concentration (ChemMet kits) and solution pH (laboratory pH meter).

When the succinate, electron acceptor, and/or RDX concentrations decreased significantly, additional quantities of each were added to the kegs in a small volume of sterile water. Repeated additions were performed to assure that each of the electron accepting conditions had been established.

2.2.3.2 Results: RDX Degradation in Dahlgren Mesocosms.

The results from this study are summarized as follows:

1. Robust RDX degradation coupled to Fe-reduction and Mn-reduction was established after about two months (**Figure 2.2.3-6**). Repeated additions of RDX were rapidly degraded, coupled with degradation of succinate and production of soluble Fe and Mn. These enrichments were subsequently used to perform RDX SIP (see **Section 2.3.4** below).

2. RDX degradation in the mesocosms that were amended with sulfate and in the unamended control was observed (**Figure 2.2.3-7**). Additional spikes of sulfate were added to the sulfate reducing enrichment to promote establishment of the sulfate reducing community before the RDX-SIP enrichments were initiated. The control mesocosm was monitored for methane production to confirm the establishment of a methanogenic community before collecting

samples for RDX-SIP analysis. Dissolved methane levels of around 0.5 mg/L were observed near the end of the experiment.

3. RDX degradation was negligible under nitrate-reducing conditions (**Figure 2.2.3-8**), which is in agreement with previous research indicating that nitrate generally inhibits RDX degradation (23). Succinate and nitrate rapidly degraded when added into the kegs, indicating good nitrate reducing conditions had been established. However, since RDX did not degrade, these enrichments were not included in the RDX-SIP enrichment experiments.

2.2.3.3 Conclusions: RDX Degradation in Dahlgren Mesocosms.

The significant accumulation of nitroso-metabolites under both iron- and manganese- reducing conditions indicates that nitro group reduction, rather than denitration, was the primary route of RDX biodegradation under these conditions. It is possible that abiotic RDX degradation by the reduced Fe and Mn mineral phases may also have occurred, but this process was not specifically examined in this study.

A very different RDX degradation pattern - without significant accumulation of nitroso-metabolites - was observed in microcosms prepared under sulfate-reducing conditions. After an acclimation period of 5 days, RDX biodegradation was observed, and the nitramine was below detection after 20 days. Only very low concentrations of nitroso-metabolites were detected as RDX degraded (<0.5 mg/L of MNX, DNX, or TNX), accounting for less than 10% of the total RDX added.

Similarly, rapid RDX degradation was observed under methanogenic conditions, with approximately 90% of added RDX being degraded after only 12 days. Nitroso-metabolites, predominantly MNX, were detected as the RDX was degrading, accounting for a maximum of 40% of added RDX on a molar basis. However, as observed under sulfate-reducing conditions, these metabolites were quickly degraded, and were below detection after 20 days.

To summarize, slow RDX degradation with high accumulation (and slow degradation) of nitroso-metabolites was observed with Mn(IV) and Fe(III) as the predominant electron acceptors. Conversely, much more rapid RDX degradation was documented in microcosms under both sulfate-reducing and methanogenic conditions, with low and transient accumulation of nitroso metabolites (10% and 40% of the added RDX at a maximum, respectively), and with MNX as the primary metabolite. The data indicate that sequential nitro group reduction was the major RDX degradation pathway under Mn(IV)- and Fe(III)-reducing conditions, whereas, a pathway involving denitration or ring cleavage likely dominated under sulfate-reducing and methanogenic conditions.

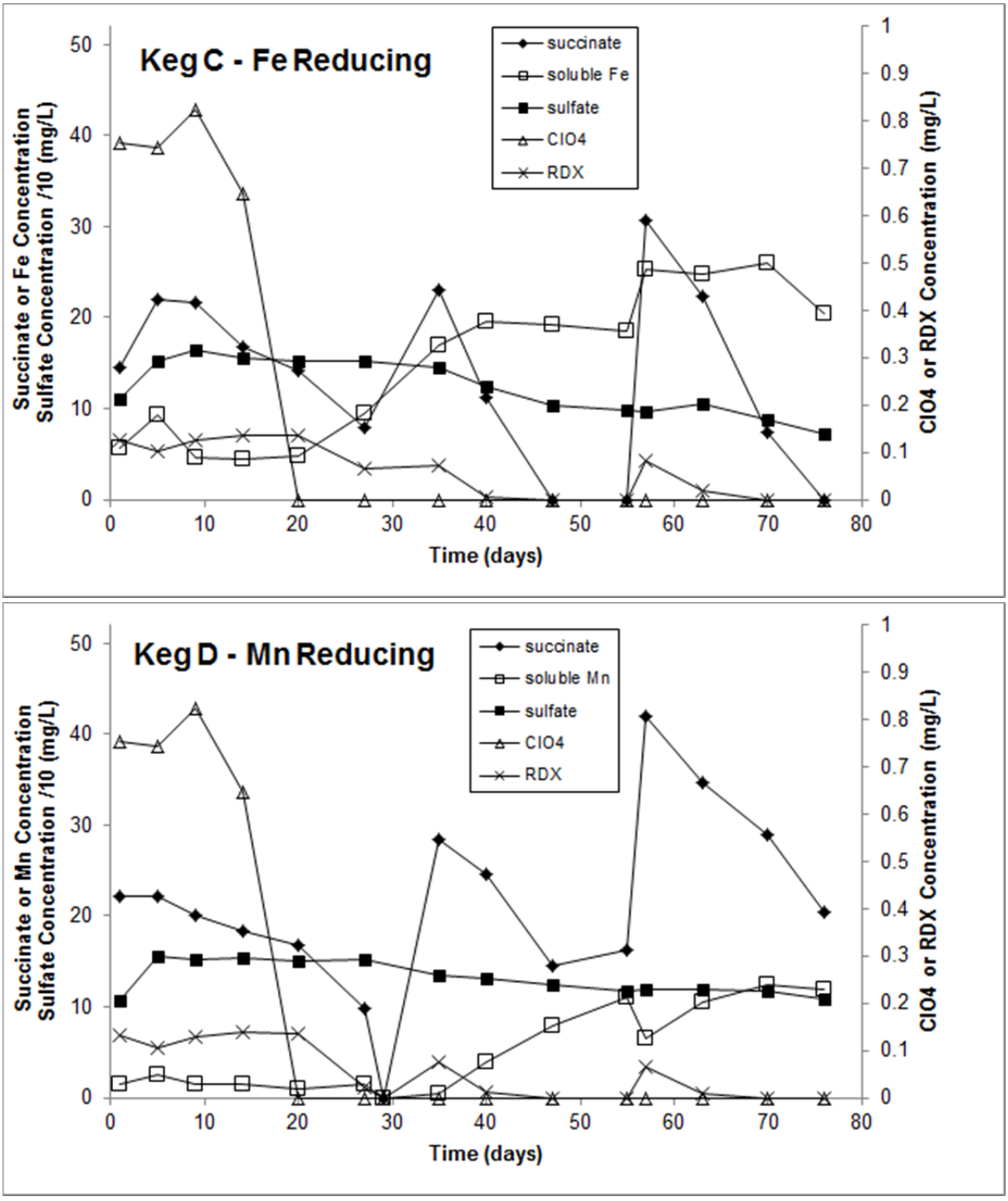

Figure 2.2.3-6. Concentrations of RDX, perchlorate, succinate, soluble metals, and sulfate over time under Fe- and Mn-reducing conditions during the Dahlgren mesocosm studies.

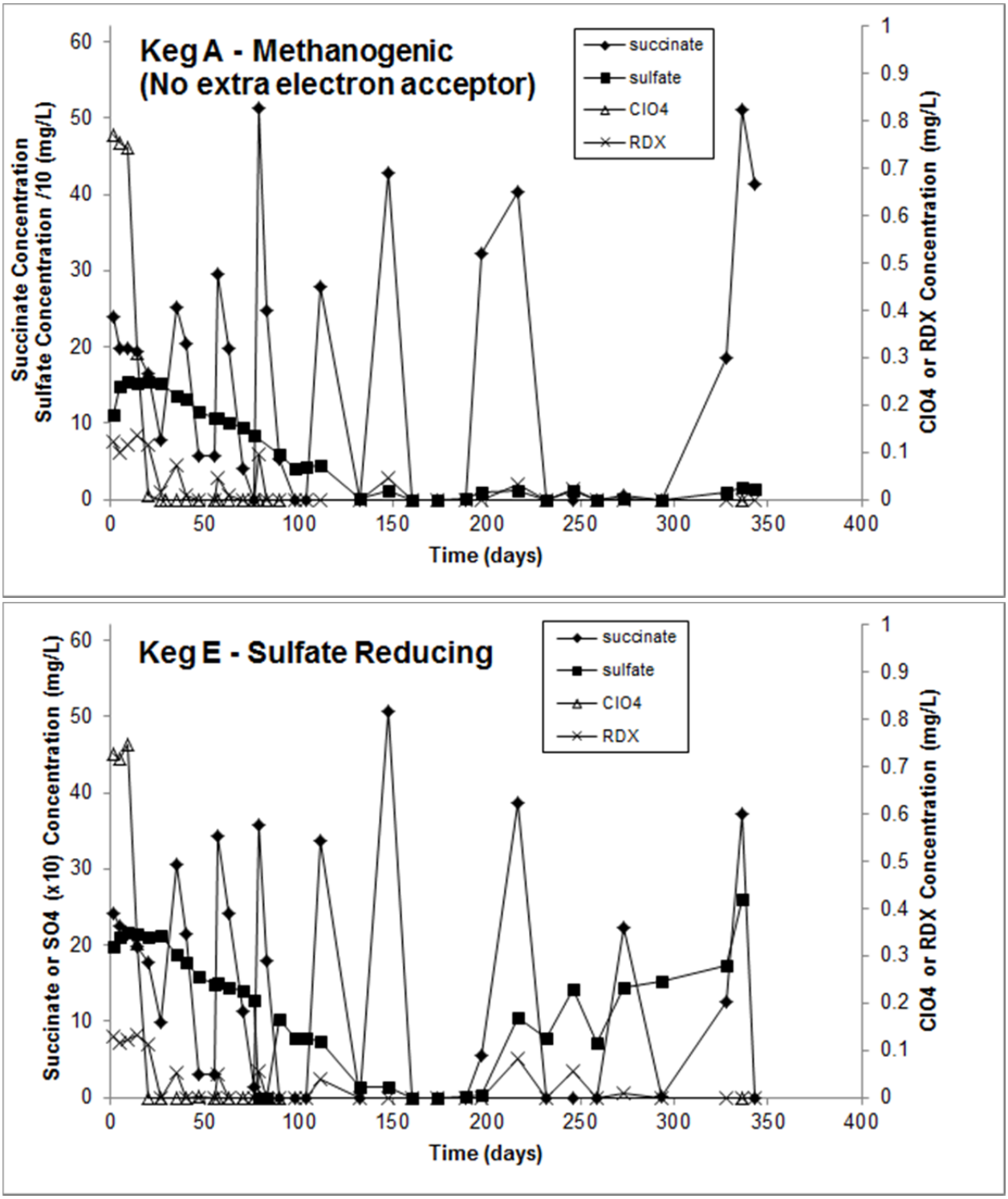

Figure 2.2.3-7. Concentrations of RDX, perchlorate, succinate, and sulfate over time in the control (no added electron donor) and under sulfate reducing conditions during the Dahlgren mesocosm studies.

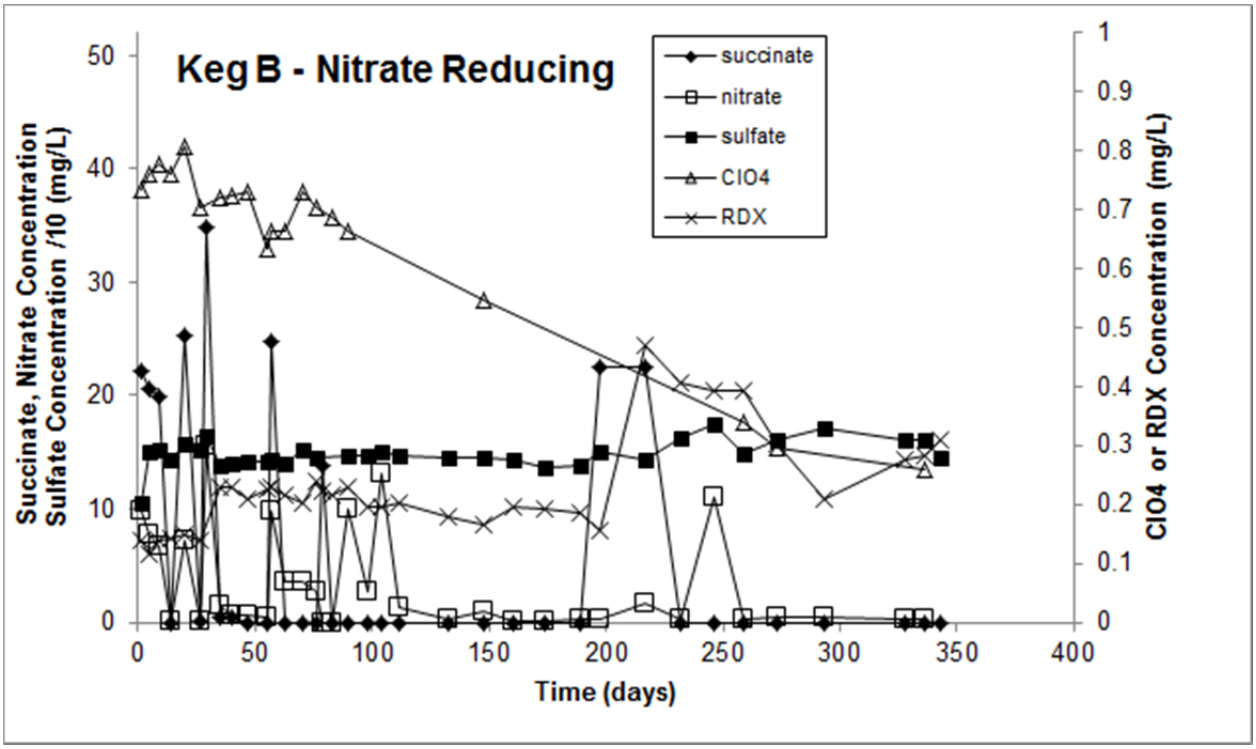

Figure 2.2.3-8. Concentrations of RDX, perchlorate, succinate, nitrate, and sulfate over time under nitrate reducing conditions in Dahlgren mesocosm studies.

2.3 Task 3 – Stable Isotope Probing (SIP) for Identification of RDX-Degrading Microorganisms

2.3.1 Objective

During this task, SIP using ^{15}N- and ^{13}C-labeled RDX was optimized for application to natural microbial communities in groundwater. These communities are characterized by low biomass and are assumed to harbor a low abundance of RDX-degrading organisms. The DNA in site and enrichment samples was isolated and subjected to density gradient centrifugation, and the resulting enriched nucleic acids were analyzed using multiple molecular techniques. Terminal restriction fragment length polymorphism (t-RFLP) analysis was used to visualize shifts in the microbial community during RDX degradation (Q-FAST; **Figure 2.3.1-1**).

2.3.2 Introduction

Direct enrichment techniques are useful for isolating and studying individual bacterial strains and their degradation pathways, but these enrichments often do not reflect the cooperative degradative processes that occur in natural environments. Moreover, enrichments performed at relatively high contaminant concentrations may not lead to isolation of the organisms that are responsible for degradation at environmentally relevant concentrations.

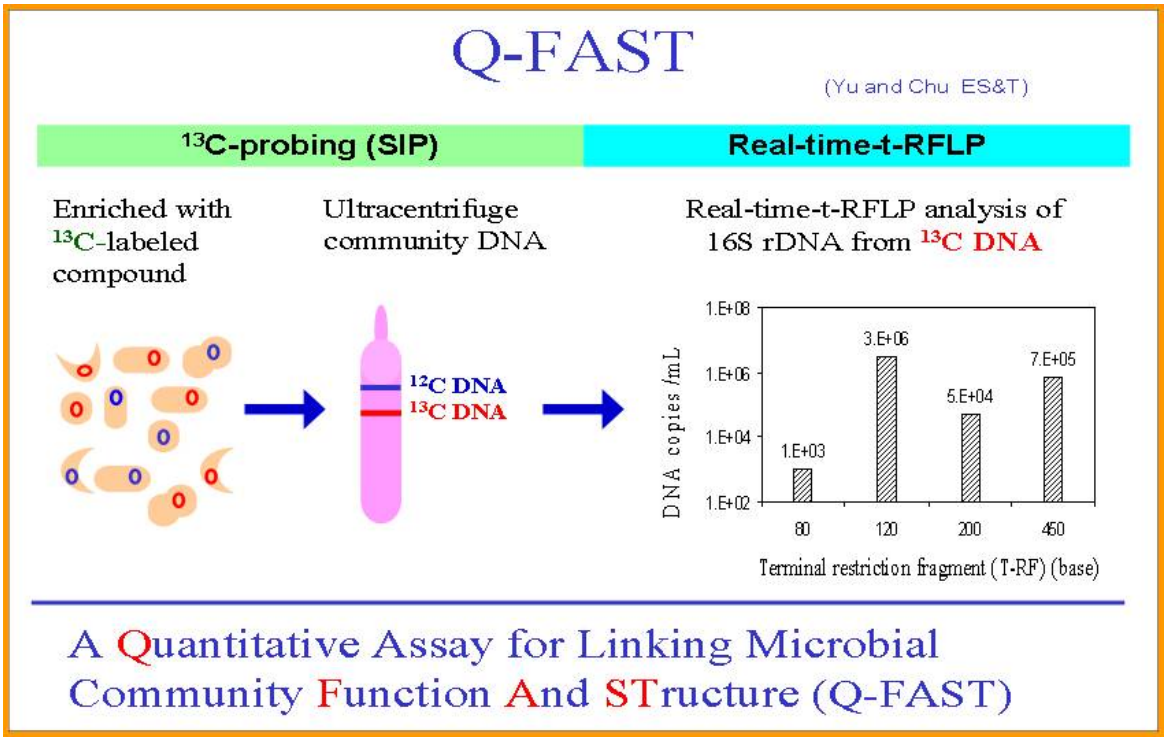

Figure 2.3.1-1. Schematic of Q-FAST technique for microbial community analysis.

A new technique called stable isotope probing (SIP) has the potential to distinguish key degradative microorganisms under natural conditions based upon their incorporation of carbon and/or nitrogen from contaminants into DNA. SIP has been applied to study the metabolism of simple and complex carbon compounds in both natural and engineered environments (17, 28, 41, 42, 73, 74). The use and tracking of ^{15}N has not yet been fully realized. However, SIP with ^{15}N may be an excellent technique to study the natural biodegradation of RDX, since a significant mechanism for the degradation of this nitramine reflects its use as a microbial nitrogen source.

2.3.3 Preparation of [^{13}C] and [^{15}N]-labeled RDX

Custom synthesis of [^{13}C] and [^{15}N]-labeled RDX was completed by Dr. Steve Fallis at the Naval Air Warfare Center Weapons Division at China Lake, CA. The starting materials for preparation of the RDX isotopomers were [^{13}C]paraformaldehyde, [^{15}N]ammonium hydroxide, and [^{15}N]sodium nitrate. From these materials, and using synthesis protocols developed at China Lake, three stable isotope-labeled RDX isotopomers were produced as depicted in **Figure 2.3.3-1**. Ring labeled ^{15}N-RDX and a small amount of ring labeled ^{13}C-RDX were already available to our project from a previous SERDP project, ands were not synthesized.

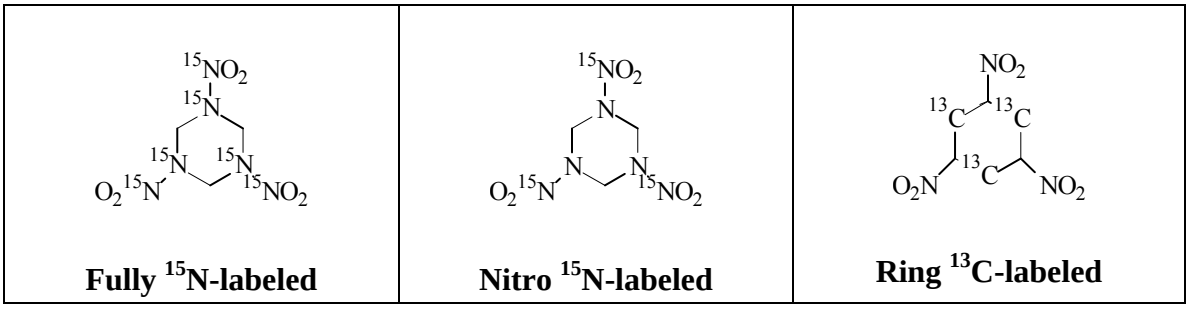

Figure 2.3.3-1. The three specific ^{13}C- and ^{15}N-RDX compounds synthesized by the Naval Air Warfare Center Weapons Division at China Lake.

2.3.4 Application of ^{13}C- and ^{15}N-RDX SIP to Picatinny Arsenal Groundwater

A subset of the results summarized in this section have been previously published:

Cho, K.-C., D. G. Lee, H. K. Roh, M. E. Fuller, P. B. Hatzinger, and K.-H. Chu. 2013. Application of ^{13}C-stable isotope probing to identify RDX-degrading microorganisms in groundwater. Environmental Pollution 178: 350-360.

2.3.4.1 Picatinny Arsenal SIP - Methods

As previously noted, one of the sites selected for further evaluation of microbial communities was Picatinny Arsenal, NJ. Groundwater was collected from Area 157 at the Picatinny Arsenal where an *in situ* biostimulation project was being conducted (ESTCP Project ER-200425; http://www.serdp.org/Program-Areas/Environmental-Restoration/Contaminated-Groundwater/ER-200425). Multiple injections of cheese whey had been performed in the preceding year, resulting in active and complete degradation of RDX and other explosive compounds in the wells within the zone of influence of the injections (**Figure 2.3.4-1**). Transient production of RDX intermediates, MNX, DNX, and TNX was also observed (**Figure 2.3.4-2**).

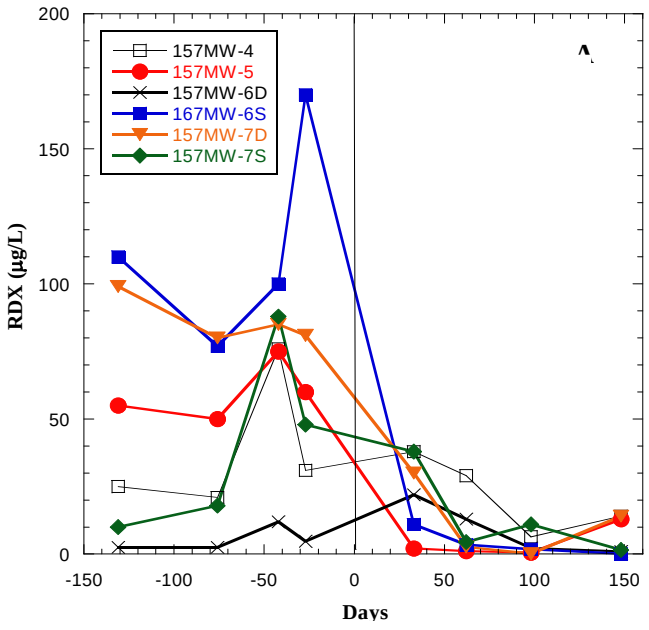

Figure 2.3.4-1. Concentrations of RDX in Picatinny treatment area monitoring wells.

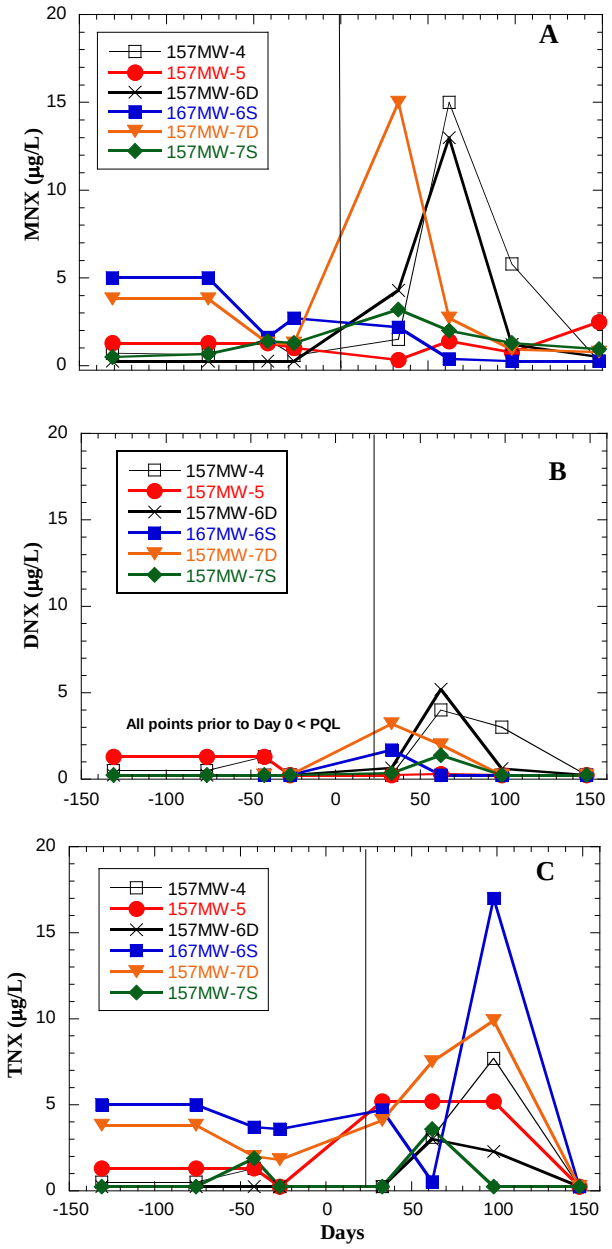

Figure 2.3.4-2 Concentrations of RDX degradation products MNX (A), DNX (B) and TNX (C) in Picatinny treatment area monitoring wells.

SIP enrichment setup: Groundwater was pumped directly from wells 157MW-5 and 157MW-7D into sterile, nitrogen purged soda kegs (total volume of 19 L), transported to the laboratory on ice, and stored at 4°C until use. The groundwater from the soda kegs was transferred aseptically into sterile 2 L Pyrex glass media bottles (1.6 L per bottle) which had been heated at 550°C overnight to remove any trace DNA (and carbon and nitrogen) and purged with sterile nitrogen

gas for 5 min. Bottle caps were irradiated for 5 minutes in a UV crosslinker to degrade any trace nucleic acids, then the caps were sterilized by autoclaving. Two bottles of each groundwater were amended with one of 5 different RDX types: unlabeled, $^{13}C_3$-RDX (ring), $^{15}N_3$-RDX (ring), $^{15}N_3$-RDX (nitro), or $^{15}N_6$-RDX (full). Three of these compounds were synthesized for the project by chemists at China Lake (see **Section 2.3.3**). Cheese whey powder was added to achieve a final concentration of 100 mg/L of TOC in half of the bottles. Bottles were shaken vigorously approximately every other day, and incubated statically at 15°C.

Bottles were sampled in a Coy anaerobic chamber with a pure nitrogen gas headspace (hydrogen-free). Samples (1 mL) were removed for RDX and metabolite analysis. The dissolved oxygen concentration in a random subset of the bottles in each set was also measured at each sampling point. RDX and metabolites was measured using HPLC (modified EPA Method 8330).

Once RDX degradation was complete, 1 L of the biomass in each bottle was collected by filtration and sent to the laboratory of Dr. Bella Chu at Texas A&M for SIP to identify key microorganisms utilizing C and N in RDX based on DNA labeling. Samples were also collected and sent to Dr. Hawari's group at BRI for metabolite analysis combined with mass spectrometry (MS) to determine product formation from differently-labeled RDX materials to be characterized and quantified. Thus, metabolite and microbial community analysis were conducted with the same samples.

Bacterial cultures: Two non-RDX-utilizers (*Escherichia coli* and *Pseudomonas fluorescens*) and one RDX-utilizer (*Rhodococcus sp*. DN22, referred as DN22 hereafter) were used to validate the ^{15}N-SIP approach. *E. coli* (~51% G+C content) and *Ps. fluorescens* (~62% G+C content) were used as reference bacteria in our previous studies. DN22 (~67% G+C content) is known to use RDX as a sole nitrogen source (N-source) (14, 15) and was kindly provided by Dr. Coleman, School of Molecular and Microbial Biosciences, University of Sydney. *E. coli* and *Ps. fluorescens* were supplied with glucose as a sole carbon source (C-source) and unlabeled NH_4^+ or $^{15}NO_3^-$ as a sole N-source. For DN22, succinate was supplied as a sole C-source and one of four N-sources (unlabeled NH_4^+, $^{15}NH_4^+$, RDX, and ring-^{15}N-labeled RDX) were supplied. To obtain ^{13}C-DNA as controls for ^{13}C-SIP experiments, *E. coli* and *Ps. fluorescens* were also grown with ^{13}C-labed glucose (400 mg/L) as a sole C-source and ammonium (NH_4^+) as a sole N-source). All the strains were grown at 30ºC overnight (optical density of cell suspension at A_{600} was about 1.0) before being harvested for DNA extraction. Extracted DNA was later used in SIP experiments.

DNA extraction: Genomic DNA of each bacterium was extracted using FastDNA kit (Q-Biogene Bio 101, Carlsbad, CA) according to manufacturer's instructions. For microcosms and groundwater samples, the FastDNA SPIN kit for soil (MP Biomedical LLC, Solon, OH) was used as described previously (74) with a modified cell lysing process: the lysing matrix tube was

processed 2 x 30s in a FastPrep instrument. Concentrations of extracted DNA were measured by using a Hoefer DyNa Quant 200 fluorometer (Pharmacia Biotech, San Francisco, CA).

^{13}C-DNA and ^{12}C-DNA separation: The ^{13}C-DNA and ^{12}C-DNA fractions were separated by equilibrium centrifugation in CsCl-EtBr density gradients as described in our previous work (74) with modification. Briefly, DNA solution was prepared in 3.5-mL Beckman centrifuge tubes containing 200 µL of EtBr (10 mg/mL) and 1.1 g/mL CsCl solution in TE buffer. The tubes were centrifuged on a table-top Beckman TLX-120 Optima ultracentrifuge in a TLA 100.3 rotor at 70,000 rpm at 20°C for 24 h. The ^{13}C-DNA and ^{12}C-DNA bands in the tubes were visualized under long-wavelength (365 nm) UV light. The ^{13}C-DNA fraction was fractionated using a fraction recovery system (Beckman Coulter, CA) and a syringe pump (Model 7801001, Fisher Scientific, Fair Lawn, NJ).

For extracting DNA from the CsCl solution, an equal volume of water-saturated n-butanol was added. The centrifuge tube was briefly vortexed before centrifugation at 450 x g for 3 min, and the n-butanol layer (i.e. the upper layer which turned pink due to the presence of EtBr) in the tube was discarded. Extraction with n-butanol was repeated five times or until no pink color was observed. Then the volume of DNA solution was brought to 1 mL in HPLC water before two volumes of ice-cold ethanol and 100 µL of 3 M sodium acetate were added. The DNA in the tube was precipitated at 0°C overnight, pelleted at 20,000 x g for 15 min at 4°C, washed with 80% ethanol, and finally re-suspended in 40 µL of HPLC water for later use. Positive controls for ^{12}C-DNA and ^{13}C-DNA were extracted from *E. coli* and *P. fluorescens* utilizing ^{12}C-glucose and ^{13}C-glucose, respectively.

Protocol modification to enhance resolution of ^{15}N- and ^{14}N-DNA separation: While we had previously demonstrated successful separation of ^{13}C-DNA and ^{12}C-DNA fractions using equilibrium centrifugation in CsCl-EtBr density gradients (74), the distance between ^{14}N- and ^{15}N-DNA bands was only half of the distance between ^{12}C-and ^{13}C-DNA bands after ultracentrifugation. This is an inherent challenge of using ^{15}N-SIP techniques, mainly due to a smaller difference of buoyant densities between the ^{15}N- and ^{14}N- nucleic acids. A recent study showed that addition of bizbenzimide would alter DNA buoyant densities to increase the distance between ^{14}N- and ^{15}N-DNA bands (11). As environmental samples commonly yield low DNA contents, a more sensitive method to view DNA bands in the ultracentrifuge tube is desirable. Our current method uses EtBr to view DNA bands in the ultracentrifuge tubes under UV light. When the DNA content is less than 5 µg, the presence of the DNA bands were not visible. A recent study reported that SYBR Safe (Invitrogen, Carlsbad, CA) is more sensitive than EtBr for DNA visualization in a ^{13}C-SIP study (43). As EtBr is a carcinogen, in this phase of study we also explored the possibility of using SYBR Safe to replace the use of EtBr.

Quantitative fingerprinting of microbial community structure using real-time-t-RFLP analysis: Quantification of each ribotype in ^{13}C-DNA and ^{12}C-DNA fractions was obtained by using real-time-t-RFLP (73). Briefly, a region of 16S rDNA sequence (~352 bp long) was amplified with a fluorescence-labeled forward primer 16S1055f (5'-hexachlorofluorescein-ATGGCTGTCGTCAGCT-3'), a reverse primer 16S1392r (ACGGGCGGTGTGTAC-3'), and a *Taq*man probe 16S*Taq*1115f (5'-[6-carboxyfluorescein]-CAACGAGCGCAACCC-[6-carboxytetramethylrhodamine]-3'). The initial copies in samples were determined based on standard curves using plasmid #931 that carries a partial 16S rRNA gene for *Nitrospira* (GenBank accession number AF420301) (18, 33). The PCR products were excised from a 1.5% agarose gel in 1X TAE buffer, recovered and purified using MicroSpin^{TM} columns (Amersham Biosciences, Piscataway, NJ), precipitated with ethanol once, and then desalted with 80% ethanol twice. The purified PCR products were then digested with restriction enzyme *Msp*I, precipitated with ethanol, and re-suspended in HPLC water. The lengths of T-RFs of digested PCR products were automatically determined on an ABI prism 310 Genetic Analyzer (Applied Biosystems Instruments, Foster City, CA) by comparing internal standards (Genescan ROX 500 size standards) using the GeneScan software 3.1 version.

PCR cloning and sequencing for RDX-degradative genes: Selected samples underwent additional probing for the RDX degrading gene *xplA*, which has been detected in a range of *Rhodococcus* strains and related genera (eg., Coleman et al., 2002). Both ^{12}C-DNA and ^{13}C-DNA fractions of microcosm samples were used as templates for PCR amplification of 16S rRNA and *xpl*A genes. DNA extracted from the groundwater was used for 16S rRNA gene sequencing only. All PCR reactions were performed in a total volume of 25 µL, with *Taq* PCR Master Mix (QIAGEN Inc., Valencia, CA), 2 to 50 ng of DNA templates, and 400 nM of primers. For 16S rRNA sequences, bacterial universal primers (8f (5'-AGAGTTTGATCMTG GCTCA G-3') and 1407r (5'-ACGGGCGGTGTGTACA-3')) and PCR thermal cycle were used as described by Yu and Chu (2005), except that less number of PCR cycle (35 cycles) was used. Forward (5'-GGTGGGGATGGAGGACTTC-3') and reverse primers (5'-CATGATGGGCAGTTTCGC-3') were newly designed for the *xpl*A gene. The *xpl*A gene primers were designed by alignment of the *xpl*A gene sequences from 14 *Rhodococcus* species in GenBank (Accession number DQ487126-DQ487137, AF449421, DQ277709). The PCR thermal cycle for *xpl*A was 95°C for 15 min, followed by 50 cycles of 95°C for 30 s, 57°C for 45 s, and 72°C for 30s, followed by a final elongation step of 72°C for 10 min. A series of diluted DNA concentrations were used as templates to examine any inhibition in PCR reactions. The fresh PCR product was cloned into the vector pCR4-TOPO (TA cloning; Invitrogen, Carlsbad, CA) as per manufacturer's instructions. Clones with inserts were verified by PCR with M13 primers and *xpl*A gene primers. The amplified fragments were cleaned using a QIA quick PCR purification kit (Qiagen Inc., Valencia, CA), followed by digestion with enzymes *Hae*III and *Hha*I (Promega Corp., Madison, WI). A total of 70 clones for the 16S rRNA gene and 60 clones for the *xpl*A gene were screened by analyzing the patterns of restriction fragment length polymorphism (RFLP) on 4% Metaphor agarose gels (Lonza, Rockland, ME). Clones with

unique RFLP patterns were selected for sequencing as described by Yu and Chu (2005). M13 primers and *xpl*A gene primers on the pCR4-TOPO plasmid were used for the sequencing of 16S rRNA genes and *xpl*A genes, respectively.

Phylogenetic analysis: A web-based program was used to assemble raw DNA sequence data from both strands into full-length sequences (www.vivo.colostate.edu/molkit /manip/index.htmL). The assembled sequences were checked for chimeras using the on-line computer tool, CHIMERA_CHECK version 2.7 of the Ribosomal Database-II Project (rdp8.cme.msu.edu/docs/chimera_doc.htmL) and carefully inspected manually. Three out of 43 sequences for 16S rRNA gene were found as suspected chimeras and removed from phylogenetic analysis. Related sequences were identified by comparing the partial 16S rRNA gene sequences or cytochrome P450 gene sequences to those in GenBank by using BLAST. The closest relatives identified from searches were aligned and analyzed with the bootstrap neighbor-joining method in the CLUSTALX2 program (68). The phylogenetic tree was created using Treeview 32 software. The sequences of 16S rRNA and the *xpl*A gene have been deposited in GenBank as accession numbers EU907865 to EU907904 for 16S rRNA genes and EU919740 to EU919745 for *xpl*A genes.

2.3.4.2 Picatinny Arsenal SIP - RDX Degradation Results

2.3.4.2.1 ^{13}C-RDX SIP

Complete degradation of RDX in the unamended bottles required a longer incubation than in the cheese whey amended bottles for microcosms established with 157MW-5 groundwater (**Figure 2.3.4-3**). In contrast, RDX degraded in unamended and cheese whey amended bottles in roughly the same time for microcosms established with 157MW-7D groundwater (**Figure 2.3.4-4**). Unlabeled and ^{13}C-RDX degraded roughly the same in all bottles, except for the unamended microcosms established with 157MW-5, in which the time for complete degradation of the intial ^{13}C-RDX required almost 300 days, compared to less than 50 days to complete degradation of both the initial and second spike of unlabeled RDX (**Figure 2.3.4-3**). The reason for this difference is not known, but it also reflected in a difference in the apparent metabolite formation compared to the other bottles as well (see below).

Dissolved oxygen was low in all of the bottles, and several of the cheese whey-amended bottles changed color from orange (assumed to be iron oxides) to grey-black (assume to be iron sulfide) (**Figure 2.3.4-5**), likely representing a shift to iron-reducing and then sulfate reducing conditions. The faster degradation in the 157MW-7D microcosms might have been the result of higher residual cheese whey, or more active biomass at time of collection, compared to the 157MW-5 microcosms. In both sets, the second spike of RDX was degraded very quickly.

The RDX metabolites MNX, DNX, and TNX were detected in small amounts in most of the microcosms (e.g., <0.5 mg/L), with MNX usually present at higher levels than DNX or TNX.

These compunds also appeared to disappear by the end of the incubation. The exception to these trends were the unamended microcosms established with 157MW-5 groundwater, in which MNX concentrations up to 3 mg/L and DNX up to around 1 mg/L were observed and persisted to the end of the incubation. These results taken together, however, do indicate that the RDX degradation did not significantly stall at the nitroso containing metabolites.

2.3.4.2.2 ^{15}N-RDX SIP

Complete degradation of RDX in the unamended bottles required a longer incubation than in the cheese whey amended bottles for microcosms established with 157MW-5 groundwater (**Figure 2.3.4-6**), the same as was observed for ^{13}C-RDX. In contrast, RDX degraded in unamended and cheese whey amended bottles in roughly the same time for microcosms established with 157MW-7D groundwater (**Figure 2.3.4-7**). No distinctions in the degradation of the three ^{15}N-labelled RDX compounds was observed in a given treatment.

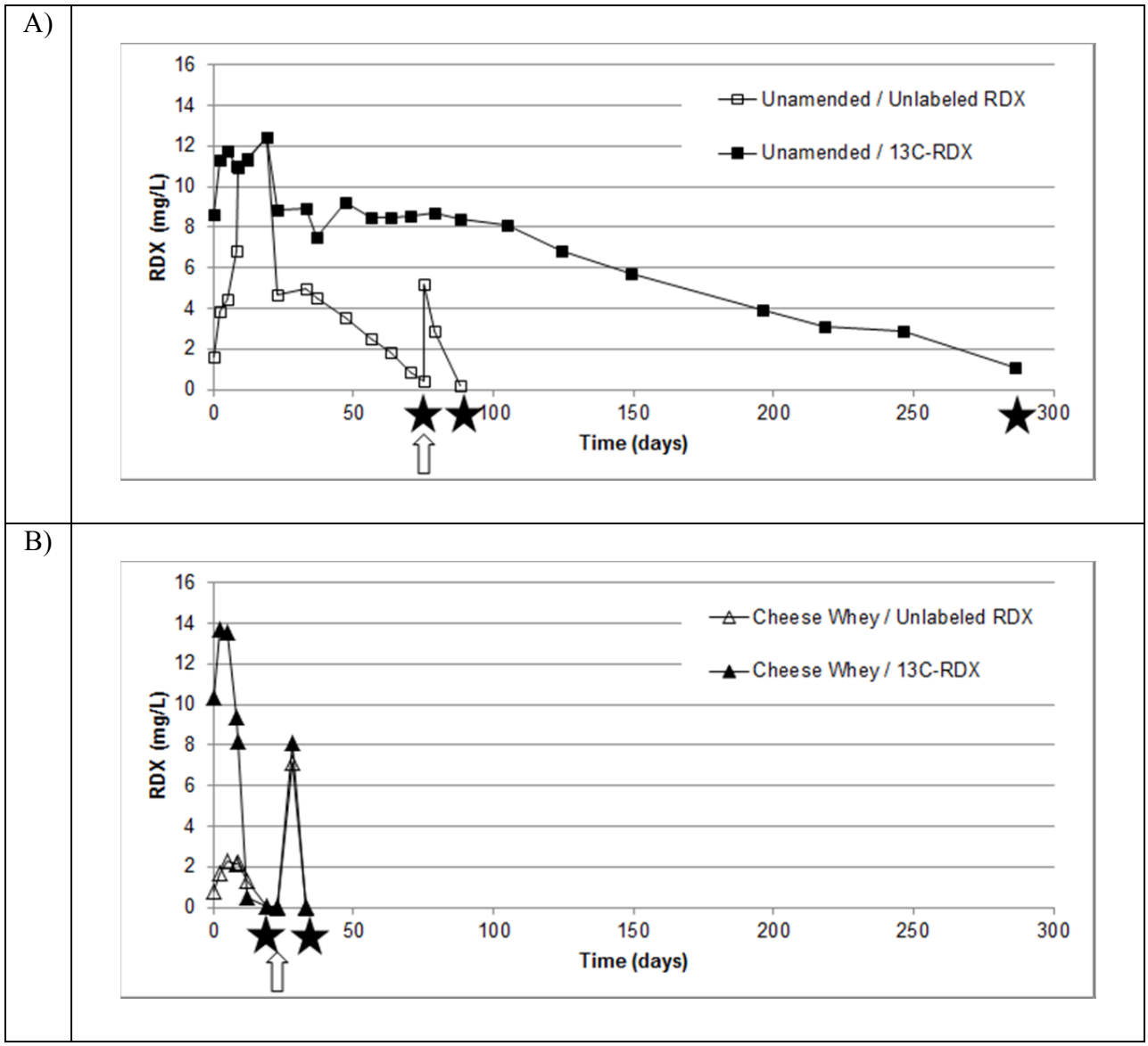

Arrows indicates when the second RDX spike was added. Stars indicate when biomass was collected for molecular analysis.

Figure 2.3.4-3. RDX concentrations in ^{13}C-SIP enrichments from Picatinny well 157MW-5 in (A) unamended bottles and (B) cheese whey amended bottles.

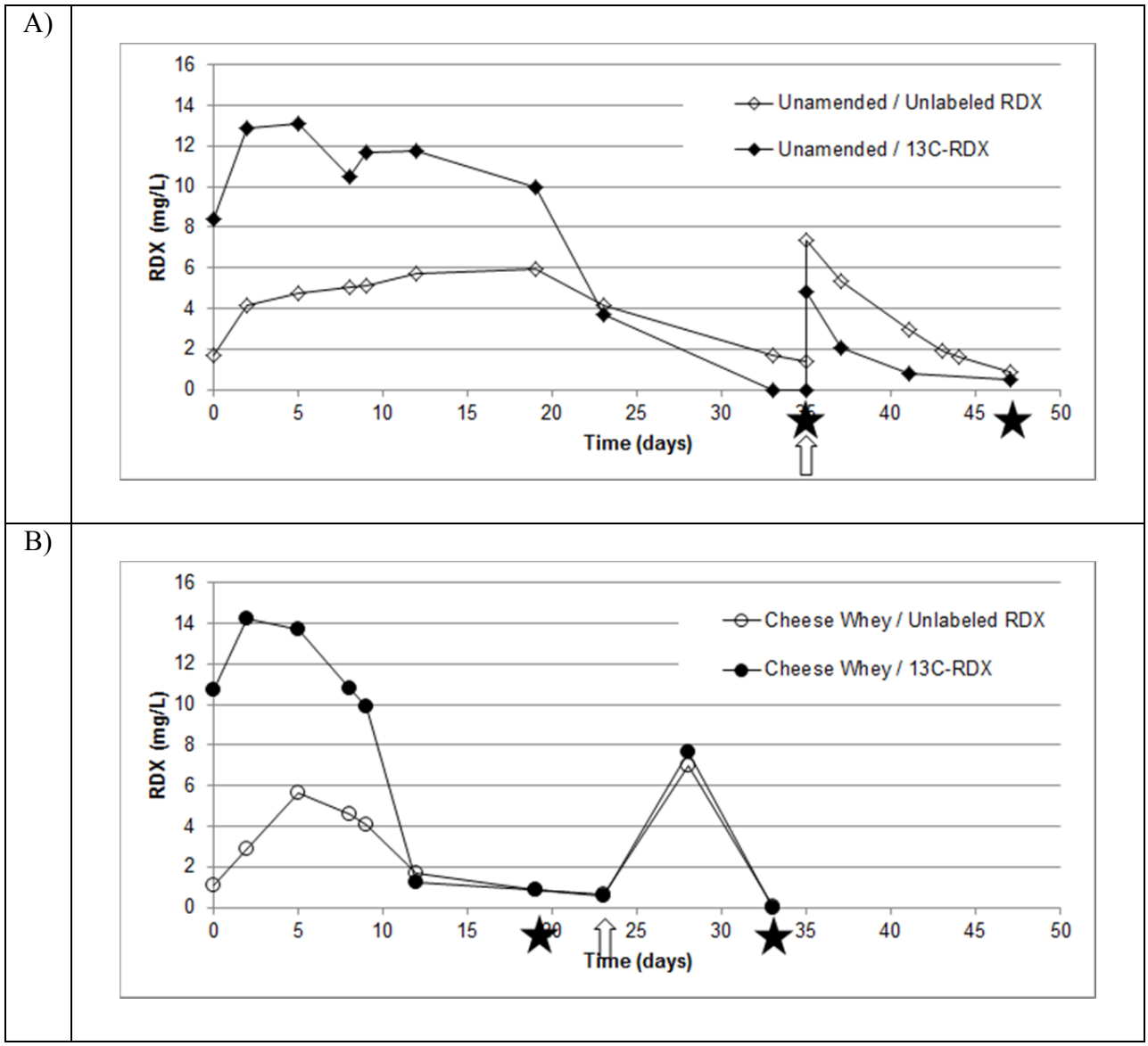

Arrows indicates when the second RDX spike was added. Stars indicate when biomass was collected for molecular analysis.

Figure 2.3.4-4. RDX concentrations in ^{13}C-SIP enrichments from Picatinny well 157MW-7D in (A) unamended bottles and (B) cheese whey amended bottles.

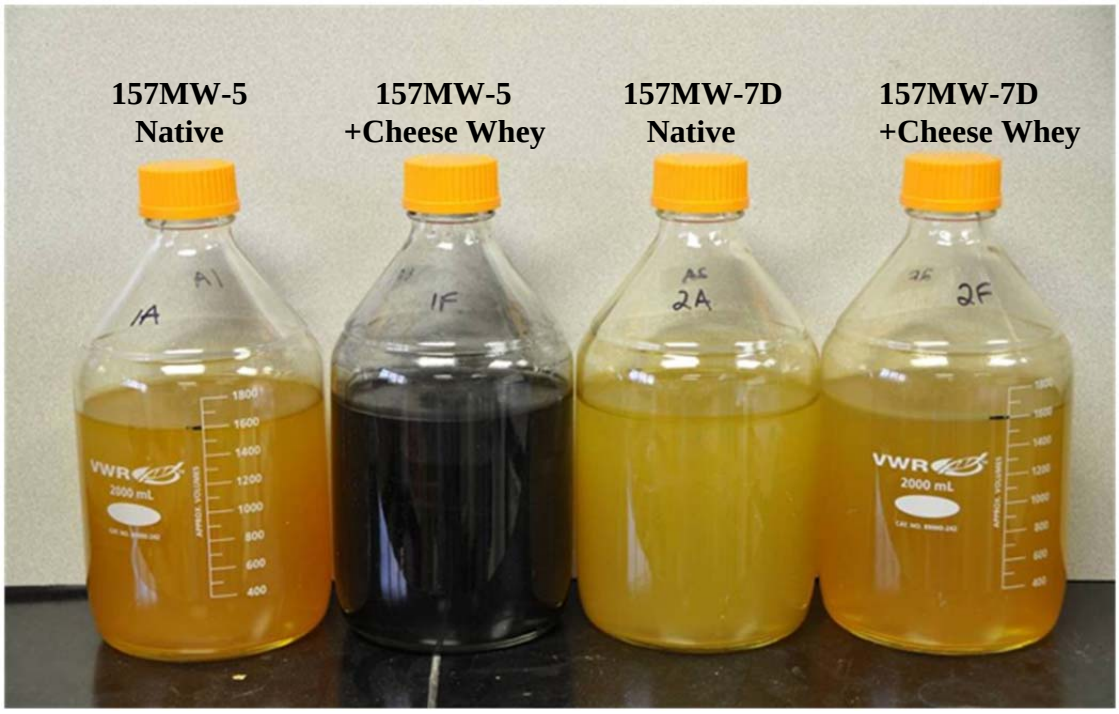

Figure 2.3.4-5. Appearance of representative SIP microcosm bottles.

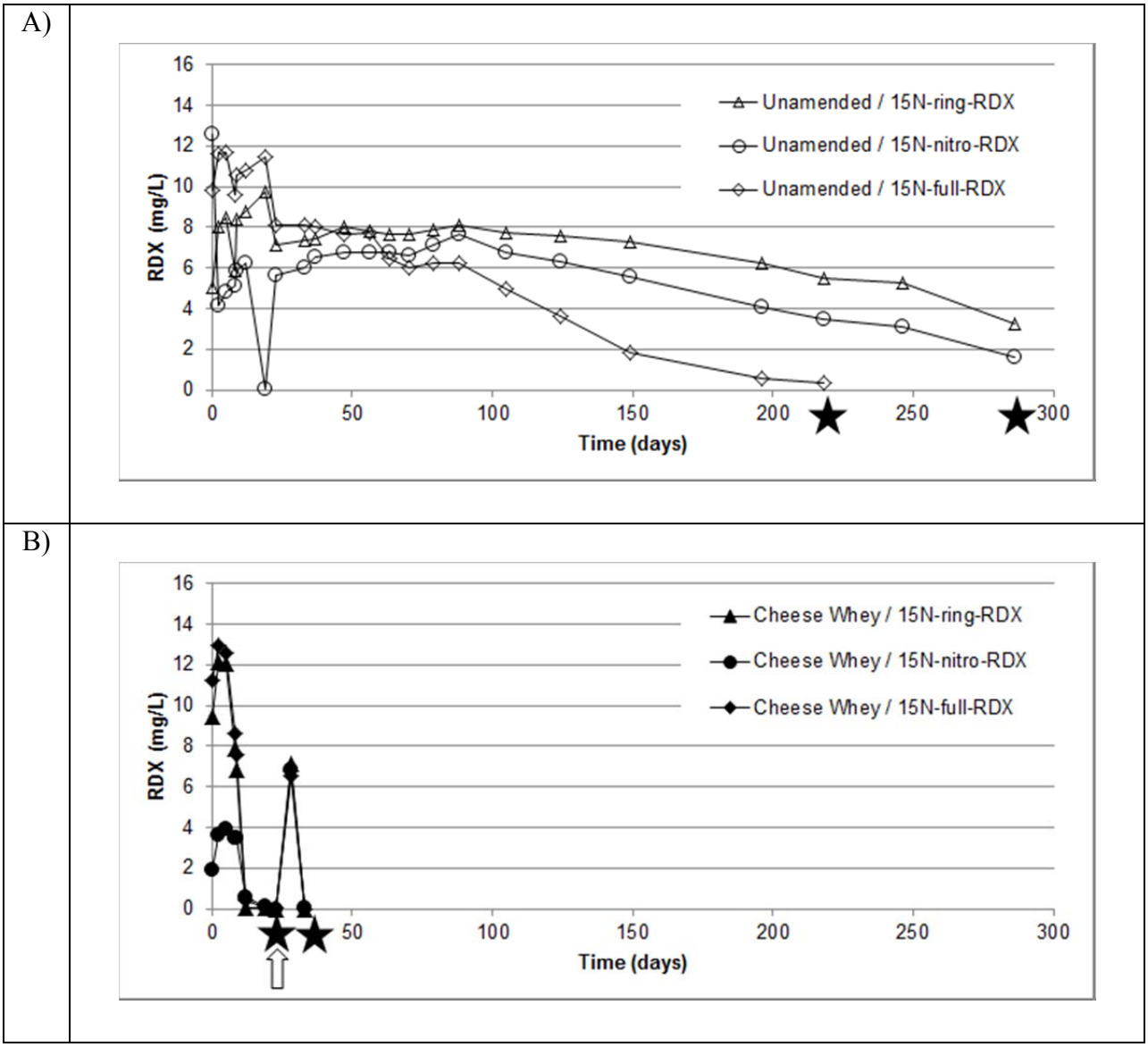

Arrows indicates when the second RDX spike was added. Stars indicate when biomass was collected for molecular analysis.

Figure 2.3.4-6. RDX concentrations in ^{15}N-SIP enrichments from Picatinny well 157MW-5 in (A) unamended bottles and (B) cheese whey amended bottles.

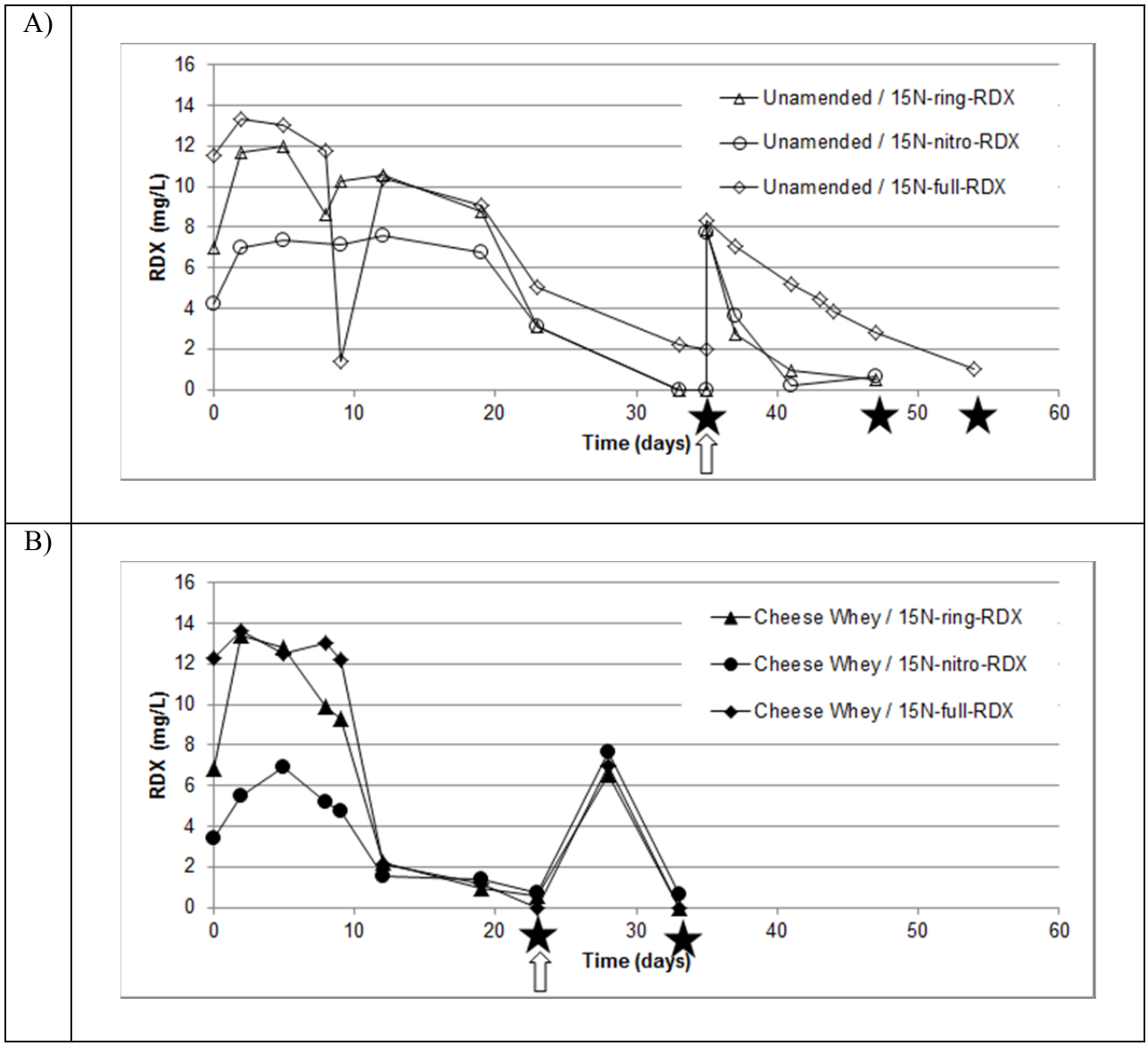

Arrows indicates when the second RDX spike was added. Stars indicate when biomass was collected for molecular analysis.

Figure 2.3.4-7. RDX concentrations in ^{15}N-SIP enrichments from Picatinny well 157MW-7D in (A) unamended bottles and (B) cheese whey amended bottles.

2.3.4.3 Picatinny Arsenal SIP - Molecular Analysis Results & Discussion

2.3.4.3.1 ^{13}C-RDX SIP

Figure 2.3.4-8 presents an example of separation of light (^{12}C) and heavy (^{13}C) DNA in CsCl-EtBr density gradients. Positive controls of light and heavy DNA from *E.coli* are also shown.

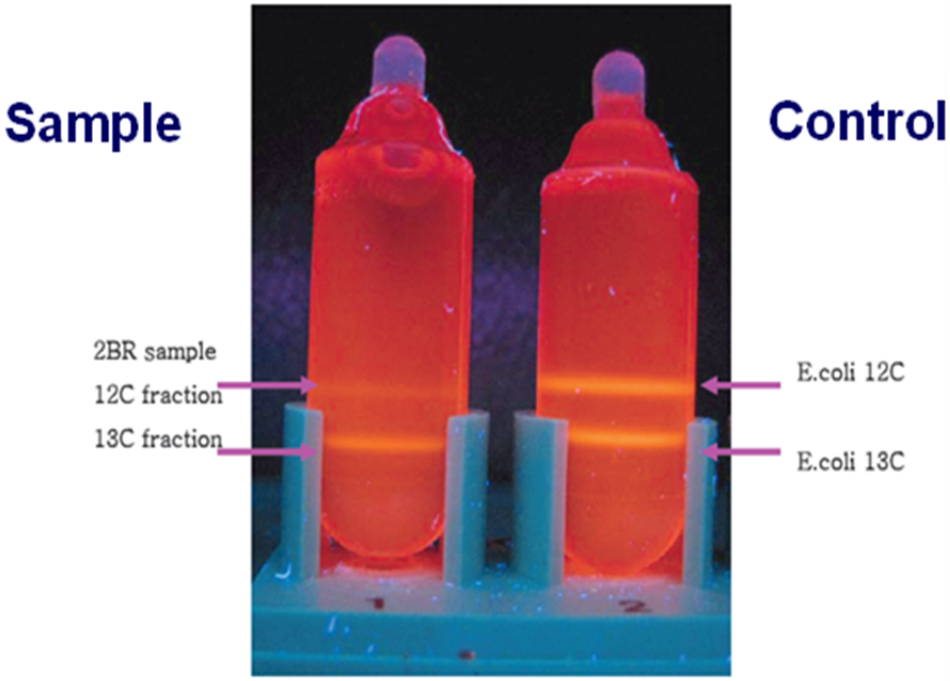

Figure 2.3.4-8. Separation of the ^{12}C- and ^{13}C- DNA bands in ultracentrifuge tubes.

To faciltate discussion of the molecular results, the microcosm samples were coded as indicated in **Table 2.3.4-1**. Wells are designated simply as "5" or "7". Unamended microcosms are designated as "0" and those receiving cheese whey as "C". Finally, microcosms spiked with unlabeled RDX are designated "U", and those receiving ^{13}C-RDX as "L", with an additional "a" or "b" indicating if the sequence was detected from biomass collected after the initial or the second RDX spike.

Table 2.3.4-1. Microcosm sample coding for the ^{13}C-RDX SIP experiments.

Groundwater source	Cheese whey addition	RDX addition	Microcosm ID	Sample ID
MW-5	No	Unlabeled	5-0-U	5-0-Ua
				5-0-Ub
MW-5	No	^{13}C-labeled	5-0-L	5-0-La
				Not available
MW-5	Yes	Unlabeled	5-C-U	5-C-Ua
				5-C-Ub
MW-5	Yes	^{13}C-labeled	5-C-L	5-C-La
				5-C-Lb
MW-7D	No	Unlabeled	7-0-U	7-0-Ua
				7-0-Ub
MW-7D	No	^{13}C-labeled	7-0-L	7-0-La
				7-0-Lb
MW-7D	Yes	Unlabeled	7-C-U	7-C-Ua
				7-C-Ub
MW-7D	Yes	^{13}C-labeled	7-C-L	7-C-La
				7-C-Lb

Active microorganisms capable of using RDX and/or RDX intermediates (MNX, DNX, TNX, MEDINA, and NDAB) as a carbon source (**Figure 2.3.4-9**) were identified from the ^{13}C-DNA fractions of groundwater microcosms receiving the first spike of ^{13}C-RDX without cheese whey (i.e. sample IDs 5-0-La and 7-0-La). Ten different 16S rRNA gene sequences were derived from sample 5-0-La, and six different 16S rRNA gene sequences were derived from sample 7-0-La. The ten sequences derived from sample 5-0-La were widespread among four different classes: α-*Proteobacteria* (2 sequences), β-*Proteobacteria* (5 sequences), δ-*Proteobacteria* (2 sequences), and *Spirochaetes* (1 sequence). The six sequences derived from sample 7-0-La clustered among four different classes: *Bacteroidia* (1 sequence), *Clostridia* (1 sequence), β-*Proteobacteria* (2 sequences), and *Spirochaetes* (2 sequences). The differences between derived sequences indicate that RDX-degrading bacteria were present and phylogenetically diverse.

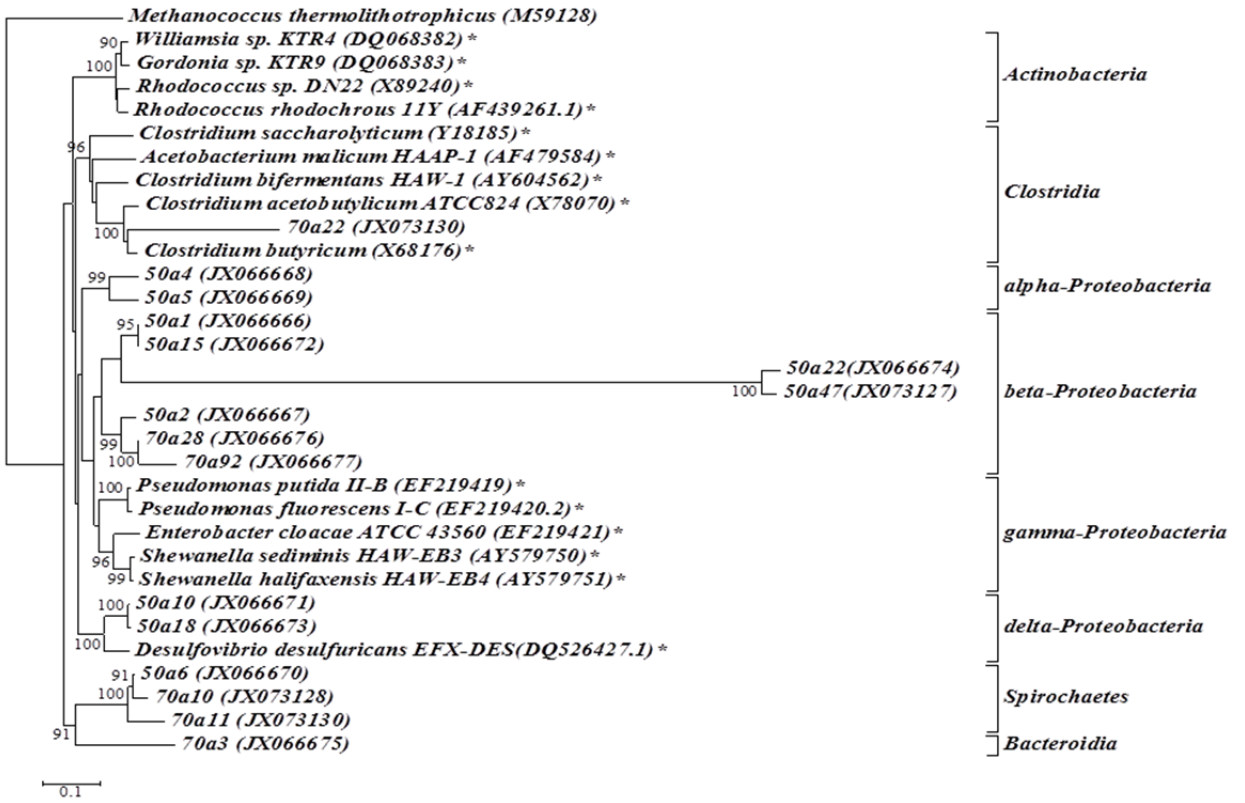

The tree was rooted with *Methanococcus thermolithotrophicus* and was constructed using the neighbor-joining algorithm. The number of clone sequences and the GenBank accession numbers are in parentheses. Only bootstrap values above 85% are shown (1000 replications). Bar, 10% estimated sequence divergence. An asterisk (*) indicates a known RDX degrader.

Samples are designated simply as "5" or "7" for 157MW-5 and 157MW-7D, respectively. Unamended microcosms are designated as "0" and those receiving cheese whey as "C". Microcosms spiked with unlabeled RDX are designated "U", and those receiving ^{13}C-RDX as "L", with an additional "a" or "b" indicating if the sequence was detected from biomass collected after the initial or the second RDX spike.

Figure 2.3.4-9. Phylogenetic tree representing 16S rRNA gene sequences derived from ^{13}C-DNA fractions of unamended groundwater microcosms receiving only ^{13}C-labeled RDX.

The difference in residual TOC from *in situ* cheese whey injection between wells MW-5 and MW-7D at the time of sampling may also have contributed to the differences in microbial community structure. A significant finding of this study was that all the 16 sequences from both wells were different from any known RDX-degraders (< 95% homology) (1, 14, 62, 69, 75, 80), which are clustered in *Actinobacteria*, *Clostridia*, and γ-*Proteobacteria.* Nine different 16S rRNA genes sequences were derived from sample 7-0-Lb, a sample taken after the depletion of the second RDX addition in the microcosms (data not shown). The nine clones were different

from the 16 clones recovered after the first RDX spike had been depleted. The nine clones might represent true rapid RDX utilizers (i.e., utilize C in parent RDX) due to enrichment, or RDX scavenger organisms that were labeled due to cross-feeding on labeled organisms that degraded the first spike of RDX. To be conservative in our analysis, these nine clones were excluded from the phylogenetic analysis.

All the derived clones are different from known RDX degraders, except for one sequence (70a22) that resides in *Clostridia*, a phylum with several known RDX degraders (75, 80). Fuller et al. (26) reported that *Clostridia* were the major 16S rRNA gene sequences recovered from groundwater samples and groundwater microcosms derived from the same contaminated aquifer. Zhang and Hughes reported that *Clostridium acetobutylicum* ATCC 824 was able to reductively transform RDX into several polar intermediates when hydrogen was supplied as the electron donor (75). The other two sequences, 50a10 and 50a18, were identified as *Desulfovibrio* sp., 97% similarity to *Desulfovibrio mexicanus* strain Lup1 (Genebank accession no. NR028776). Several studies have reported that *Desulfovibrio* sp. were capable of mineralizing RDX and using RDX as a carbon source under anoxic conditions (2, 77, 82). As RDX biodegradation has been reported under sulfate-reducing conditions (10), the detection of these two sequences, 50a10 and 50a18, suggested that some *Desulfovibrio* sp. might be able to utilize RDX or RDX metabolites as a carbon source.

Sequences 50a4 and 50a5 fell within the cluster of Order *Rhizobiales*, which are nitrogen-fixing bacteria. Using ^{15}N-RDX SIP, our previous study (56) identified three ^{15}N clones (RDX clones 15N-2, -8, and -13) that were very close to *Azospirillum* sp. (a nitrogen-fixing bacterium). It is interesting to note that the same groups of nitrogen-fixing organisms were detected via both ^{15}N-RDX and ^{13}C-RDX SIP. Overall, these results implicated the presence of nitrogen-fixing strains that are also capable of using RDX as a nitrogen source and/or a carbon source.

With the aid of ^{13}C-RDX SIP, we observed 11 out of 16 clones in the *Bacteroidia* (70a3), the β-*Proteobacteria* (50a1, 50a2, 50a15, 50a22, 50a47, 70a28, 70a92) and the *Spirochaetes* (50a6, 70a10, 70a11). To our knowledge, this is the first report of RDX degradation attributed to these taxonomic groups. Sequences 50a1 and 50a15 showed 97% similarity to the iron-reducing bacteria, *Rhodeferax fermentans* strain FR2 (Genbank accession no. NR025840). Increasing numbers of *Rhodoferax* sp. were reported during RDX degradation in aquifer materials amended with acetate or lactate (37). Since iron-reducing bacteria are ubiquitous in groundwater, future studies are needed to investigate the role of *Rhodoferax* sp. in RDX biodegradation (29, 44, 47, 63).

Sequences 50a2, 70a28 70a92 fell with the cluster *Rhodocyclaceae*, a family of denitrifying bacteria. These findings suggest that many unknown RDX-degrading bacteria play an important role during *in situ* RDX biodegradation. Future research is needed to explore the significance of

these strains, such as *Desulfovibrio* sp., *Azospirillum* sp., and *Rhodoferax* sp., during intrinsic biodegradation of RDX. These strains might be important biomarkers for assessing *in situ* RDX biodegradation when monitored natural attenuation is selected as a remediation option. Research efforts focusing on isolating these strains from sites for detailed biochemical studies are also warranted.

Addition of cheese whey changed the types and distribution of microorganisms capable of using RDX and/or RDX metabolites as a carbon source. Fourteen different ^{13}C-clones were derived from 157MW-5 groundwater microcosms (samples 5-C-La and 5-C-Lb). Unlike the wide distribution of ^{13}C-clones obtained from microcosms receiving only ^{13}C-labeled RDX, these 14 clones clustered in γ-*Proteobacteria* and *Bacilli* (**Figure 2.3.4-10**). The seven sequences (5Ca2, 5Ca12, 5Ca25, 5Ca31, 5Cb2, 5Cb5, 5Cb10) were identified as *Pseudomonas sp.* and clustered in γ-*Proteobacteria* with two known RDX degraders, *Pseudomonas fluorescens* I-C and *Pseudomonas putida* II-B (9, 25, 49). This observation is consistent with the findings of Fuller et al (26), in which many *Pseudomonas* sp. sequences were recovered from groundwater and laboratory enrichments when biostimulation was performed to promote RDX degradation. Our results also suggest that *Pseudomonas* sp. play a key role in the transformation of RDX and other nitramine explosives in the environment, as some strains have been shown to transform RDX under anoxic conditions (25). The rest of the clones were clustered in the *Bacilli* (discussed below).

From microcosms derived from 157MW-7D (sample 7-C-La and 7-C-Lb), another 10 distinct ^{13}C-clones were recovered, distributed among three phyla: β-*Proteobacteria*, *Actinobacteria*, and *Bacilli* (**Figure 2.3.4-10**). Among the 10 clones, four sequences (7Ca15, 7Ca21, 7Cb6 and 7Cb11) reside in *Actinobacteria*, a phylum with four known RDX degraders: *Rhodococcus sp.* DN22, *Rhodococcus rhodocrous* 11Y, *Gordonia* sp. KTR9, and *Williamsia* KTR4. However, only sequence 7Cb11 in the present study was identified as a *Rhodococcus* sp. Although some *Rhodococcus* strains have recently been shown to degrade RDX slowly under microaerophilic conditions (24), the anoxic conditions maintained in the microcosms during this study may have limited their activity.

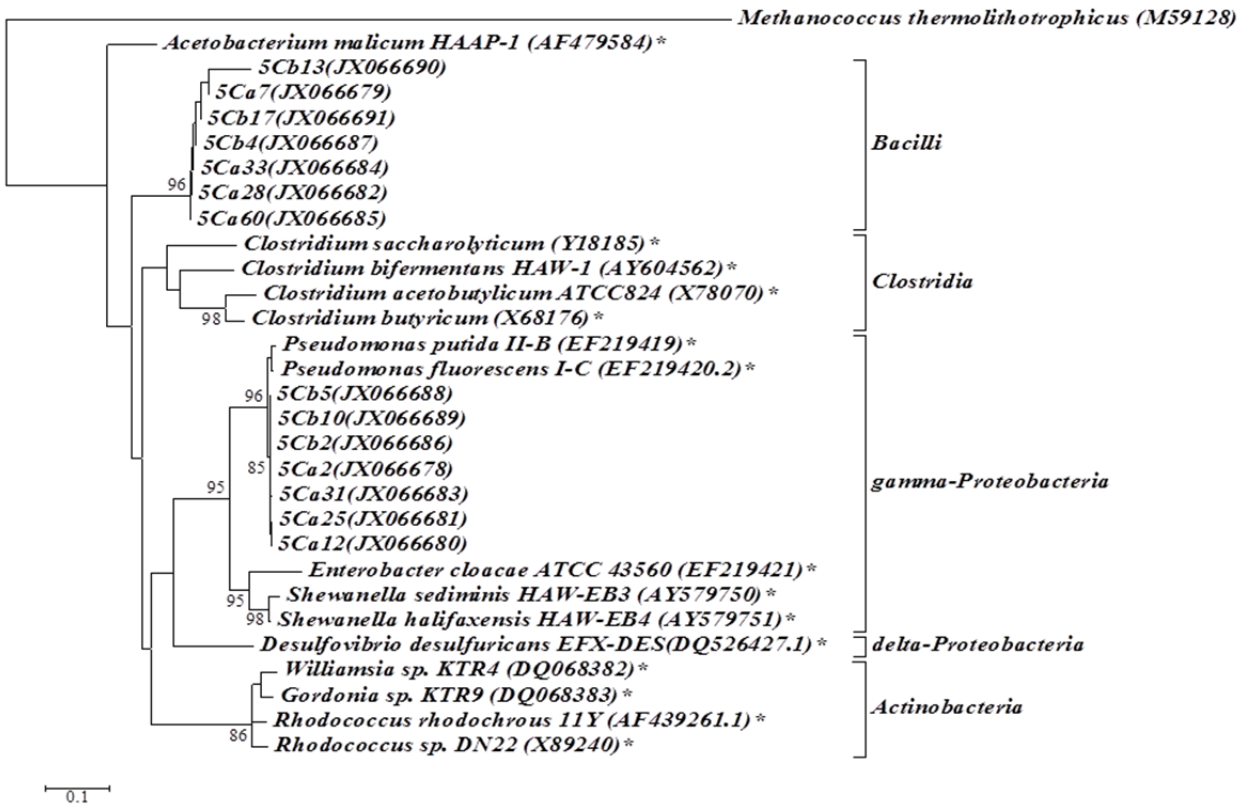

The tree was rooted with *Methanococcus thermolithotrophicus* and was constructed using the neighbor-joining algorithm. The number of clone sequences and the GenBank accession numbers are in parentheses. Only bootstrap values above 85% are shown (1000 replications). Bar, 10% estimated sequence divergence. An asterisk (*) indicates a known RDX degrader.

Samples are designated simply as "5" or "7" for 157MW-5 and 157MW-7D, respectively. Unamended microcosms are designated as "0" and those receiving cheese whey as "C". Microcosms spiked with unlabeled RDX are designated "U", and those receiving ^{13}C-RDX as "L", with an additional "a" or "b" indicating if the sequence was detected from biomass collected after the initial or the second RDX spike.

Figure 2.3.4-10. Phylogenetic tree representing 16S rRNA gene sequences derived from 13C-DNA fractions of cheese whey amended groundwater microcosms derived from 157MW-5 groundwater.

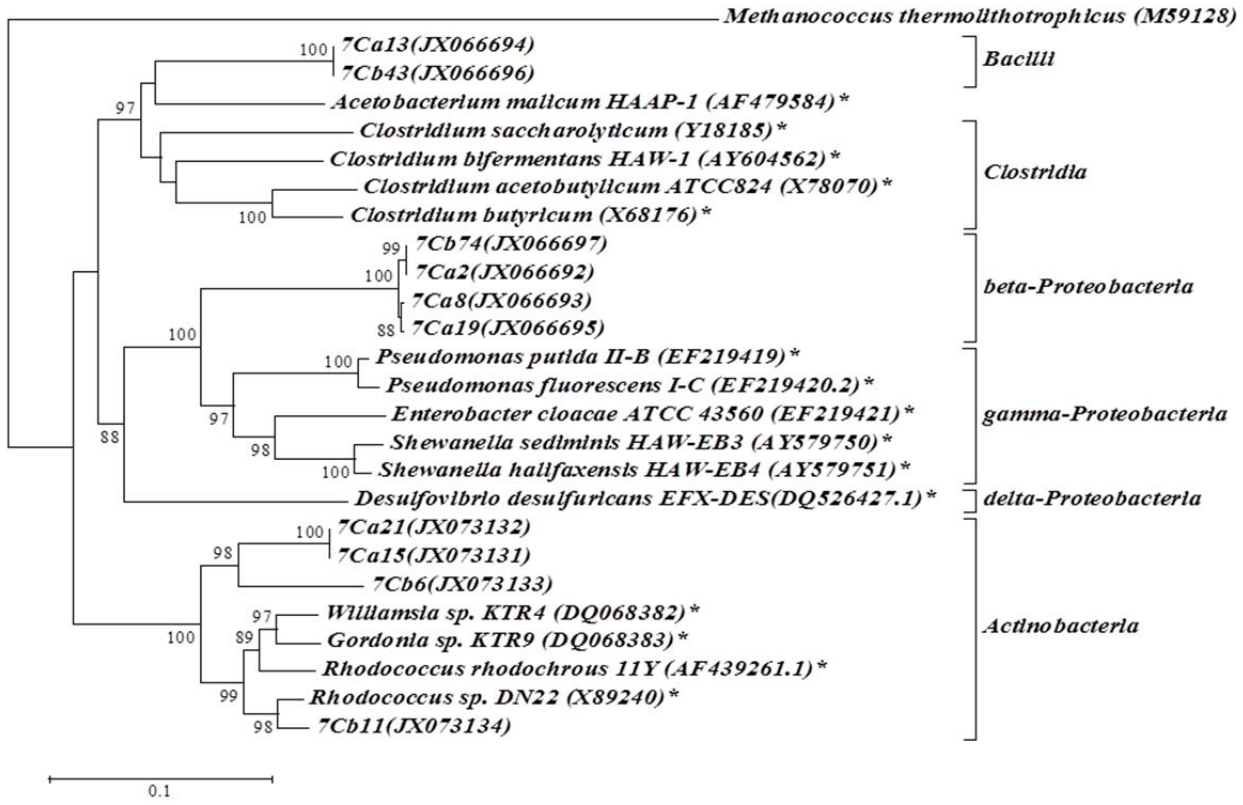

The tree was rooted with *Methanococcus thermolithotrophicus* and was constructed using the neighbor-joining algorithm. The number of clone sequences and the GenBank accession numbers are in parentheses. Only bootstrap values above 85% are shown (1000 replications). Bar, 10% estimated sequence divergence. An asterisk (*) indicates a known RDX degrader.

Samples are designated simply as "5" or "7" for 157MW-5 and 157MW-7D, respectively. Unamended microcosms are designated as "0" and those receiving cheese whey as "C". Microcosms spiked with unlabeled RDX are designated "U", and those receiving ^{13}C-RDX as "L", with an additional "a" or "b" indicating if the sequence was detected from biomass collected after the initial or the second RDX spike.

Figure 2.3.4-11. Phylogenetic tree representing 16S rRNA gene sequences derived from ^{13}C-DNA fractions of cheese whey amended groundwater microcosms derived from 157MW-5 groundwater.

A significant number of clones derived from cheese whey-amended microcosms were found clustered in *Bacilli*. For example, seven sequences recovered from microcosm 5-C-L (5Ca7, 5Ca28, 5Ca33, 5Ca60, 5Cb4, 5Cb13, 5Cb17) and two sequences from microcosm 7-C-L (7Ca13, 7Cb43) cluster in *Bacilli*. The reason that a high number of clones in the cheese whey-amended microcosms are *Bacilli* is unknown. However, the addition of nutrients (particularly the high amounts of the sugar lactose (typically 70-75% (w:w) of cheese whey) (46, 48) is known to promote reactivation of spores (60), which may have been present in both the groundwater and

the cheese whey itself. Nevertheless, our SIP results clearly indicated that the *Bacilli* were stimulated by the cheese whey addition and that they assimilated ^{13}C initially derived from ^{13}C-labeled RDX in our microcosms.

2.3.4.3.2 ^{15}N-RDX SIP

As with the ^{13}C-RDX SIP molecular results, the ^{15}N-RDX SIP microcosm samples were coded as indicated in **Table 2.3.4-2**. Wells are designated simply as "5" or "7". Unamended microcosms are designated as "0" and those receiving cheese whey as "C". Microcosms spiked with ^{15}N-ring-, ^{15}N-nitro-, and ^{15}N-fully labeled RDX are designated "R", "N", and "F", respectively.

Table 2.3.4-2. Microcosm sample coding for the ^{13}C-RDX SIP experiments.

Groundwater source	Cheese whey addition	RDX addition	Microcosm ID	Sample ID
MW-5	No	^{15}N-ring	50-R	No degradation
		^{15}N-nitro	50-N	50-Na
		^{15}N-full	50-F	50-Fa
MW-5	Yes	^{15}N-ring	5C-R	5C-Ra
		^{15}N-nitro	5C-N	5C-Na
		^{15}N-full	5C-F	5C-Fa
MW-7D	No	^{15}N-ring	70-R	70-Ra
		^{15}N-nitro	70-N	70-Na
		^{15}N-full	70-F	70-Fa
MW-7D	Yes	^{15}N-ring	7C-R	7C-Ra
		^{15}N-nitro	7C-N	7C-Na
		^{15}N-full	7C-F	7C-Fa

By using the ^{15}N-DNA fractions of five unamended microcosms (50-Na, 50-Fa, 70-Na, 70-Ra and 70-Fa) as templates, a total of fifteen 16S rRNA gene sequences were derived. These sequences were contributed from metabolically active bacteria capable of using RDX and/or RDX intermediates as a nitrogen source. These sequences were clustered in three major phyla: *Clostridia* (2 sequences), β–*Proteobacteria* (7 sequences), and *Spirochaetes* (6 sequences) (**Figure 2.3.4-12**), indicating that RDX-degrading bacteria were present and they are

phylogenetically diverse in groundwater. Most of, the 15 sequences were different from any previously described RDX degraders (1, 14, 62, 69, 75, 80).

As the same groundwater was used in our previous ^{13}C-RDX study (13), the clone libraries in the previous study were compared to those established in this study. Common clones in both libraries of ^{13}C-SIP and ^{15}N-SIP studies would indicate that these common clones might be able to use RDX or its metabolites as both a nitrogen and carbon source. Two sequences (70-Ra22 and 70-Na4) in β-*Proteobacteria* showed high homology (>97%) to one clone derived from background groundwater (GW clone 16, EU907859), and one clone (^{13}C-RDX clone 50-a1, JX066666) identified from the ^{13}C-RDX SIP study (13), suggesting that these two clones likely are able to use RDX as both a carbon and nitrogen source.

The sequence 70-Ra22, detected in the ^{15}N-ring- RDX sample has a high sequence similarity to two iron-reducing strains: *Rhodeferax ferrireducens* strain T118 (accession number: NR074760) and *Rhodeferax fermentans* strain FR2 (accession number: NR025840) (19). Increased numbers of *Rhodoferax* sp. in aquifer materials was reported when acetate or lactate was amended to promote RDX biodegradation (37). A recent study reported a shift of the dominant Fe(III)-reducers in the RDX-contaminated groundwater, changing from β-*Proteobacteria* to δ- , β-*Proteobacteria* (*Geobacter* sp.) when acetate was amended to enhance RDX biodegradation (40).

Four sequences (50-Fa13, 70-Fa2, 70-Fa3, and 70-Fa12) in β-*Proteobacteria* also showed high similarity (>95%) to the two ^{13}C-RDX clones 70-a28 and 70-a92 (13). These four sequences show 92% homology to *Ferribacterium limneticum* (accession number: NR026464.1), a Fe(III)-reducing bacteria, isolated from mining-impacted sediment (16). The high homology of these four sequences to Fe (III)-reducing bacteria (such as *Albidiferax* sp. (basonym *Rhodoferax*) and *Ferribacterium* sp.) also suggests that Fe-reducers might be able to use RDX as a carbon and nitrogen source.

An additional six clones (50-Na22, 50-Na28, 50-Na32, 50-Fa14, 50-Fa33, and 70-Fa15) were closely related to *Spirochaetes*, and are similar (>98%) to the ^{13}C-RDX clone 50-a6 (accession number: JX066670) isolated during our previous ^{13}C-RDX study (13). This genus has only been tied to RDX degradation on these two occasions.

Interestingly, several clones derived from ring-, nitro-, and fully-labeled ^{15}N-RDX were identical. These identical clones were clustered within *Clostridia*, β-*Proteobacteria* and *Spirochaetes*. The nearest relatives for these clones is *Desulfosporosinus meridiei* (accession number: NR074129), belonging to a family of sulfate-reducing bacteria. *D. meridiei* was previously isolated from a gasoline contaminated soil. A number of *Desulfosporosinus* sp. can utilize a wide spectrum of carbon sources, ranging from aromatic compounds to short-chained

fatty acids (53). Several sulfate-reducing bacteria are known to utilize RDX as a nitrogen source (3, 10, 82) under anaerobic condition. Thus, these two clones (50-Na8 and 50-Fa19) are very likely to be *Desulfosporosinus* sp., and they are also capable of using the N from the nitro-groups of RDX. Interestingly, *Desulfosporosinus* sp. were also detected as RDX degraders in ^{13}C and ^{15}N-SIP studies using samples from Dahlgren, VA incubated under a range of different electron-accepting conditions (see **Section 2.3.5**).

Finally, from the unamended microcosms, a sequence related to *Herbaspirillum lusitanum* (70-Fa7, accession number: NR028859) was recovered. This genus is a nitrogen-fixing bacterium associated with root nodules of *Phaseolus vulgaris* (71) and has not previously been associated with RDX degradation.

Addition of cheese whey altered the types and distributions of RDX-degrading microbial community populations when compared to those observed in microcosms 50-N, 50-F, 70-R, 70-N, and 70-F. A total of 28 sequences were derived from these cheese-whey-receiving microcosms (5C-Na, 5C-Ra, 5C-Fa, 7C-Na, 7C-Ra, and 7C-Fa). These sequences were grouped into *Bacteroidia, Bacilli,* α-, β-, and γ-*Proteobacteria* (**Figure 2.3.4-13**), with the majority in *Proteobacteria*. Once again, none of the derived sequences were an exact match to any of known RDX degraders.

By comparing the clone libraries of ^{13}C-SIP and ^{15}N-SIP studies, there were three overlapping groups: β-, γ-*Proteobacteria* and *Bacilli*. Two sequences (5C-Ra12 and 5C-Na12), derived from microcosms 5C-Ra and 5C-Na, showed high similarity (95%) to two known RDX degraders, *Pseudomonas fluorescens* I-C and *Pseudomonas putida* II-B (9, 49). *Pseudomonas* sp. are aerobes and/or facultative anaerobes that have been identified in many contaminated soil and groundwater environments. Our results are consistent with previous findings that many *Pseudomonas* sp. sequences can be recovered from groundwater or laboratory enrichments when biostimulation was performed to enhance RDX degradation (13, 26, 56). *P. fluorescens* I-C and *P. putida* II-B strains can transform RDX using xenobiotic reductases XenA and XenB under both aerobic and anaerobic conditions (25). RDX transformation by these reductases was much faster anaerobically than aerobically, as oxygen can inhibit the activity of the enzymes. Along with previous findings, these results suggest that *Pseudomonas* sp. play an important role in transforming RDX and other nitramine explosives in the environment. In addition, the catabolic genes that code the xenobiotic reductases can be a useful biomarker to assess potential and/or progress of RDX biodegradation under anoxic conditions.

A total of 12 sequences were derived from cheese whey amended microcosms. These sequences were clustered in *Bacilli*. Among the 12 sequences, seven sequences (5C-Ra27, 5C-Ra29, 5C-Na2, 5C-Na3, 5C-Na3, 5C-Na4, and 5C-Fa7) were derived from microcosms 5C-Na, 5C-Ra and 5C-Fa. The other five sequences (7C-Ra22, 7C-Na22, 7C-Fa1, 7C-Fa2, and 7C-Fa9) were

derived from microcosms 7C-Na, 7C-Ra, and 7C-Fa. Most of these sequences were highly homologous (>97%), and were repetitively observed in microcosms receiving ring-, nitro-, or fully-labeled ^{15}N-RDX.

These results are similar to the previous ^{13}C-SIP study results presented above in that the high numbers of sequences in *Bacilli* (nine sequences in ^{13}C-SIP study, 5Ca7, 5Ca28, 5Ca33, 5Ca60, 5Cb4, 5Cb13, 5Cb17, 7Ca13, and 7Cb43) were associated with the cheese whey amended microcosms. These 12 sequences were very close to *Trichococcus flocculiformis* (accession number: NR042060), a low G+C content strain capable of utilizing various carbohydrates for acid production (39). Although no studies have reported the RDX degradation ability of *Trichococcus* sp., our results clearly indicate that the *Bacilli* were stimulated by cheese whey addition and that they can assimilate ^{15}N from ^{15}N-labeled RDX.

Based on derived sequences, our results once again indicate the diversity of active microorganisms associated with RDX biodegradation in the environmental samples. When cheese whey was absent, none of the known RDX-degraders were detected in this study. Some, but not all, clones identified from this study were highly similar to those obtained during the ^{13}C-SIP study described in **Section 2.3.4.3.1** above. With cheese whey addition, RDX degradation was significantly enhanced and the active microbial community structure shifted dramatically.

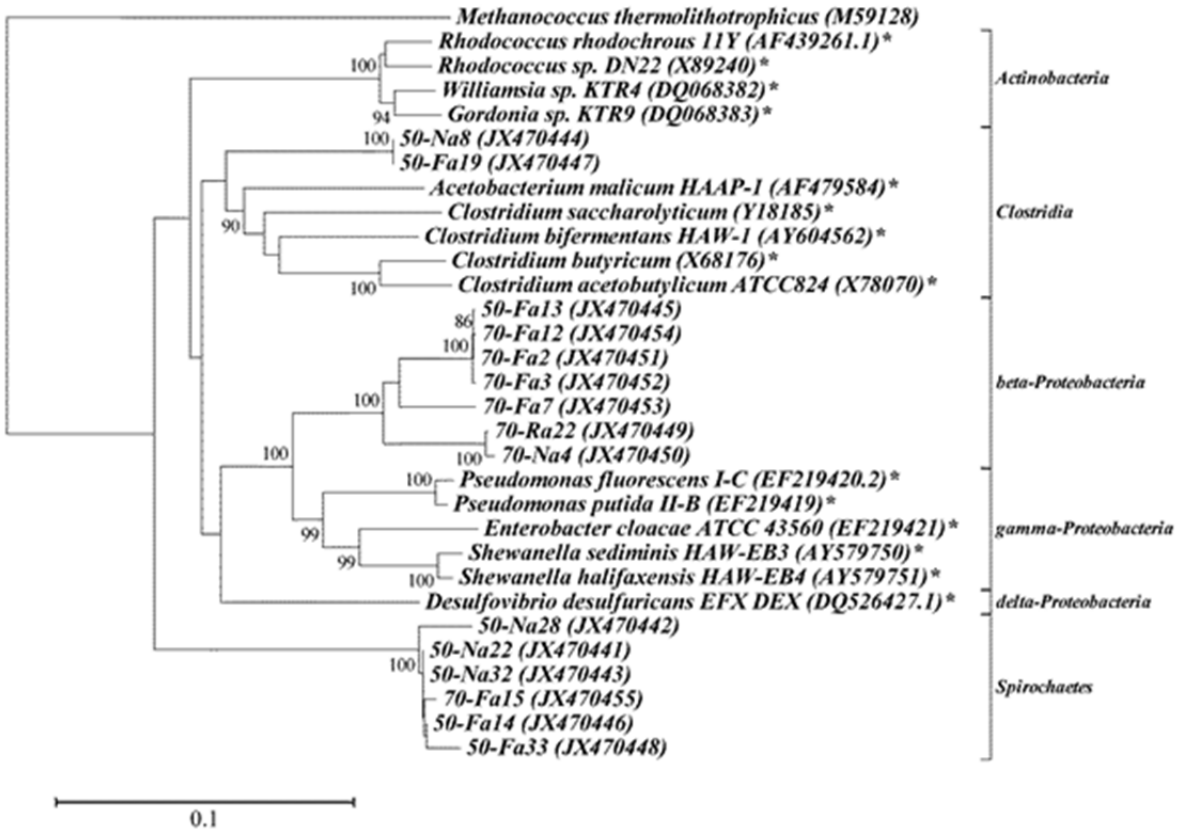

The tree was rooted with *Methanococcus thermolithotrophicus* and was constructed using the neighbor-joining algorithm. The number of clone sequences and the GenBank accession numbers are in parentheses. Only bootstrap values above 85% are shown (1000 replications). Bar, 10% estimated sequence divergence. An asterisk (*) indicates a known RDX degrader.

Samples are designated simply as "5" or "7" for 157MW-5 and 157MW-7D, respectively. Unamended microcosms are designated as "0" and those receiving cheese whey as "C". Microcosms spiked with ^{15}N-ring-, ^{15}N-nitro-, and ^{15}N-fully labeled RDX are designated "R", "N", and "F", respectively.

Figure 2.3.4-12. Phylogenetic tree representing 16S rRNA gene sequences derived from ^{15}N-DNA fractions of unamended microcosms derived from 157MW-5 and 157MW-7D groundwater receiving ^{15}N-ring-, ^{15}N-nitro-, and ^{15}N-fully labeled RDX.

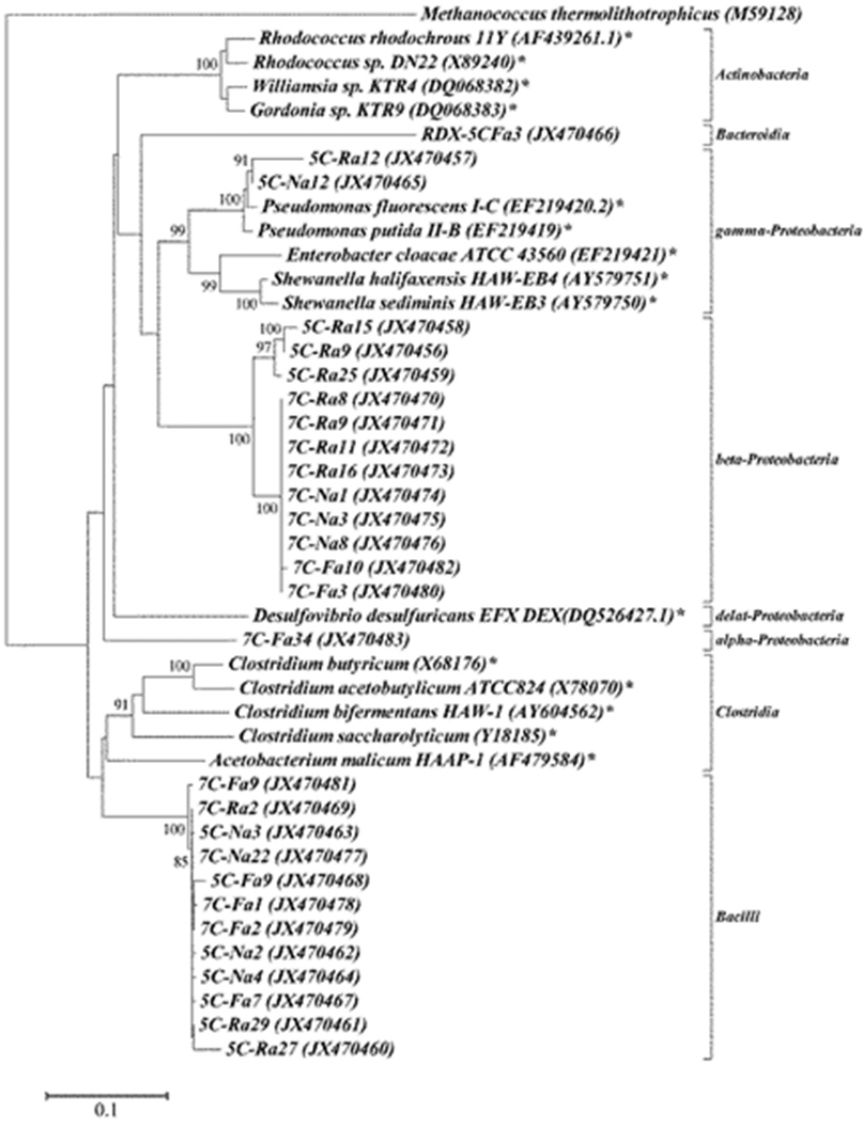

The tree was rooted with *Methanococcus thermolithotrophicus* and was constructed using the neighbor-joining algorithm. The number of clone sequences and the GenBank accession numbers are in parentheses. Only bootstrap values above 85% are shown (1000 replications). Bar, 10% estimated sequence divergence. An asterisk (*) indicates a known RDX degrader.

Samples are designated simply as "5" or "7" for 157MW-5 and 157MW-7D, respectively. Unamended microcosms are designated as "0" and those receiving cheese whey as "C". Microcosms spiked with ^{15}N-ring-, ^{15}N-nitro-, and ^{15}N-fully labeled RDX are designated "R", "N", and "F", respectively.

Figure 2.3.4-13. Phylogenetic tree representing 16S rRNA gene sequences derived from ^{15}N-DNA fractions of cheese whey amended microcosms derived from 157MW-5 and 157MW-7D groundwater receiving ^{15}N-ring-, ^{15}N-nitro-, and ^{15}N-fully labeled RDX.

2.3.5 Application of ^{13}C- and ^{15}N-RDX SIP to Dahlgren Mesocosms Incubated under Different Electron Accepting Conditions

2.3.5.1 Dahlgren SIP - Methods

Methods for establishment of RDX degradation in Dahlgren sediment and groundwater mesocosms under various dominant electron accepting conditions were described previously in **Section 2.2.4**. The degradation of RDX and the formation of degradation products under different electron-accepting regimens also were described in detail in this section.

When the dominant electron accepting conditions were confirmed to be stable, the contents of a given mesocosm were divided among five 2 L glass bottles (glass heated at 550°C and caps UV irradiated and autoclaved, respectively) and amended with variously labeled [^{13}C-RDX (ring) or ^{15}N-RDX (ring, nitro, or full)] or unlabeled RDX at 20 mg/L, additional succinate, and the corresponding electron acceptor. The bottles were incubated at 15°C and sampled approximately weekly for measurement of RDX. If RDX degradation stalled, additional electron donor, electron acceptor, and/or inorganic nutrients were added. When >90% of the RDX had degraded past the point of the nitroso-containing products (MNX, DNX, TNX), the solutions were filtered to collect the biomass and subjected to DNA extraction and molecular analysis (methods as described in **Section 2.3.4** above).

2.3.5.2 Dahlgren SIP - RDX Degradation Results

The results from the Dahlgren SIP study were as follows:

1. In the samples initially incubated under Fe-reducing conditions in mesocosms, an initial transformation of all the RDX to TNX was observed in the SIP bottles (**Figure 2.3.5-1**). RDX was transformed to TNX in all of the Fe-reducing enrichments, and the TNX then was degraded to non-identifiable metabolites. Once TNX degradation was nearly complete, the biomass was collected by filtration and the samples were shipped to Texas A&M for DNA extraction and analysis.

2. In the samples initially incubated under Mn-reducing conditions in mesocosms, the degradation of RDX occurred after a much longer lag phase than observed under Fe-reducing conditions (~ 100 days compared to 10 days, respectively) (**Figure 2.3.5-2**). However, Conversion of all the RDX to TNX was observed after a small addition of mineral nutrients. TNX degradation followed, and the biomass was collected for DNA extraction and phylogenetic analysis once TNX degradation was nearly complete.

3. RDX-SIP coupled to sulfate reduction and under no added electron donor conditions (methanogenic conditons) resulted in very rapid reductions in RDX concentrations in the SIP bottles (**Figures 2.3.5-3** and **2.3.5-4**). Very small and transient amounts (<2 mg/L) of TNX were formed and rapidly disappeared after RDX was exhausted. The biomass was collected for DNA extraction and phylogenetic analysis once RDX and TNX degradation were nearly complete.

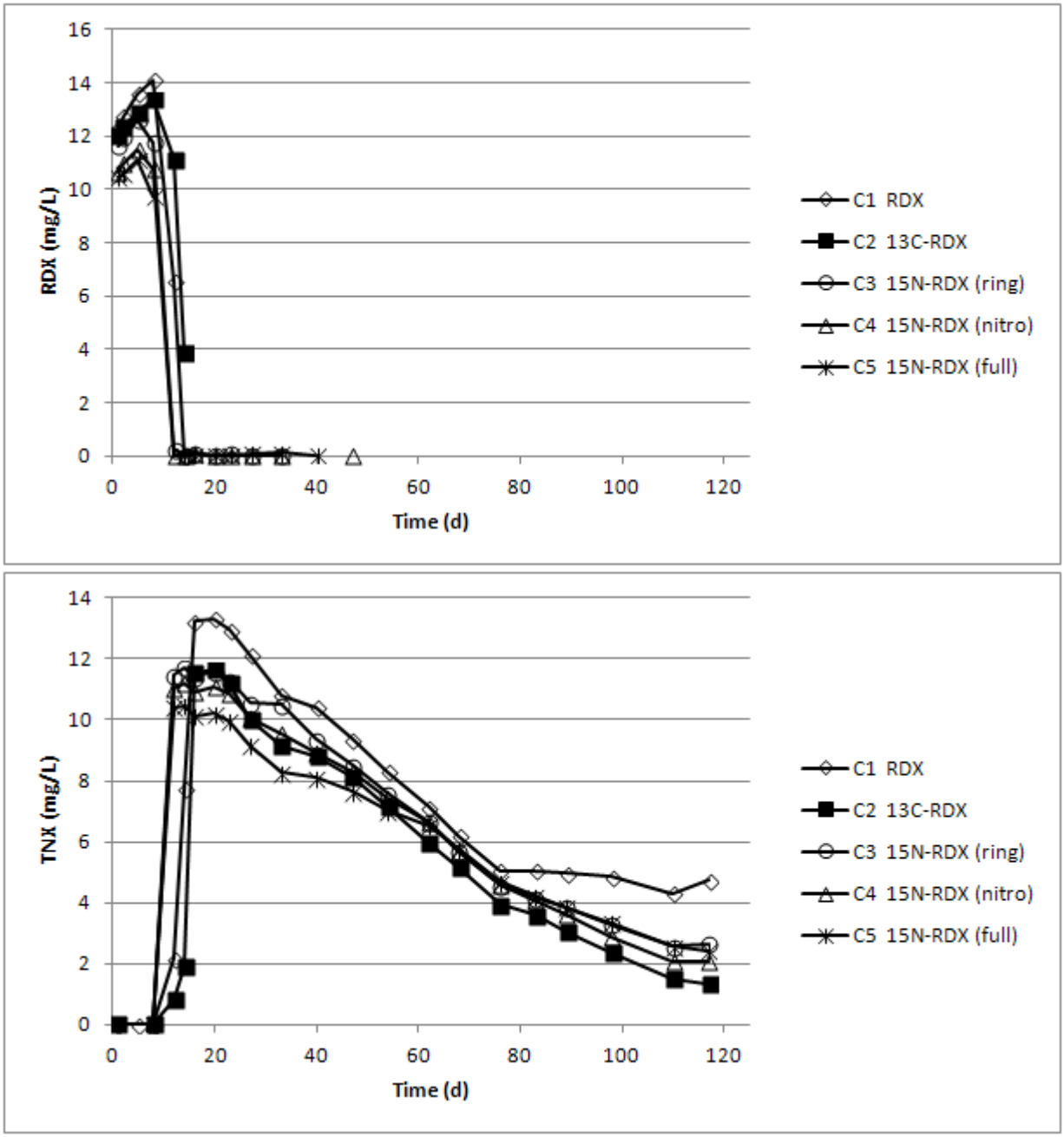

Figure 2.3.5-1. Concentrations of RDX and TNX over time under Fe reducing conditions in Dahlgren SIP enrichments.

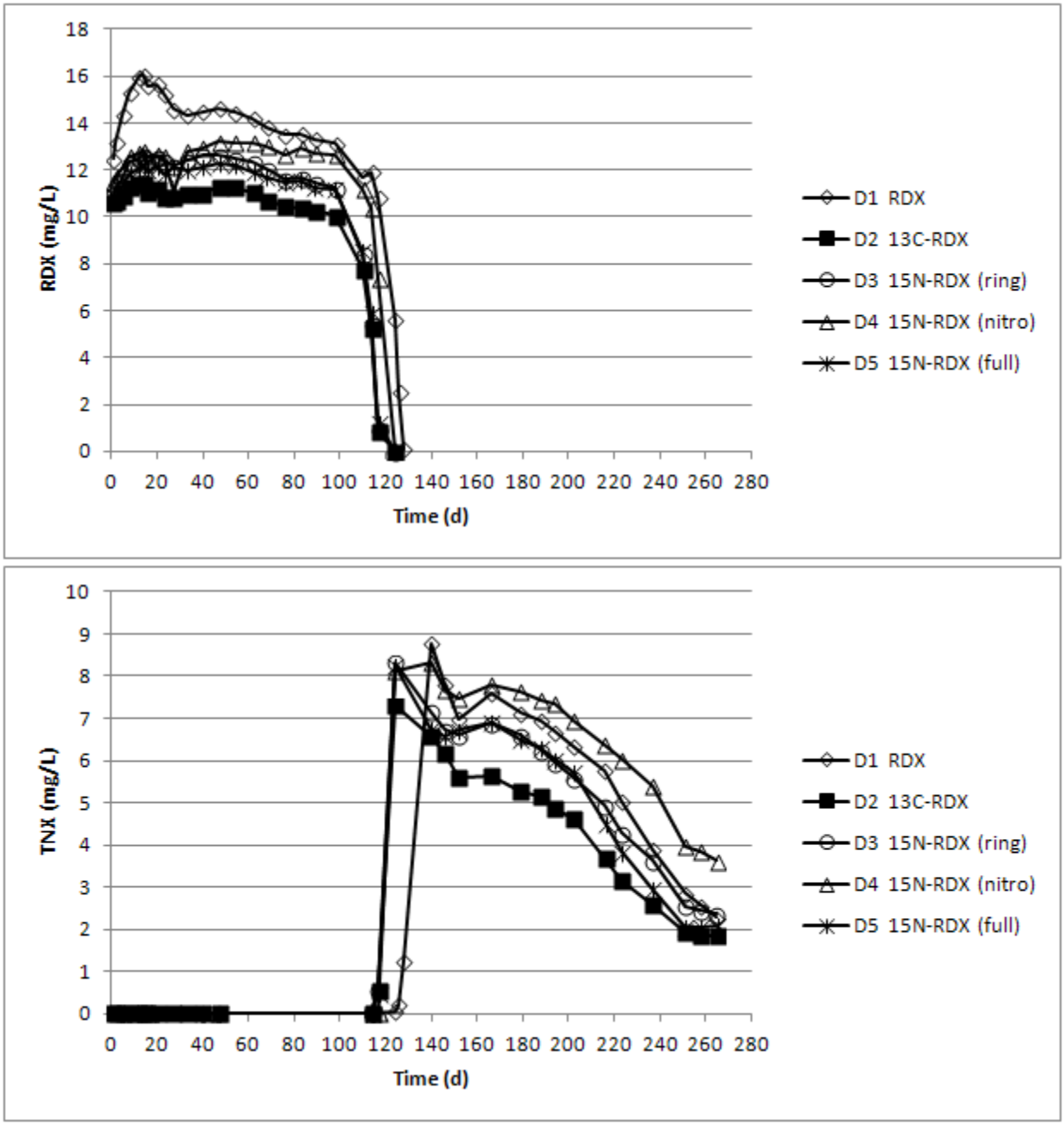

Figure 2.3.5-2. Concentrations of RDX and TNX over time under Mn reducing conditions in Dahlgren SIP enrichments.

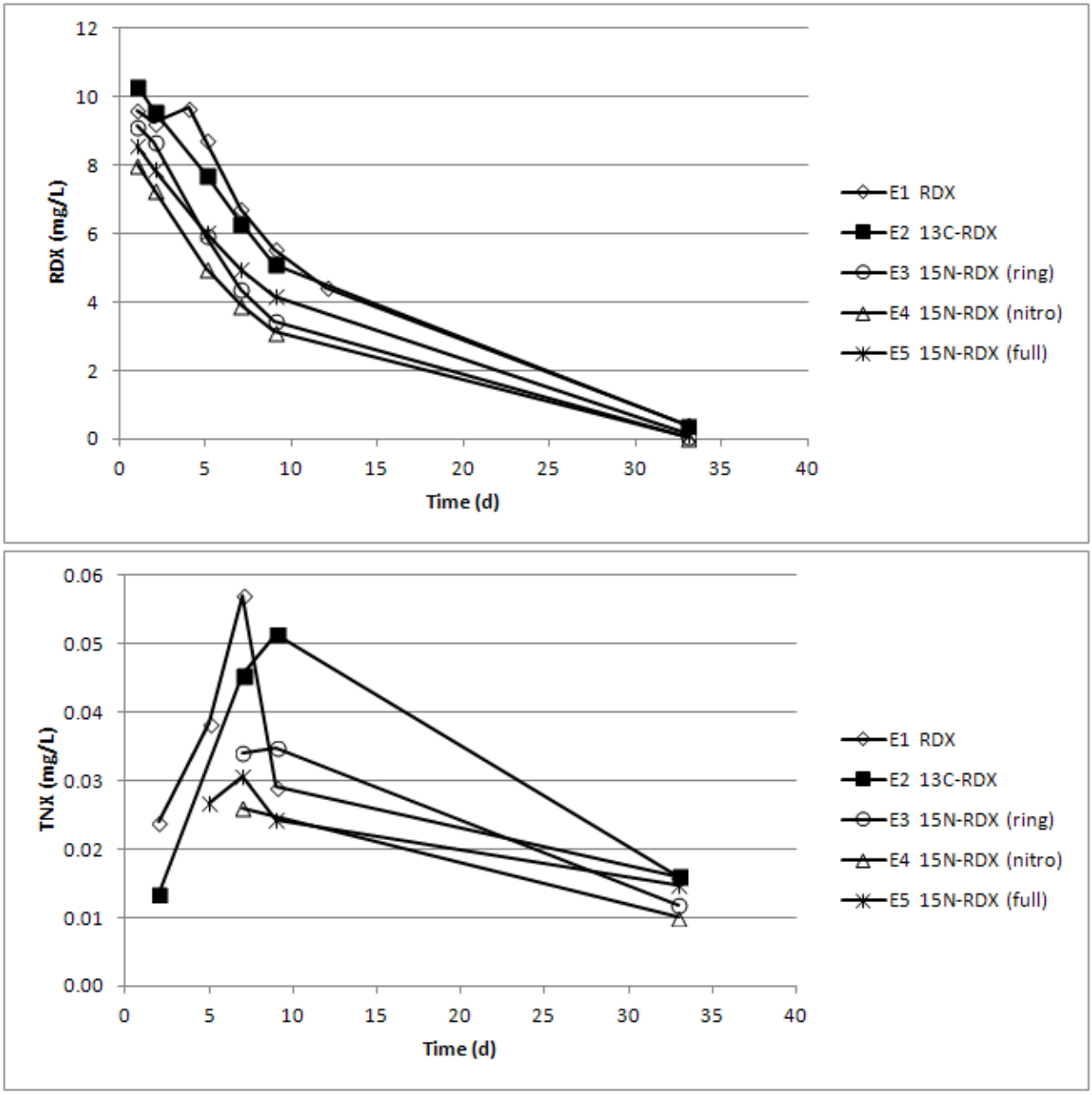

Figure 2.3.5-3. Concentrations of RDX and TNX over time under sulfate reducing conditions in Dahlgren SIP enrichments.

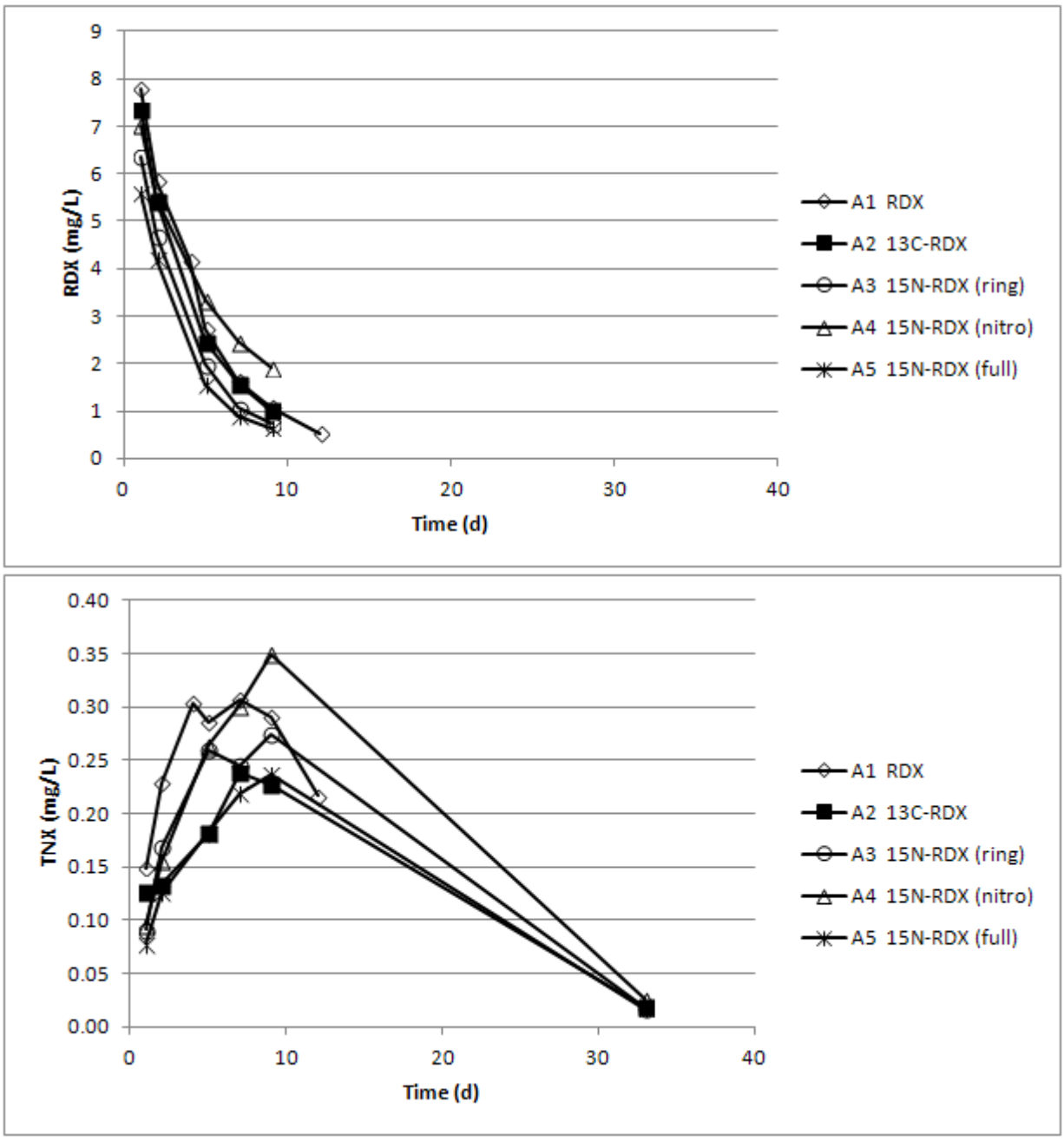

Figure 2.3.5-4. Concentrations of RDX and TNX over time under methanogenic conditions in Dahlgren SIP enrichments.

2.3.5.3 Dahlgren SIP - Molecular Analysis Results & Discussion

By using the ^{13}C-DNA fractions from the microcosms that had received ^{13}C-labeled RDX as templates for cloning and sequencing, identities of active bacteria capable of using RDX and/or RDX intermediates as a carbon source were determined. A total of fifteen 16S rRNA sequences were derived. These sequences resided in four major clusters: *Actinobacteria (Eggerthella)*, α-*Proteobacteria* (unclassified *Rhizobiales*), γ-*Proteobacteria* (*Pseudomonas)*, and *Clostridia* (*Desulfosporosinus*) (**Figure 2.3.5-5**).

Similarly, a total of twenty seven sequences were derived from ^{15}N-DNA fractions from the microcosms which received ring-, nitro- and fully-labeled ^{15}N-RDX, respectively (**Figure 2.3.5-6**). Interestingly, the clone library assembly from ^{15}N-DNA fractions was similar to that from the ^{13}C-DNA fractions. These sequences formed the three major groups in α-*Proteobacteria* (unclassified *Rhizobiales*), γ-*Proteobacteria* (*Pseudomonas*), and *Clostridia* (*Desulfosporosinus*). One sequence (manganese D2H5, derived from the microcosm D2) in *Actinobacteria* in shows a close match to *Eggerthella* sp., whereas, two sequences (manganese D2H2 and D2H6) were grouped in α-*Proteobacteria* (unclassified *Rhizobiales*). In contrast, three sequences (manganese D3H2, manganese D4H6, and sulfate E4H2) in α-*Proteobacteria* were derived from microcosms receiving ring- and nitro-labeled ^{15}N-RDX, respectively. No previous studies have reported these genera of bacteria to be associated with RDX degradation. Additionally, the derived sequences data from ^{13}C- and ^{15}N-SIP implied these unknown bacteria in α-*Proteobacteria* can use RDX or metabolites as carbon and/or a nitrogen sources.

Three sequences (manganese D2H4, sulfate E2H6 and methanogenic A2H3,) in γ-*Proteobacteria* were derived from microcosms receiving ^{13}C-labeled RDX under manganese-reducing, sulfate-reducing, and methanogenic conditions, respectively. These three sequences were identified as the closest matches (95% homology) to the known RDX degraders, *Pseudomonas fluorescens* I-C and *Pseudomonas putida* II-B. Both *P. fluorescens* I-C and *P. putida* II-B strains transform RDX with xenobiotic reductases XenA/XenB (25), and degrade RDX via a ring-cleavage (pathway B, **Figure 2.1.2-1**). Interestingly, the *Pseudomonas* sp. were also found in the ^{15}N-fractions clone library. Three sequences (manganese_D3H1, sulfate_E3H5 and methanogenic_A3H2) in γ-*Proteobacteria* were derived from microcosms receiving ring-labeled ^{15}N-RDX, while one sequence (manganese_D4H6) in γ-*Proteobacteria* was derived from the microcosm receiving nitro-labeled ^{15}N-RDX. The common sequences identified the *Pseudomonas* sp. from both clone libraries in ^{13}C- and ^{15}N-SIP studies suggested that *Pseudomonas* sp. are likely to use RDX or its metabolites as a carbon and/or a nitrogen source. These results differ from Fuller et al., (25) who reported that *Pseudomonas* sp. with xenobiotic reductases were capable of degrading RDX, but these strains could not utilize RDX as sole carbon or nitrogen source. It is possible that the *Pseudomonas* sp. isolated here utilized a different enzyme for RDX degradation or that they scavenged nitrogen or carbon-containing

metabolites of RDX after the parent molecule was partially degraded by a different organism in the enrichment.

A major group of *Desulfosporosinus,* a family of sulfate-reducing bacteria, was identified from both ^{13}C-SIP and ^{15}N-SIP clone libraries. *Desulfosporosinus* sp. were also previously detected in ^{15}N SIP studies with groundwater samples from Picatinny Arsenal (**Section 2.3.4.3.2**), suggesting that they are potentially an important, but previously unreported RDX degrader in the environment. A total of eight sequences (iron C2H10, iron C2H13, iron C2H27, iron C2H33, sulfate E2H1, sulfate E2H9, methanogenic A2H6, and methanogenic A2H18) were derived from microcosms under iron-reducing, sulfate-reducing and methanogenic conditions in samples receiving ^{13}C-RDX. In addition, a total of twenty two sequences were derived from microcosms under manganese-reducing, iron-reducing, sulfate-reducing, and methanogenic conditions, respectively, from samples receiving ring-, nitro, and fully-labeled ^{15}N-RDX. These sequences were found to be highly similar in both ^{13}C-SIP and ^{15}N-SIP clone libraries with the closest matches (95% to 99% homology) being to the species *Desulfosporosinus lacus* (accession number: NR042202) and *Desulfosporosinus meridiei* (accession number: NR074129). *Desulfosporosinus* sp. can reduce sulfate for energy, and some species can also grow by using nitrate, Fe(III), or As(V) as terminal electron acceptors or by fermentative processes (53). One isolate of this genus was isolated from acid mine drainage, and was shown to be able to reduce iron and manganese oxides in addition to sulfate (57), which may explain why this organism apparently thrived under a range of electron acceptor conditions. While *Desulfosporosinus* sp. have been isolated from or detected in other organic pollutant contaminated environments (12, 27, 38, 54, 55, 72), no previous studies have shown that this genus is involved in RDX biodegradation. However, several studies revealed that sulfate-reducing bacteria, such as *Desulfovibrio* sp., are able to utilize RDX as a nitrogen source (3, 10).

The ^{13}C- or ^{15}N- labeled gradient fractions were used as templates for characterizing the active RDX-degrading microbial community structures under different electron accepting conditions via real-time-t-RFLP analysis. Four ribotypes (t-RFs = 101, 106, 109 and 329 bp) were observed in all microbial community profiles in microcosms under all four different electron-accepting conditions (**Figure 2.3.5-7**). Three other peaks (t-RFs 107, 108 and 118 bp) were observed in the iron-reducing microbial communities. The 16S rRNA gene copies were higher in 106 and 109 bp t-RFs than in other t-RFs.

Compared to those derived from $^{13}C_3$-RDX fractions, different and more diverse microbial community profiles were observed in the microcosms receiving ring-, or nitro-$^{15}N_3$-RDX, and fully-labeled $^{15}N_6$-RDX under the different dominant electron-accepting conditions (**Figure 2.3.5-7**). The common t-RFs (106, 109, and 116 bp) were dominated in all treatments by t-RF=116 bp in microcosms receiving ring-labeled $^{15}N_3$-RDX. However, the patterns were shifted to the common peaks 135, 138, 140, and 150 bp t-RFs in microcosms receiving the nitro-$^{15}N_3$-

RDX and fully-labeled $^{15}N_6$-RDX under manganese-reducing, sulfate-reducing, and methanogenic conditions. The shifts might be due to the fact that different bacterial groups were able to use nitrogen of RDX derived from both the nitro groups and the ring structure.

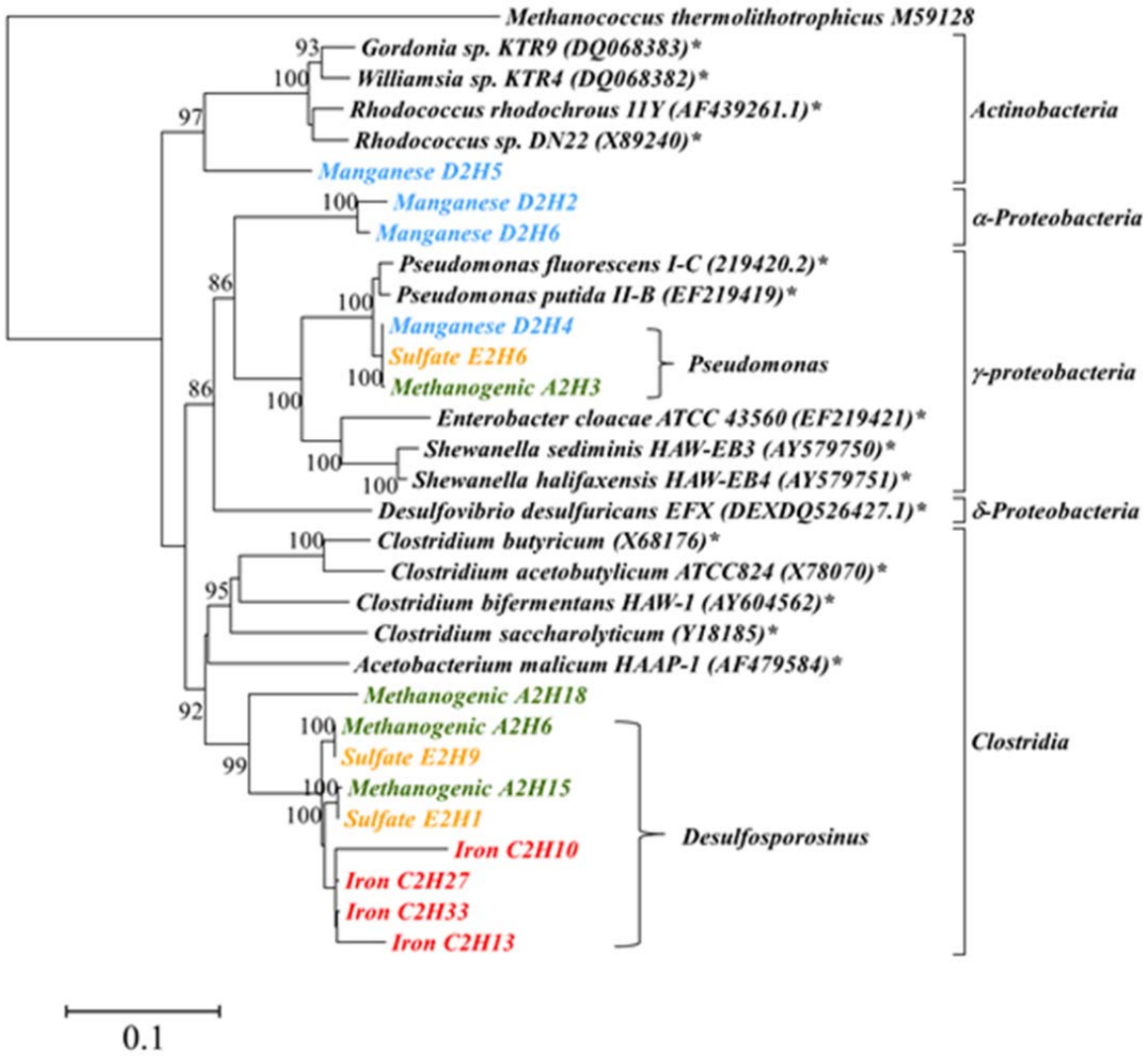

The tree was rooted with *Methanococcus thermolithotrophicus* and was constructed using the neighbor-joining algorithm. Only bootstrap values above 85% are shown (1,000 replications). Bar, 10% estimated sequence divergence. An asterisk (*) indicates a known RDX degrader.

Figure 2.3.5-5. Phylogenetic tree representing 16S rRNA gene sequences derived from ^{13}C-RDX SIP of groundwater microcosms receiving under different electron accepting conditions (manganese, iron, sulfate and CO_2).

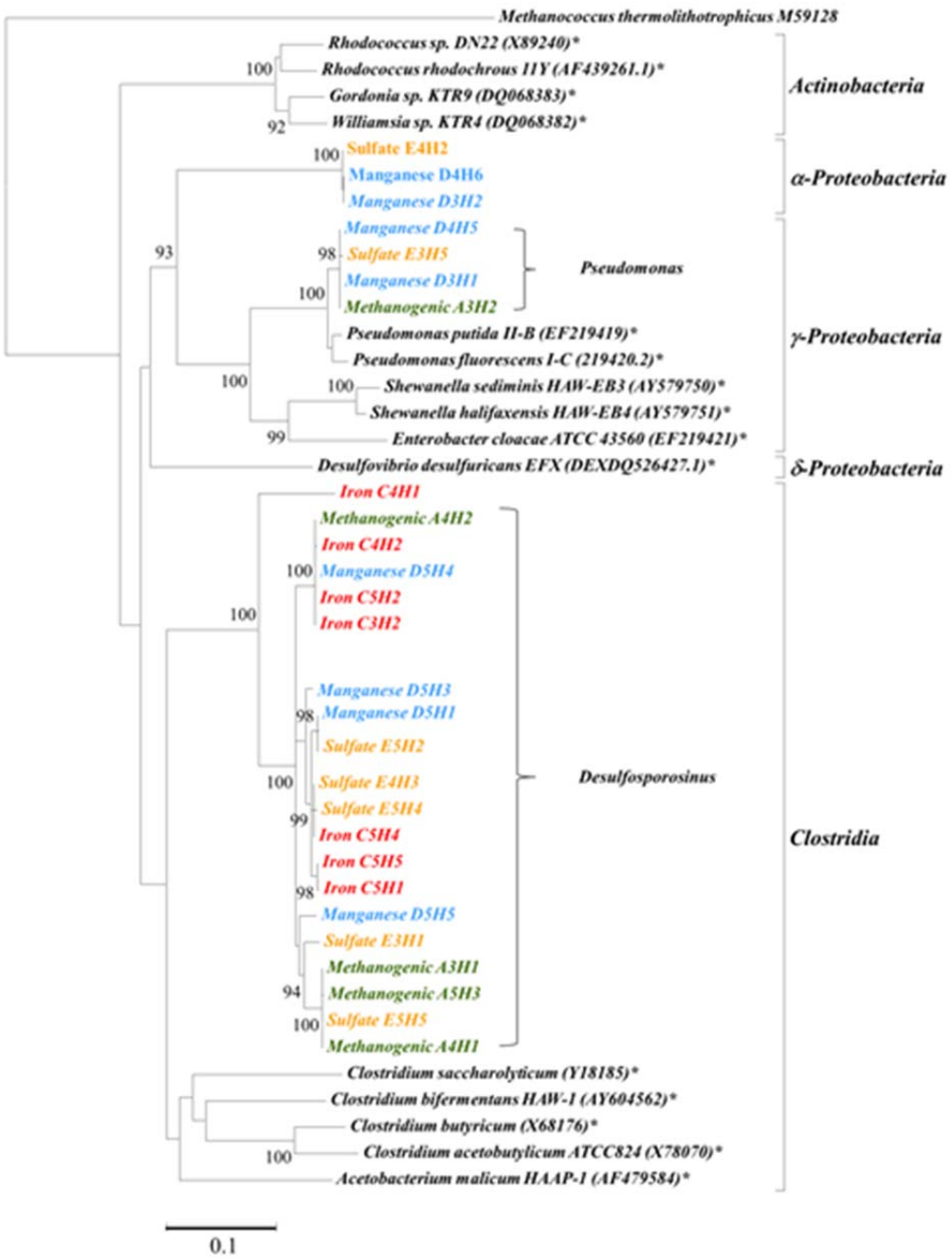

The tree was rooted with *Methanococcus thermolithotrophicus* and was constructed using the neighbor-joining algorithm. Only bootstrap values above 85% are shown (1,000 replications). Bar, 10% estimated sequence divergence. An asterisk (*) indicates a known RDX degrader.

Figure 2.3.5-6. Phylogenetic tree representing 16S rRNA gene sequences derived from ^{15}N-RDX SIP of groundwater microcosms under different electron accepting conditions (manganese, iron, sulfate and CO_2).

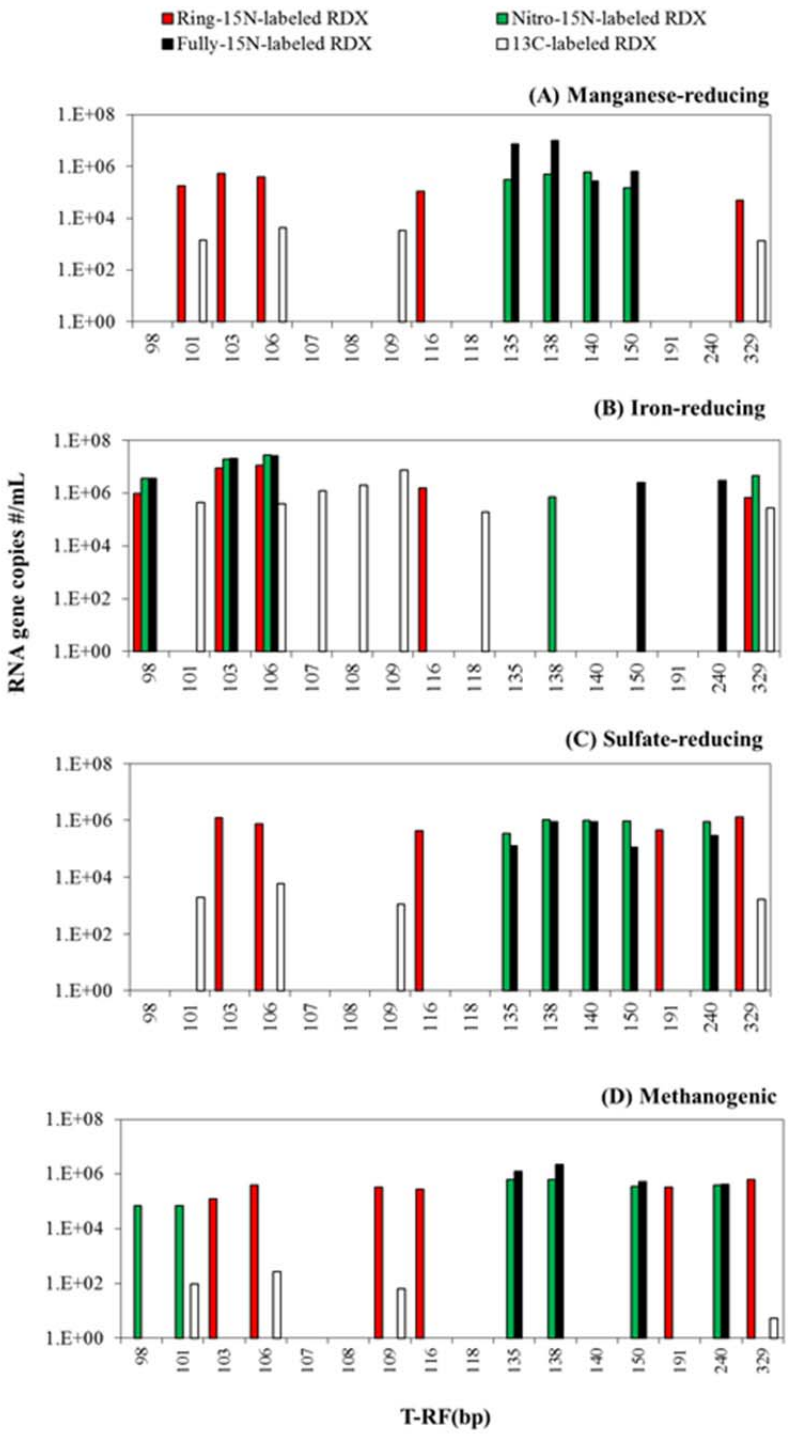

Figure 2.3.5-7. Microbial community structure of the ^{13}C- and ^{15}N-RDX SIP microcosms under (A) manganese-reducing (B) iron-reducing, (C) sulfate-reducing, (D) methanogenic conditions.

2.3.6 Unique Metabolite Formation from Stable Isotope-Labeled RDX

In conjunction with the microbial community studies detailed in **Section 2.3.4**, the metabolites produced during microbial degradation of ^{13}C- or ^{15}N-labeled RDX in Picatinny Arsenal SIP microcosms were also evaluated.

2.3.6.1 Metabolite Methods

During these studies, ^{13}C- or ^{15}N-labeled RDX and breakdown products from these RDX isotopomers were analyzed from the same bottles used for SIP analysis. Samples were collected and sent to Dr. Jalal Hawari at BRI for analysis. RDX, MNX, NDAB, and MEDINA were analyzed in samples prepared without sea salts by LC-MS. NDAB and MEDINA were quantified in samples prepared with and without sea salts by HPLC. Formaldehyde (HCHO) was analyzed in samples prepared with MeOH containing non-labeled and ^{13}C-labeled RDX after being derivatized by GC-MS and quantified by HPLC/UV. Nitrous oxide (N_2O) was quantified by GC-ECD in samples sent in serum bottles.

2.3.6.2 Metabolite Results and Discussion

LC-MS analysis of samples without sea salts prepared with non-labeled (F), ^{13}C- (G), ^{15}N-ring (H), ^{15}N-nitro (I) and ^{15}N-fully (J) labeled RDX was done using negative electrospray ionization mode (ES^-). The mass spectra of MNX, NDAB, and MEDINA are characterized by the deprotonated molecular mass ions $[M–H]^-$ and TFA adduct mass ions $[M+TFA]^-$, respectively. **Table 2.3.6-1** shows the calculated m/z of $[M+TFA]^-$ of RDX and MNX and $[M–H]^-$ of NDAB and MEDINA using the non-labeled, ^{13}C-, ^{15}N-ring, ^{15}N-nitro and ^{15}N-fully labeled compound.

Interestingly, NDAB was detected in all samples and was quantified in the series of samples prepared with and without sea salts (**Table 2.3.6-2**). RDX, MNX and MEDINA were not detected. The presence of NDAB in these enrichments under anoxic/anaerobic conditions is interesting, given that NDAB is generally considered to be a product of aerobic RDX degradation. However, as noted above, more recent research in our laboratory has indicated that NDAB can be produced under low oxygen conditions by *Rhodococcus* sp. (24).

Another compound that has not previously been observed during RDX degradation was detected with several ($[M–H]^-$) appearing at m/z 134, 136,136,135 and 137 for samples prepared with unlabeled, ^{13}C-, ^{15}N-ring, ^{15}N-nitro and ^{15}N-fully labeled RDX, respectively. We attributed these mass ions to an empirical formula $C_2H_5N_3O_4$ having two nitrogen atoms from the ring and one nitrogen atom from the nitro group in the molecule. Interestingly, a new peak with a UV spectrum similar to NDAB was observed at 8.8 min. showing higher intensity in the presence of sea salt **(Table 2.3.6-3)**. The two peaks that we observed in the LC-MS spectrum and in the HPLC chromatogram likely represent the same product. We suspect that this detected product is either a hydroxylated NDAB derivative or a carboxylic derivative, but more work is needed to

identify this product, which to our knowledge, has not previously been reported during RDX biodegradation.

Table 2.3.6-4 shows nitrous oxide (N_2O) concentrations measured by GC-ECD in samples designated for N_2O analysis. No MS analysis was done due to insufficient concentrations. Formaldehyde was analyzed in samples 1F (^{12}C-RDX, 1.99 mg/L), 2F (^{12}C-RDX, 2.50 mg/L), 1G (^{13}C-RDX, 1.69 mg/L), 2G (^{13}C-RDX, 1.81 mg/L) and in the MeOH control (0.045 mg/L) as its pentadione derivative by GC-MS. HCHO was detected using the characteristic mass at m/z 194 (^{13}C) and m/z 193 (^{12}C). The m/z ratio 194/193 of HCHO standard was 12.3 ± 0.3 similar to the theoretical value (12.3%). Surprisingly, in samples 1F and 2F (prepared with ^{12}C-RDX) the ratio was 11.6% ± 0.4, whereas in samples 1G and 2G (prepared with ^{13}C-RDX) the ratios were 13.1% and 14.4%, respectively, suggesting that 6.1 and 16.6% of formaldehyde originated from ^{13}C-RDX in samples 1G and 2G prepared with ^{13}C-RDX.

Table 2.3.6-1. Calculated m/z values ($[M+TFA]^-$) of RDX and MNX and ($[M–H]^-$) of NDAB and MEDINA from labeled RDX.

Description	RDX $[M+TFA]^-$	MNX $[M+TFA]^-$	NDAB $[M–H]^-$	MEDINA $[M–H]^-$
Unlabeled RDX	335	319	118	135
$^{13}C_3$-labeled RDX	338	322	120	136
$^{15}N_3$-ring labeled RDX	338	322	120	137
$^{15}N_3$-nitro labeled RDX	338	322	119	137
$^{15}N_6$-fully labeled RDX	441	325	121	139

Table 2.3.6-2. Molecular mass ions of NDAB detected by LC-MS and its quantification by HPLC/UV.

ID number	RDX Label	w/o sea salts $[M–H]^-$	HPLC/UV[a] (mg/L)	HPLC/UV[b] (mg/L)
PA GW SIP#3 – 1F	Unlabeled	118	1.68	1.37
PA GW SIP#3 – 1G	$^{13}C_3$	120	3.92	3.68
PA GW SIP#3 – 1H	$^{15}N_3$-ring	120	3.94	3.73
PA GW SIP#3 – 1I	$^{15}N_3$-nitro	119	1.76	1.28
PA GW SIP#3 – 1J	$^{15}N_6$-full	121	3.17	2.93
PA GW SIP#3 – 2F	Unlabeled	118	4.04	3.82
PA GW SIP#3 – 2G	$^{13}C_3$	120	4.57	4.55
PA GW SIP#3 – 2H	$^{15}N_3$-ring	120	4.44	4.26
PA GW SIP#3 – 2I	$^{15}N_3$-nitro	119	3.73	3.31
PA GW SIP#3 – 2J	$^{15}N_6$-full	121	4.14	3.95

[a]Without sea salt added.

[b]With sea salt added.

Table 2.3.6-3. HPLC/UV and molecular mass ions of the new RDX product detected.

ID number	RDX Label	w/o sea salts $[M–H]^-$	HPLC/UV[a] area x 10^{-5}	HPLC/UV[b] area x 10^{-5}
PA GW SIP#3 – 1F	Unlabeled	134	0.64	1.82
PA GW SIP#3 – 1G	$^{13}C_3$	136	0.55	1.30
PA GW SIP#3 – 1H	$^{15}N_3$-ring	136	0.32	0.75
PA GW SIP#3 – 1I	$^{15}N_3$-nitro	135	1.03	3.02
PA GW SIP#3 – 1J	$^{15}N_6$-full	137	0.51	1.37

[a]Without sea salt added.

[b]With sea salt added.

Table 2.3.6-4. Nitrous oxide (N_2O) concentrations measured by GC-ECD

ID number	RDX Label	N_2O (µg/L)
PA GW SIP#3 – 1F	Unlabeled	0
PA GW SIP#3 – 1G	$^{13}C_3$	0
PA GW SIP#3 – 1H	$^{15}N_3$-ring	6.2
PA GW SIP#3 – 1I	$^{15}N_3$-nitro	4.8
PA GW SIP#3 – 1J	$^{15}N_6$-full	0
PA GW SIP#3 – 2F	Unlabeled	14.5
PA GW SIP#3 – 2G	$^{13}C_3$	11.4
PA GW SIP#3 – 2H	$^{15}N_3$-ring	10.3
PA GW SIP#3 – 2I	$^{15}N_3$-nitro	23.9
PA GW SIP#3 – 2J	$^{15}N_6$-full	14.5

Note: Samples 1G, 2G, 1J and 2G designated for N_2O analysis were analyzed for NDAB by LC-MS. NDAB was found only in samples numbered 2 (G and J).

2.3.7 Conclusions from Dahlgren SIP Studies

A wide variety of organisms were identified using the ^{13}C- and ^{15}N-labeled RDX SIP approaches during this project, many of which have not formerly been associated with RDX biodegradation. It is reasonable to assume that the organisms identified in the methanogenic and sulfate reducing SIP enrichments were more likely to be directly responsible for RDX degradation, given the shorter incubation period (<40 days) and the relatively low percentages of persistent nitroso metabolites. In contrast, the longer incubation periods (100 to 260 days), and the overall persistence of nitroso metabolites observed with the iron and manganese reducing SIP enrichments would tend to indicate that the identified sequences likely included more "scavenger" organisms that incorporated the label from RDX metabolites.

Three major groups in α-*Proteobacteria* (unclassified *Rhizobiales*), γ-*Proteobacteria* (*Pseudomonas*), and *Clostridia* (*Desulfosporosinus*) were present and responsible for RDX and/or RDX-intermediate degradation under various electron- accepting conditions. Some *Desulfosporosinus* species are known for their adaptable metabolism, including their ability to use not only sulfate, but also nitrate, Fe(III), or As(V) as terminal electron acceptors (53). This might explain why the majority of clones detected in this study are clustered in the genus of *Desulfosporosinus* under each of the different electron-accepting conditions where RDX degradation was observed. Similarly, the frequent detection of sequences identified as *Pseudomonas* likely reflects the unique ability of this genus to use many different electron acceptors. The detection of sequences identified as *Pseudomonas* sp. from highly anaerobic enrichments (e.g., sulfate reducing and methanogenic conditions) has been reported previously

(50, 76, 83). The detection of *Pseudomonas* sp. during this study under differing geochemical conditions, and with both C and N SIP, highlights the wide diversity of this genus, and their importance in many environmental processes.

Our data suggest that, from a remediation perspective, sulfate-reducing or methanogenic conditions are desirable for RDX treatment in order to avoid the long-term accumulation of nitroso-intermediates. The selection of carbon substrate added during biostimulation may be one means of driving the degradative processes in a favorable direction. Use of emulsified vegetable oils has been shown to generate good sulfate-reducing and methanogenic conditions (unpublished data), and also serves as a long-term source of short chain organic acid that may favor the growth of preferred degradative genera like *Pseudomonas*. The data also suggest, surprisingly, that some groups of bacteria, such as *Desulfosporosinus,* can play an important role in RDX degradation under a variety of different dominant electron–accepting conditions. This genus is related to the *Clostridia*, which were also detected at a high frequency during previous field survey work at explosives-contaminated sites (26). One area for future study is better understanding of the roles of *Desulfosporosinus* and *Pseudomonas* (and closely-related species) during *in situ* RDX degradation.

Furthermore, the presence of NDAB as an intermediate was detected under anoxic conditons. This compound is typically detected during aerobic but not anoxic degradation of RDX. In addition, use of the differentially-labeled RDX molecules has allowed the detection of a possible new RDX metabolite, likely either a hydroxylated NDAB derivative or a carboxylic derivative. However, additional studies are needed to further identify this product which, to our knowledge, has not previously been reported during RDX biodegradation.

2.4 Task 4 – Compound-Specific Stable Isotope Analysis of RDX as a Measure of Biodegradation

2.4.1 Objective

During this task, methods were developed at the University of Illinois at Chicago (UIC) to analyze stable isotope ratios of both nitrogen ($\delta^{15}N$) and carbon ($\delta^{13}C$) in RDX. Unlike the SIP described in Task 3, RDX enriched in ^{15}N or ^{13}C was not required for this task; rather, this approach is applicable for RDX as it is found in the environment (i.e., with isotopes at natural abundance).

2.4.2 Introduction

Compound-specific stable isotope ratio analysis is increasingly being applied as an analytical tool to assess the biodegradation and environmental fate of industrial and military pollutants, including chlorinated solvents (64, 66) and, most recently, perchlorate (65, 67). This technique relies on the fact that bacteria biodegrade heavier isotopologues (e.g., RDX with ^{15}N vs. ^{14}N) more slowly than lighter ones due to the greater bond stability of the heavier molecules. This leads to the enrichment of parent molecules in heavier isotopes as biodegradation proceeds. An analysis of stable isotope ratios of a contaminant along the flow path of a plume and/or in contaminated groundwater compared to the contaminant source material can be utilized to conclusively document biodegradation and natural attenuation *in situ*. Thus, stable isotope analysis can be used as a powerful tool to quantify biodegradation in natural environments, and during enhanced bioremediation efforts.

2.4.3 Methods and Method Development

Solid Phase Extraction (SPE): A SPE technique was employed to concentrate RDX from aqueous solution. Superclean ENVI Chrom P SPE tubes (Supelco; 6 mL) were pretreated, which entailed washing each tube with 30 mL of acetonitrile followed by 50 mL of reagent-grade deionized water. For sample analysis, samples were passed slowly (<10 mL/min) through the SPE tubes under vacuum. Some samples were spiked with a 10 μL volume of surrogate (trinitrotoluene; 125 mg/L) to assess sample recovery. The tubes were dried for 15 min under vacuum. Sorbed RDX (and surrogate) were eluted from the SPE tubes under gravity flow with 12 mL of acetonitrile, and then briefly placed under vacuum to remove any remaining acetonitrile. Each extract was then brought to a final volume of 1 mL using a Turbo-Vap II (Zymark, Hopkinton, MA) and placed in a screw capped 2-mL GC vial.

Gas Chromatography - Isotope Ratio Mass Spectrometry (GC-IRMS): GC-IRMS techniques were developed at UIC for analysis of both $\delta^{15}N$ and $\delta^{13}C$ in RDX. Because bacterial degradation of RDX sometimes entails an initial denitration step (breaking a N-N bond), development of a precise technique for analysis of $\delta^{15}N$ in RDX is critical for estimating and documenting environmental biodegradation.

Carbon Isotope Analysis ($\delta^{13}C$): For analysis of $\delta^{13}C$ in RDX, C was converted to CO_2 gas after chromatographic separation of RDX. Different GC columns were initially tested for separation of RDX from other explosives and intermediates prior to combustion. The most effective column was determined to be a RTX-5MS (15 m length x 0.53 mm inner diameter x 0.5 μm film thickness; Restek, Inc.), with a 20 mL/min flow of He. During initial studies, RDX was observed to decompose at the column inlet. Reducing the inlet temperature to 190°C resolved this issue. The following GC program was used for C separation: 75°C x 1.5 min, ramp at 10°C/min to 200°C, then ramp 20°C/min to 300°C, which was maintained for 5 min. From the GC column the sample passed through a pre-oxidized Ni/Cu/Pt combustion furnace at 940°C, and the combustion products were then reduced in a separate furnace of Cu at 600°C. The resulting CO_2 was introduced to the mass spectrometer (Themo Finnigan Delta Plus XP) by an open split interface (Thermo Finnigan GCCIII) for quantification of C isotope amounts.

The C isotope ratio in RDX was reported as $\delta^{13}C$:

$$\delta^{13}C_{sample} = (^{13}C/^{12}C_{sample}) / (^{13}O/^{12}C_{VPDB}) - 1, \quad (1)$$

where VPDB is Vienna Pee Dee Belemnite. The $\delta^{13}C$ data are reported in parts per thousand (‰), and were calibrated by analyzing a laboratory reference material [ChemService (West Chester, PA) RDX concentration standard, 1000 μg/mL in acetonitrile, lot 388-132B] having a $\delta^{13}C$ value of -32.2 [calibrated against US Geological Survey isotopic reference materials USGS-40 and USGS-41 (L-glutamic acid)]. The average reproducibility of normalized $\delta^{13}C$ values is approximately ± 1.0 ‰, based on 300 replicate analyses.

Nitrogen Isotope Analysis ($\delta^{15}N$): The N in RDX was converted to N_2 gas prior to IRMS analysis. The basic method for ^{15}N analysis of N_2 gas generated from RDX was the same as that detailed for CO_2 with a few small modifications. The GC column is RTX-5MS (15 m length x 0.53 mm inner diameter x 0.5 um film thickness), with a 20 mL/min flow of He. The He inlet temperature was 190°C, and the GC oven temperature program was as follows: 75°C x 1.5 min, ramp at 10°C/min to 220°C, then ramp at 20°C/min to 300°C which was maintained for 5 min. From the GC column the sample passed through a Ni/Cu/Pt combustion furnace at 940°C. This furnace was not pre-oxidized (as is the case for CO_2) in order to minimize formation of NO. The combustion products then passed through a Cu reduction furnace at 600°C. CO_2 was trapped using liquid nitrogen, and the analyte N_2 was introduced to the mass spectrometer (Thermo Finnigan Delta Plus XP) by an open split interface (Thermo Finnigan GCCIII). The trapped CO_2 was flushed away after each sample.

The N isotope ratio in RDX was reported as $\delta^{15}N$:

$$\delta^{15}N_{sample} = (^{15}N/^{14}N_{sample}) / (^{15}N/^{14}N_{AIR}) - 1, \quad (2)$$

where AIR is N_2 in air. The $\delta^{15}N$ data are reported in parts per thousand (‰), and were calibrated by analyzing a laboratory reference material [ChemService (West Chester, PA) RDX concentration standard, 1000 µg/mL in acetonitrile, lot 388-132B] having a $\delta^{15}N$ value of 0.22 ‰ [calibrated against US Geological Survey isotopic reference materials USGS-40 and USGS-41 (L-glutamic acid)]. The average reproducibility of normalized $\delta^{15}N$ values is approximately ± 0.7 ‰, based on 400 replicate analyses.

Isotopic Fractionation Factor: The isotopic fractionation factor, α, is defined as

$$\alpha = R_A/R_B \quad (3)$$

where R is an isotope amount ratio, and A and B are two compounds (in the present case, product and reactant, respectively). For C and N in RDX, R represents the isotope ratios $^{13}C/^{12}C$, and $^{15}N/^{14}N$, respectively. Values of α can be determined from experimental data by assuming the function

$$R/R_0 = f^{\alpha-1} \quad (4)$$

where R and R_0 are the C or N isotope ratios of the residual RDX and the initial (unreacted) RDX, respectively, and f is the fraction of RDX remaining during the experiment. In terms of the δ values, Equation 4 can be rewritten as:

$$(\delta + 1)/(\delta_0 + 1) = f^{\alpha-1} \quad (5)$$

where δ is the isotopic composition of RDX at any value f, and δ_0 is the stable isotope ratio at f = 1. The value of α can be obtained from the natural log of Equation 5:

$$\alpha - 1 = \ln (R/R_o)/\ln f \quad (6)$$

This describes the mass-dependent Rayleigh-type isotopic fractionation that accompanies biodegradation and other natural processes. Isotopic fractionation factors are commonly expressed in terms of ε, where

$$\varepsilon = \alpha - 1. \quad (7)$$

2.4.4 Fractionation of C and N Isotopes by RDX-Degrading Pure Cultures

2.4.4.1 Methods

Bacterial strains: Bacterial strains capable of RDX biodegradation were acquired from several sources as follows: *Rhodococcus rhodochrous* 11Y (NCIMB 40820) (59), Dr. Neil C. Bruce, University of York, GB (via NCIMB Ltd., Aberdeen, UK) ; *Rhodococcus* sp. strain A and *Rhodococcus* sp. DN22 (14), Dr. Diane Fournier, National Research Council, Canada ; *Gordonia* sp. KTR9 (69) and *Shewanella oneidensis* MR-1, Dr. Fiona Crocker, U.S. Army Corps of Engineers, Engineer Research and Development Center (ERDC); *Klebsiella pneumoniae* SCZ-1 (78) and *Clostridium bifermentans* HAW-1 (81), Dr. Jian-Shen Zhao, National Research Council, Canada; *Pseudomonas fluorescens* I-C and *Pseudomonas putida* II-B, Dr. Brian Fox, University of Wisconsin (9); *Clostridium acetobutylicum* ATCC 824 (75), American Type Culture Collection; *Desulfovibrio* sp. EFX-DES, Dr. Clint Arnett, U.S. Army Corps of Engineers, Construction Engineering Research Laboratory (CERL) (3). Strains were stored as frozen stocks, and revived in appropriate media to check for purity prior to use.

Isotope fractionation studies: All isotopic fractionation tests were performed with initial RDX concentrations of approximately 20 mg/L. A minimum of duplicate experiments was performed with each strain. The *Rhodococcus* and *Gordonia* strains were screened in basal salts medium (BSM) (32) prepared without nitrilotriacetic acid (NTA). Sodium succinate was added initially at 1 g/L. Cultures were assayed in 950-mL amber glass bottles with stirring (400 rpm), and the headspace in the bottles was continuously purged with sterile humidified air to maintain aerobic conditions. The two *Pseudomonas* strains were screened in BSM amended with sodium succinate (1 g/L), and ammonium chloride (2 g/L). Cultures were assayed in 950-mL amber glass bottles with stirring (400 rpm), and the headspace in the bottles was continuously purged with sterile humidified nitrogen to maintain anoxic conditions. *Shewanella oneidensis* MR-1 and *Klebsiella pneumoniae* SCZ-1 were screened in a similar anoxic manner, substituting BSM amended with sodium lactate (1 g/L), sodium fumarate (3.6 g/L), trace minerals (mg/L: H_3BO_3, 5; $Na_2MoO_4 \cdot 2H_2O$, 2.5; $NiCl_2 \cdot 6H_2O$, 2.5; $CuCl_2 \cdot 2H2O$, 2.5; $NaSeO_3 \cdot 5H_2O$, 0.05; $NaWO_4 \cdot 2H_2O$, 0.05) and vitamins (0.1%, v:v; Sigma-Aldrich B6891) for *Shewanella*, and PYG medium (per L: peptone, 10; yeast extract, 5; glucose; 3) for *Klebsiella*, respectively.

Desulfovibrio and the *Clostridium* strains were screened under strict anaerobic conditions using autoclavable Applicon bioreactors (Cole Palmer, Vernon Hills, IL, USA) equipped with pH, temperature, DO, and mixer controls. *Desulfovibrio* was grown in anaerobic mineral medium (RAMM, prepared without sodium sulfide and resazurin) (61) amended with sodium lactate (1.35 g/L), Na_2SO_4 (1.42 g/L), yeast extract (150 mg/L), and ATCC vitamin supplement (1%, v:v). *Clostridium* strains were grown in reinforced clostridia broth (ATCC medium #2107) (http://www.atcc.org/Attachments/3260.pdf) amended with 1 g/L ammonium chloride during RDX degradation.

During isotope fractionation screening, samples were periodically removed, filtered through glass microfiber filters (GMF, 13 mm x 0.45 µm pore size), and analyzed for residual RDX concentrations using HPLC (see below). Additional nutrients were added as needed to sustain RDX degradation. Larger samples (40 mL to 250 mL) were removed over the course of the incubation, representing fractional RDX degradation in the range of approximately 0.05 to 0.95. Larger samples were filtered through GMF filters (25 mm x 0.45 µm pore size) to remove cells. The cleared sample was then passed over a pre-conditioned Supelclean™ ENVI-Chrom P solid phase extraction column (250 mg packing; Sigma-Aldrich, St. Louis, MO, USA). An aliquot (20 mL) of the supernatant was preserved at elevated pH with a pellet of KOH, and the remainder was frozen at -20°C. The analytes on the SPE column were eluted with acetonitrile according to the manufacturer's instructions, and the extract was dried to a volume of 1 mL. Final RDX and RDX breakdown product concentrations were determined using HPLC (see below). Additional culture aliquots were removed, filtered through 0.2 µm nylon syringe filters, and analyzed for nitrate and nitrate using either ion chromatography according to EPA Method 300.0 (www.nemi.gov/pls/nemi_pdf/nemi_data.download_pdf?p_file=152) or colorimetrically (Hach Company, Loveland, CO, USA).

After SPE concentration, the RDX samples were sent to the UIC laboratory for GC-IRMS analyses of C and N isotope ratios as described in **Section 2.4.3** above.

2.4.4.2 Results and Discussion

The fractionation of C and N isotopes in RDX was tested in 11 different strains, representing the three major pathways of RDX biodegradation as shown in **Figure 2.1.2-1**. Four strains were tested that aerobically degrade RDX using the the XplA/B cytochrome P450 system (*Rhodococcus* sp. DN22, *Rhodococcus rhodochrous* 11Y, *Rhodococcus* sp. strain A, and *Gordonia* sp. KTR9; Pathway A in **Figure 2.1.2-1**). The other 7 strains that were examined degrade RDX under anaerobic conditions using one or both of the pathways shown in **Figure 2.1.2-1** (Pathway A and Pathway B). We initially compared C and N fractionation under aerobic and anaerobic conditions, irrespective of the anaerobic pathway of degradation.

For the seven anaerobic strains tested, we attempted to obtain strains that degraded RDX either via Pathway A or Pathway B in **Figure 2.1.2-1,** and we measured total nitroso-intermediates to evaluate the extent to which the organisms reduced nitro ($N–NO_2$) groups in RDX to the corresponding nitroso (N–NO) groups resulting in the initial formation of MNX, followed by DNX and TNX (hereafter, NXs), and then possibly ring cleavage. In the absence of these intermediates, we assumed that strains were following Pathway B in **Figure 2.1.2-1,** which entails ring cleavage to the labile intermediate MEDINA, which was not measured during these studies. However, there were complications when studying these strains: (1) with one exception, strains that were presumed to degrade RDX primarily via Pathway A (nitro reduction) did not produce stoichiometric amounts of NXs during degradation, leaving the possibility that either

both pathways were operating at the same time, or that the NXs were being degraded more rapidly than RDX; (2) some of the strains that were reported to degrade RDX via a ring cleavage mechanism were observed to product NXs at some level, indicating that organisms degraded RDX via both pathways; and, (3) the reactions that initiate ring cleavage in RDX (and the enzymes catalyzing those reactions) may differ by strain, and entail direct ring cleavage by α-hydroxylation of a CH_2 group, N-denitration followed by ring cleavage, or another mechanism, potentially resulting in different extents of C and N fractionation. These different considerations are addressed on a strain-by-strain basis below.

Among four aerobic strains that were tested, degradation of RDX occurred in <30 hrs, and there was no detection of NXs, as expected based on the aerobic degradation pathway (**Figure 2.4.4-1**). For each of these strains, significant fractionation of N but not C was observed **Figure 2.4.4-2** and **Table 2.4.4-3**). The mean $\varepsilon^{15}N$ for the four strains was -2.4 ± 0.5 ‰, and the $\varepsilon^{13}C$ was -0.3 ± 1.0 ‰ (i.e., not statistically different from zero). The $\varepsilon^{15}N$ values calculated for the aerobic strains tested in this study are consistent with those previously calculated for three *Rhodococcus* sp. which varied from -1.9 to -2.3 ‰ (4, 5). This same group also reported no significant fractionation of C isotopes by the strains tested (5). From a mechanistic perspective, the enrichment in $\delta^{15}N$ but not $\delta^{13}C$ during aerobic RDX degradation is consistent with the initial cleavage of a N-N bond by the P450 enzyme(8, 15, 58), rather than a C-H bond as has also been postulated (30). If a C-H bond cleavage was the initial reaction, a significant enrichment in $\delta^{13}C$ rather than $\delta^{15}N$ would be expected as a primary isotope effect. Most importantly, the significant and consistent N isotope enrichment during aerobic biodegradation by all the strains tested suggests that CSIA analysis of N isotope ratios in RDX may be a useful tool to detect aerobic degradation of RDX *in situ.*

Two different pseudomonads that express xenobiotic reductase A (XenA; *P. putida* II-B) or xenobiotic Reductase B (XenB; *P. fluorescens* I-C) and degrade RDX under anoxic conditions were tested (25). Between these strains, only a trace of transient MNX was observed in one replicate (<5 % of total RDX on a molar basis; **Figure 2.4.4-1)**, which is generally consistent with a previous study showing no production or MNX, and hypothesizing that these strains degrade RDX via ring cleavage to MEDINA (Pathway B in **Figure 2.1.2-1** (25, 34)), rather than nitro-group reduction. A large N fractionation ($\varepsilon^{15}N$ = -13.0 ± 1.2 ‰) was observed for these cultures (**Figure 2.4.4-3)**. Carbon isotope fractionation in these strains was not as large but still significant and consistent ($\varepsilon^{13}C$ = -3.3 ± 0.6 ‰). The exact mechanism of enzymatic attack of XenA or XenB on RDX is not known, but may entail an initial denitration reaction based on the production of some nitrite during degradation (25). In this case, the observed C fractionation is likely a secondary isotope effect.

Four of the strains tested produced NXs in non-stoichiometric quantities **(Figure 2.4.4-1)**, suggesting that both degradation pathways may have been operating. Two of the strains,

Klebsiella pneumoniae SCZ-1 (78) and *Desulfovibrio* sp. EFX-DES (3) were each assumed to biodegrade RDX primarily through a ring cleavage mechanism based on previous pathway studies with each organism, although each produced small quantities of NXs, suggesting that some level of nitro reduction also occurred. The precise mechanism of ring cleavage during RDX degradation by these strains is not known, but possibilities include direct ring cleavage by α-hydroxylation of a CH_2 group or N-denitration followed by ring cleavage (6, 78). Other mechanisms are also possible. During our studies, *K. pneumoniae* SCZ-1 produced ~20 % NXs from the initial RDX on a molar basis, and the *Desulfovibrio* produced ~5 to 15 % NXs in different replicate samples. Thus, although some NXs were produced by these strains, the data suggest that they each metabolized RDX primarily through a ring cleavage pathway. Significant N and C stable isotope fractionation was observed for both strains. The mean $\varepsilon^{15}N$ and $\varepsilon^{13}C$ values for *Desulfovibrio* sp. EFX-DES were -10.6 ± 1.0 ‰ and -2.1 ± 0.0 ‰ and $\varepsilon^{15}N$ and $\varepsilon^{13}C$ values for *K. pneumoniae* SCZ-1 were -6.8 ± 0.9 ‰ and -4.0 ± 1.2 ‰, respectively. As previously noted, the differing C and N fractionation factors between these strains may reflect different initial mechanisms of enzymatic attack on RDX.

The final three strains, *Shewanella oneidensis* MR-1, *Clostridium acetobutylicum* ATCC 824,and *Clostridium bifermentans* HAW-1were selected because they were previously reported to degrade RDX primarily through nitro-reduction to MNX (52, 80) or possibly MNX plus hydroxylamino- and amino- derivatives of RDX without ring cleavage (75). The enzyme involved in RDX nitro-reduction by strain MR-1 was reported to be a c-type cytochrome involved in electron transport (51), while that used by *Clostridium acetobutylicum* was likely a nitroreductase enzyme (36, 75). *Clostridium bifermentans* HAW-1 was the only one of the three strains that appeared to stoichiometrically produce NXs from RDX (**Figure 2.4.4-1).** Unfortunately, components of the growth medium used for this strain caused interference during CSIA analysis, particularly for $\delta^{13}C$, and only one value of $\varepsilon^{15}N$ (-7.8 ‰) was obtained for the strain (**Figure 2.4.4-2** and **Table 2.4.4-3**). The other two strains produced between 20% and 55% NXs from RDX on a molar basis (**Figure 2.4.4-1**). Thus, these strains either degraded RDX via a ring cleavage pathway in addition to nitro-reduction or perhaps degraded the NXs after production. The mean $\varepsilon^{15}N$ and $\varepsilon^{13}C$ values for *S. oneidensis* MR-1 were -9.7 ± 0.3 ‰ and -7.1 ± 0.5 ‰ and $\varepsilon^{15}N$ and $\varepsilon^{13}C$ values for *Clostridium acetobutylicum* were -10.7 ± 4.1 ‰ and -4.5 ± 0.6 ‰, respectively. Significant C fractionation would not be expected by a pure nitro-reduction pathway, but each of these strains had the highest average values of $\varepsilon^{13}C$ of any of the strains tested. Thus, as suggested by analysis of NXs, other pathways of RDX transformation to be operating in these strains in addition to nitro-reduction.

Among all of the anaerobic strains tested, the mean $\varepsilon^{15}N$ and $\varepsilon^{13}C$ values were -10.4 ± 2.6 ‰ and -4.0 ± 1.7 ‰, respectively (**Table 2.4.4-3**). There are few other comparable isotope fractionation data for RDX during anaerobic biodegradation. Bernstein et al., (2008) reported an $\varepsilon^{15}N$ value of -5.0 ± 0.3 ‰ during RDX biodegradation by an anaerobic enrichment culture of unknown

composition, which is appreciably lower than the mean of our pure culture studies. However, the $\varepsilon^{15}N$ for the *Klebsiella* sp. we tested was -6.8 ‰ ± 0.9 ‰, which is only slightly higher than that of Bernstein et al., (4). To our knowledge no other values of $\varepsilon^{15}N$ or $\varepsilon^{13}C$ during anaerobic RDX degradation are currently available.

It would be very informative to obtain $\varepsilon^{13}C$ values for strains or pure enzymes that catalyze nitro-reduction reactions on RDX, forming MNX as an initial product. We were not able to obtain such values, either because we could not confirm that this was the only reaction that was occurring or, in the one case where this was the only reaction based on NX production, due to analytical issues from other compounds in the growth medium. It would also be important to confirm $\varepsilon^{15}N$ values under a strict nitro reduction pathway, as we were only able to obtain data for one sample.

2.4.4.3 Conclusions

The CSIA data presented herein for RDX indicate that N stable isotope ratio analysis can be useful for documenting both aerobic and anaerobic biodegradation of RDX, and potentially for discerning the two processes. In addition, C stable isotope analysis can be useful for documenting anaerobic (but not aerobic) biodegradation. Graphs showing all of the compiled $\delta^{15}N$ and $\delta^{13}C$ data for the aerobic and anaerobic strains are provided in **Figure 2.4.4-5** and **Figure 2.4.4-6**, respectively. As is apparent in **Figure 2.4.4-5**, significant and consistent fractionation of N is apparent under anaerobic conditions for all of the different strains tested, representing multiple mechanisms of RDX degradation (-11.5 ‰; r^2 = 0.9), and lesser but consistent fractionation is also apparent during aerobic degradation (-2.5 ‰; r^2 = 0.9). Moreover, these data are in general concurrence with the few previous reports using different microbial strains or enrichments, although our $\delta^{15}N$ values for anaerobic degradation are appreciably higher (4, 5). In contrast, there was no appreciable C fractionation in RDX during aerobic degradation, which is expected based upon the proposed mechanism of degradation by the XplA/B cytochrome P450 system (-0.8 ‰; r^2 = 0.2; **Figure 2.4.4-6)**. Interestingly, there was significant C fractionation during anaerobic RDX degradation for all of the strains for which data were available, although the extent of fractionation was highly variable (-4.3 ‰; r^2 = 0.5). This variability most likely reflects the fact that (1) strains appear to degrade RDX by multiple pathways in many instances; and, (2) the initial degradative step for RDX as it breaks down to MEDINA (which may be a multi-step process) may vary by strain, and reflect attack by different enzymes and mechanisms. Further work is required to better understand fractionation of C and N in RDX at an enzymatic and mechanistic level. However, the data presented herein suggest that CSIA may have broad application for documenting RDX biodegradation in groundwater. Additional studies are necessary to evaluate fractionation of C and N in RDX in natural systems and under differing geochemical conditions.

Figure 2.4.4-1. RDX biodegradation and breakdown product formation (when applicable) by pure cultures.

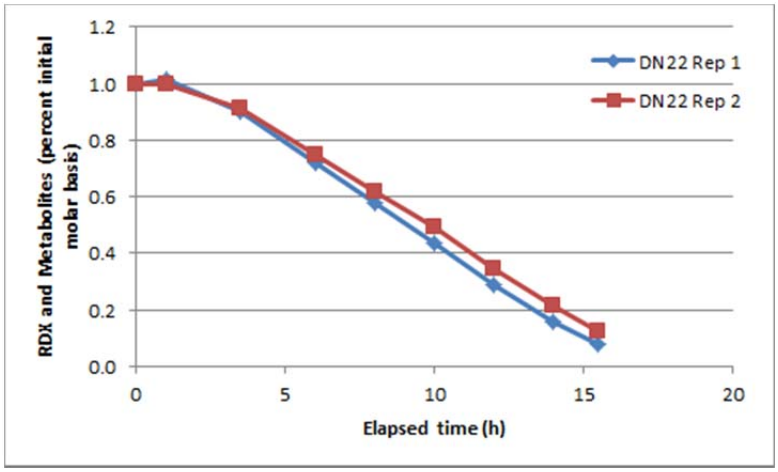

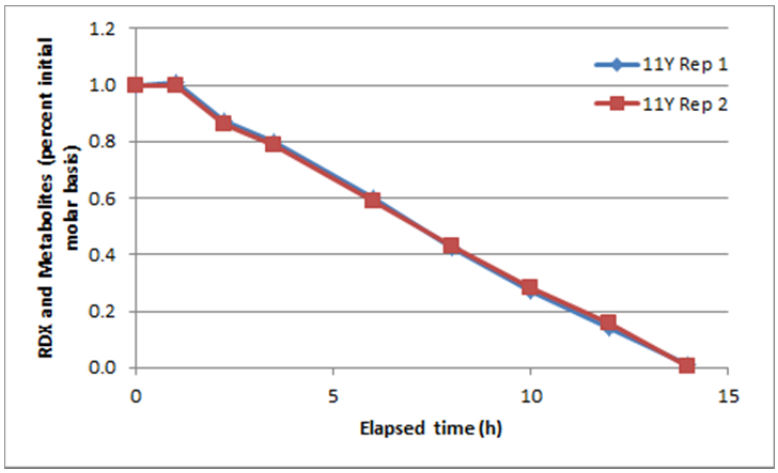

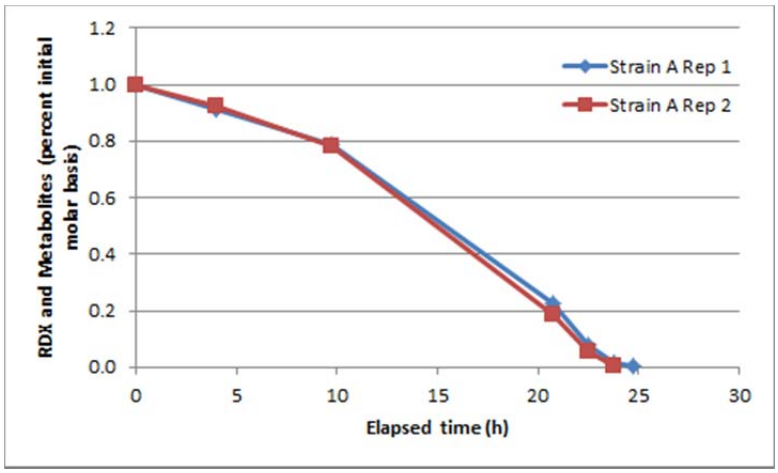

Figure 2.4.4-1. (cont.)

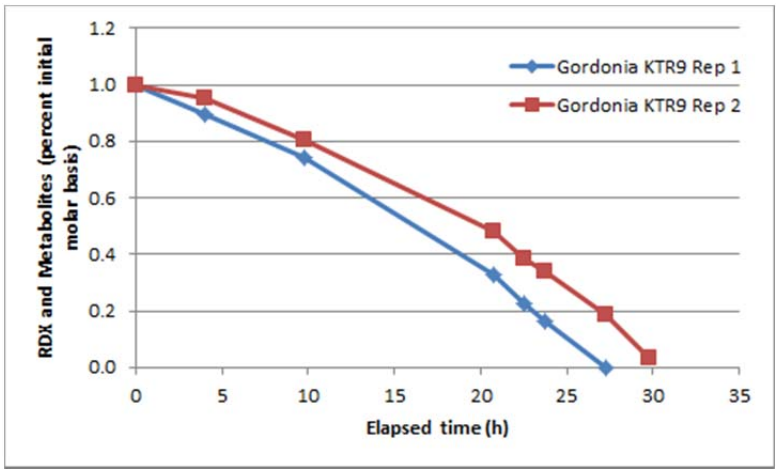

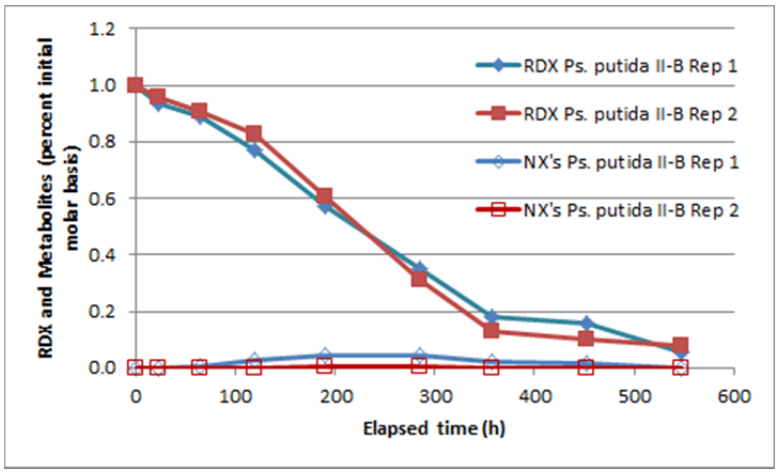

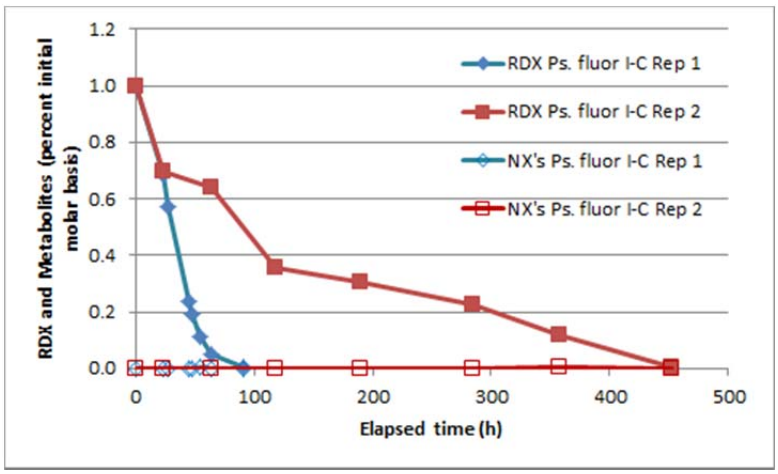

Figure 2.4.4-1. (cont.)

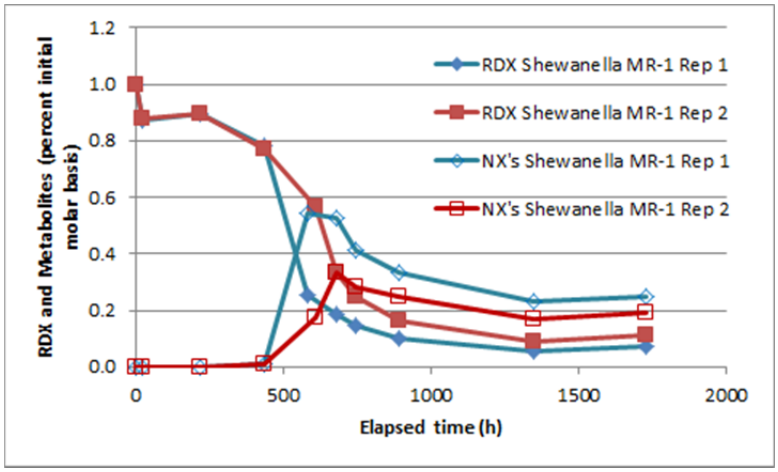

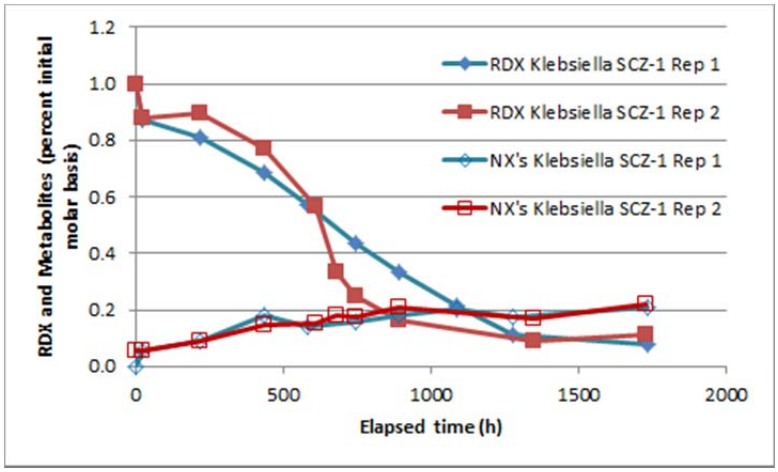

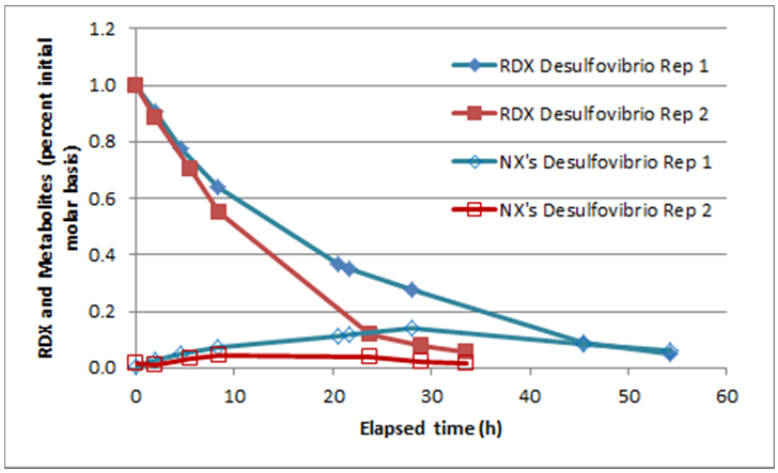

Figure 2.4.4-1. (cont.)

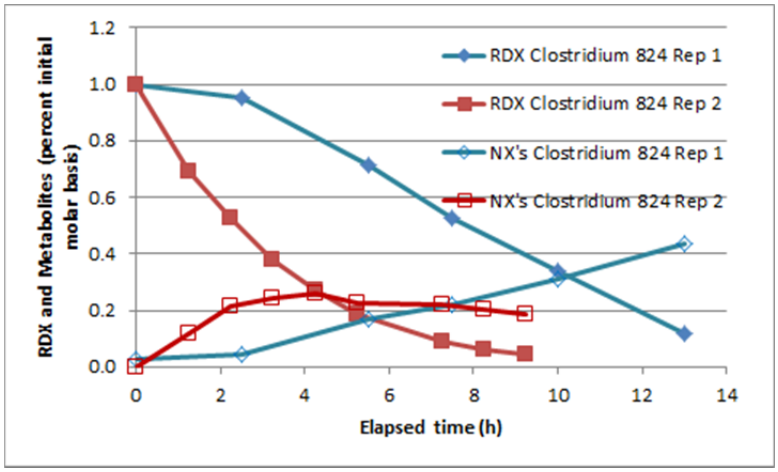

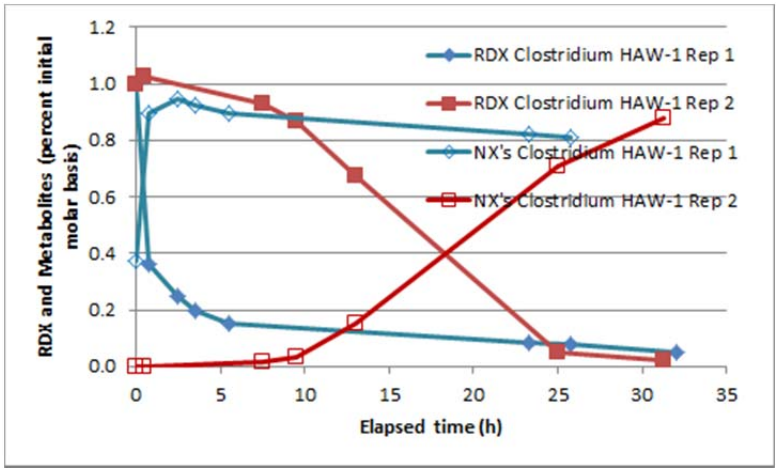

Figure 2.4.4-2. ^{13}C and ^{15}N fractionation during RDX biodegradation by pure cultures under aerobic conditions (Pathway C, Figure 2.4.4-6).

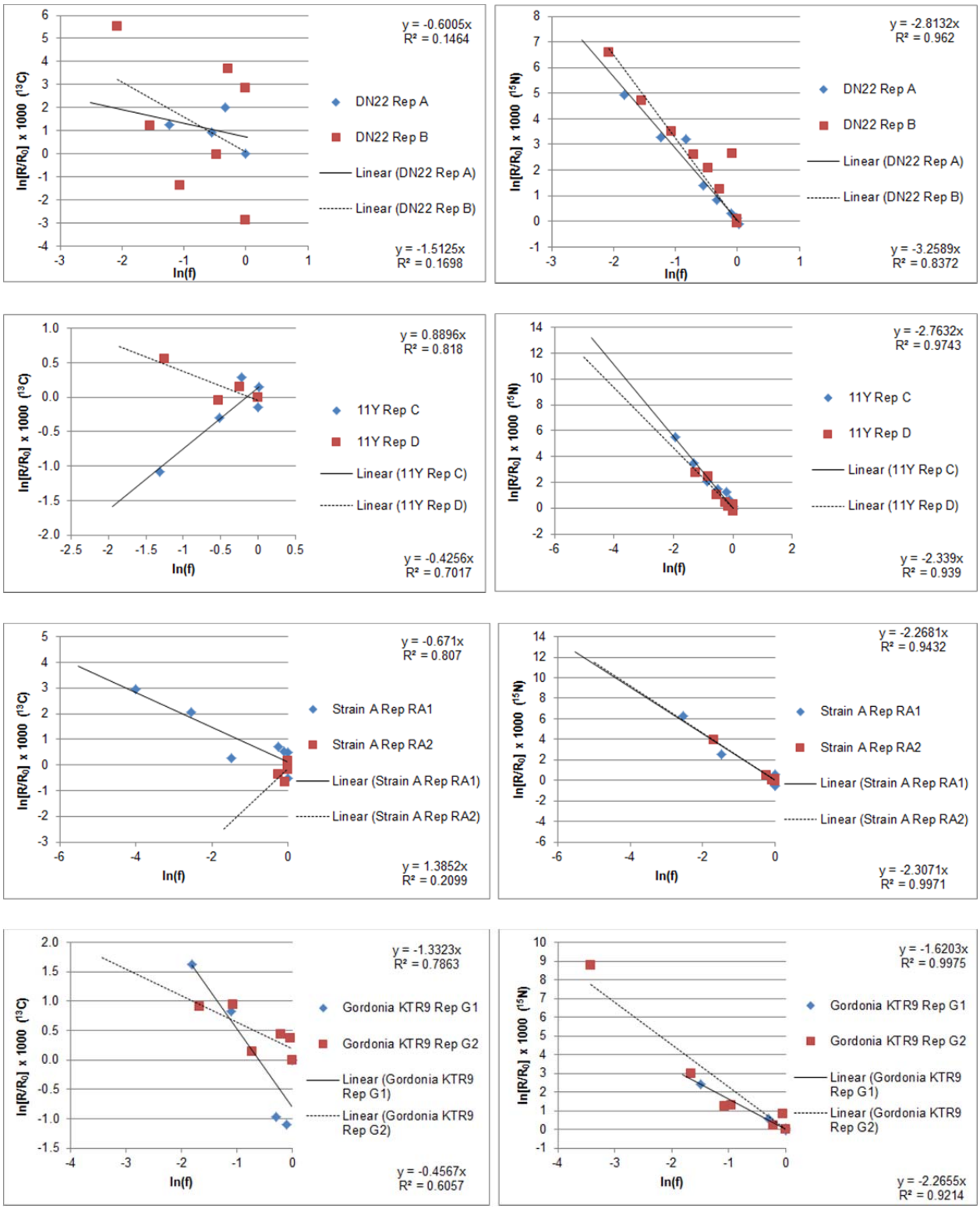

Figure 2.4.4-3. ^{13}C and ^{15}N fractionation during RDX biodegradation by pure cultures under anaerobic conditions (Pathway B, Figure 2.4.4-6).

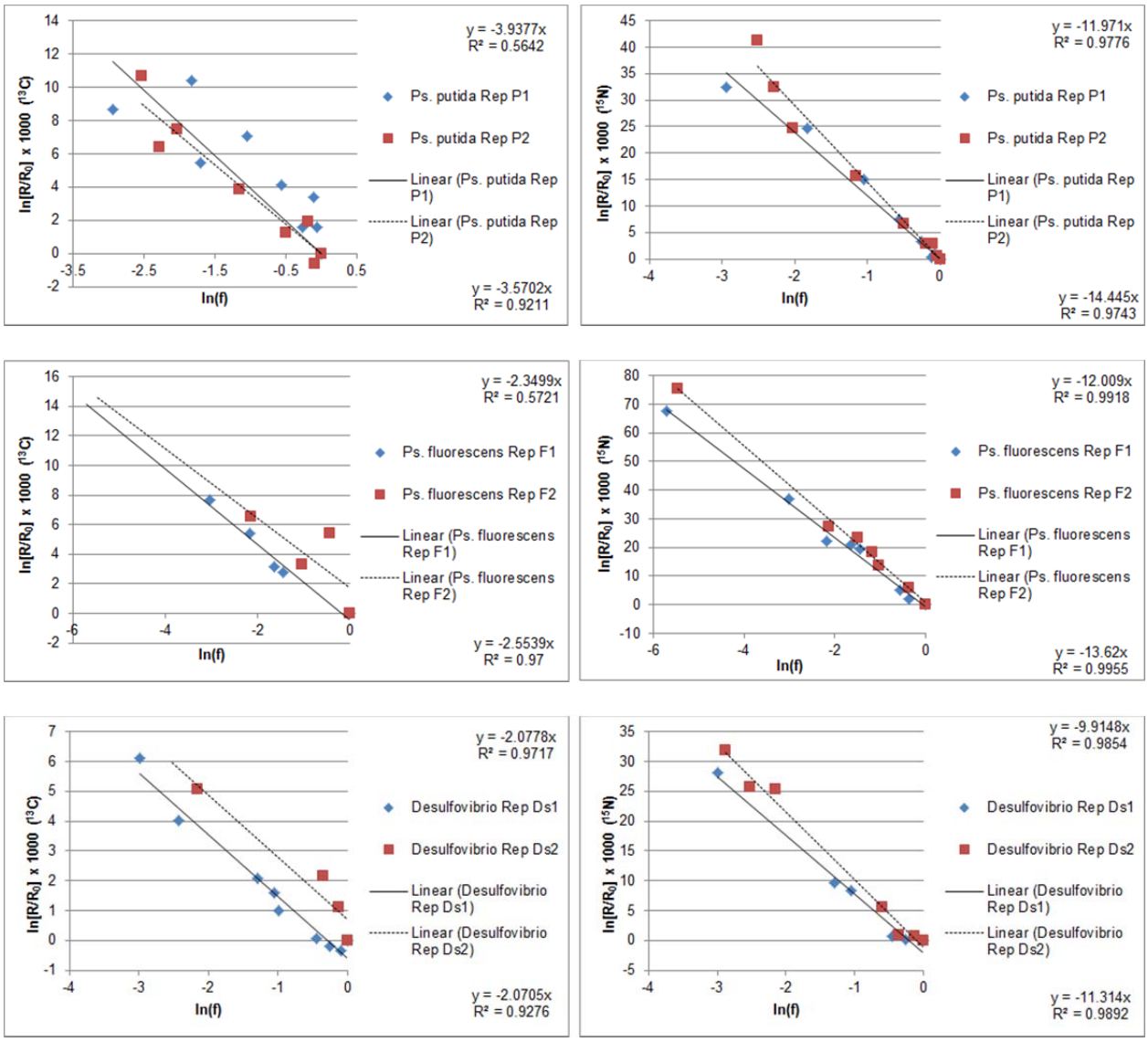

Figure 2.4.4-4. ^{13}C and ^{15}N fractionation during RDX biodegradation by pure cultures under anaerobic conditions (Pathway A, Figure 2.4.4-6).

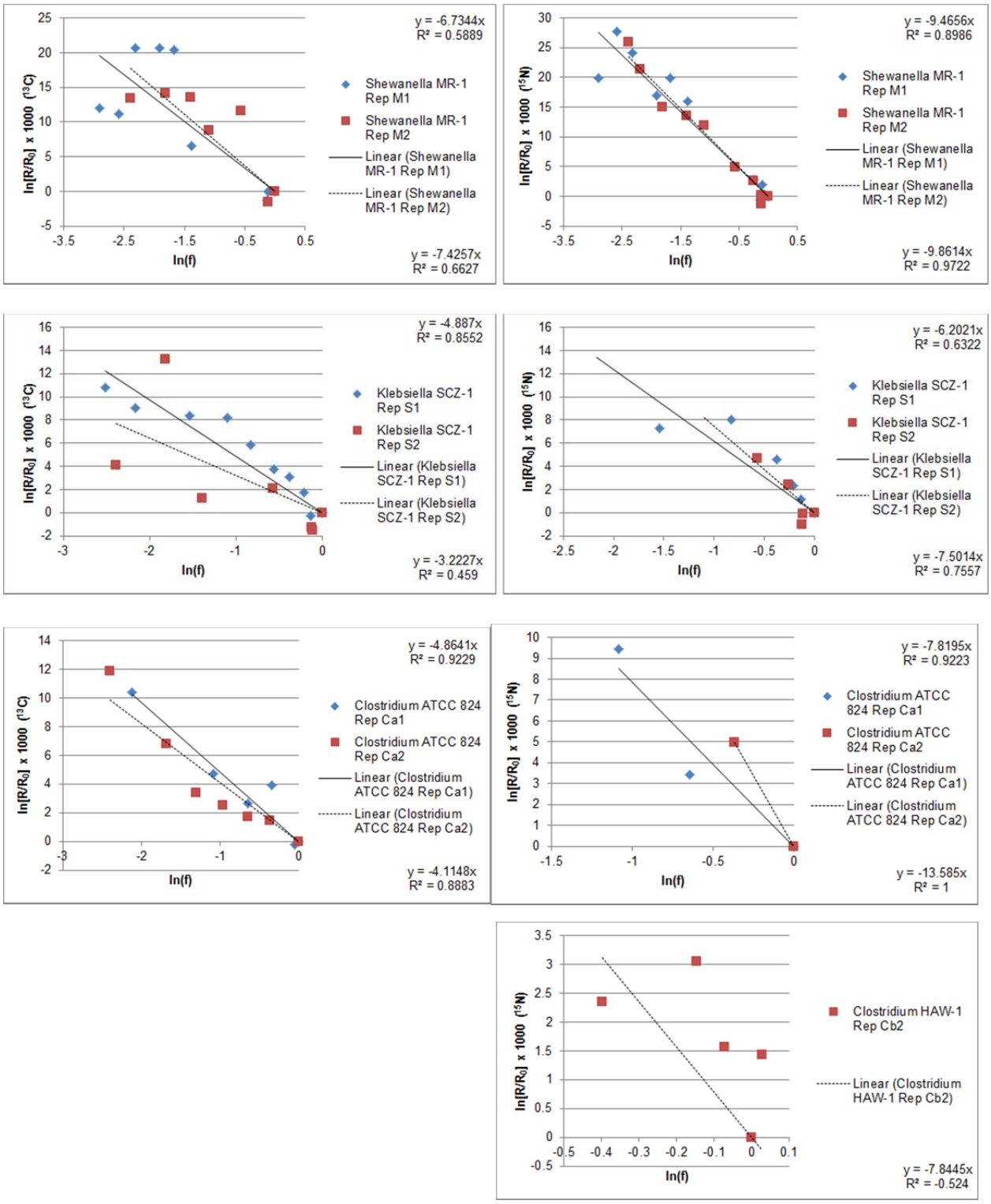

Figure 2.4.4-5. Nitrogen fractionation during RDX biodegradation by pure cultures using different degradation pathways.

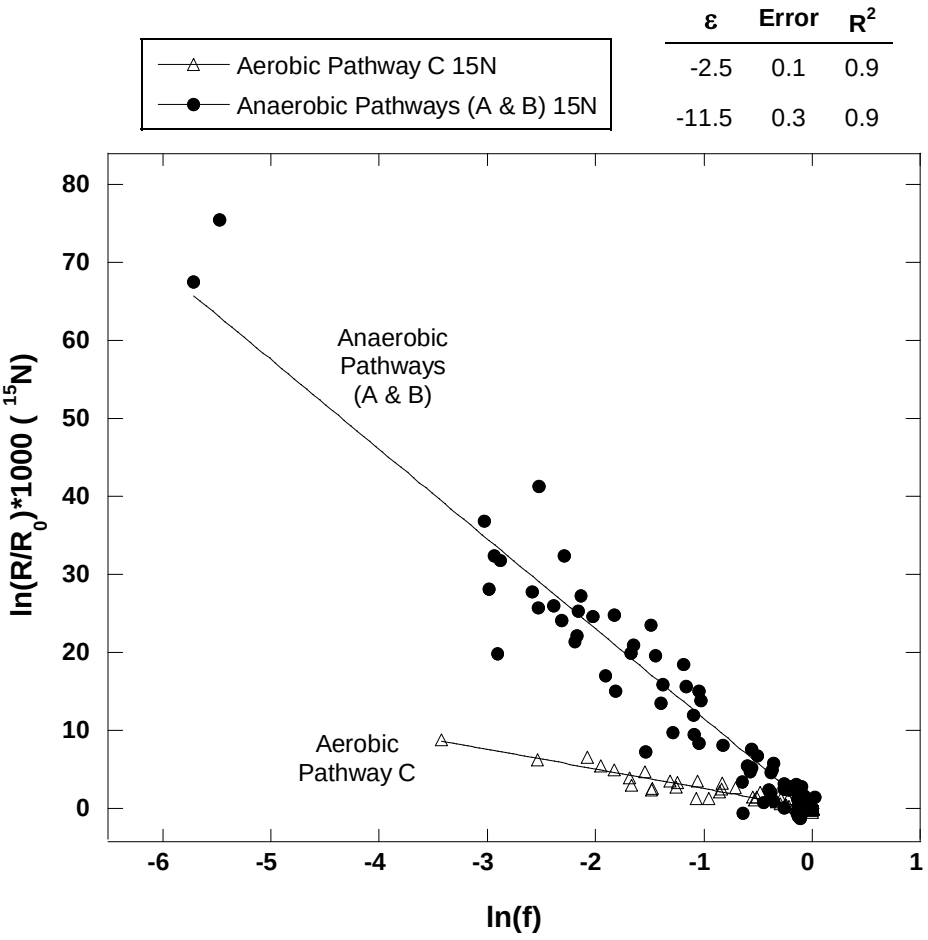

Figure 2.4.4-6. Carbon fractionation during RDX biodegradation by pure cultures using different degradation pathways.

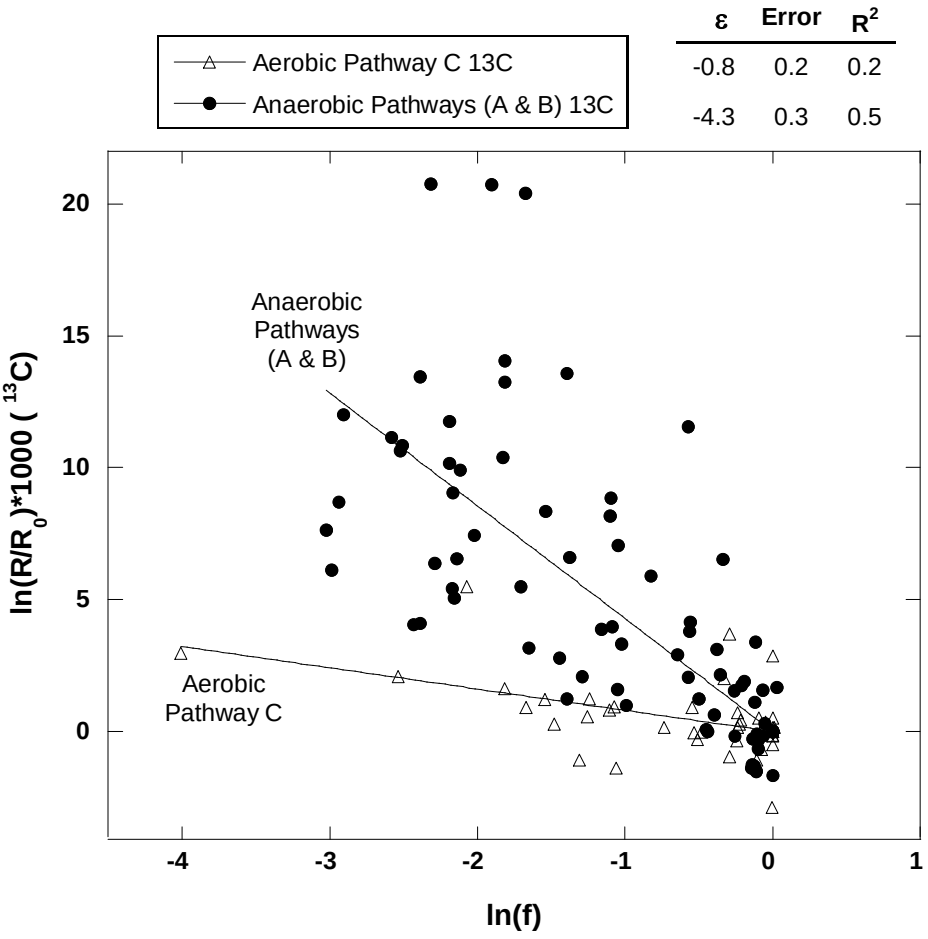

Table 2.4.4-3. ^{15}N and ^{13}C ε values from pure culture RDX biodegradation experiments.

	ε ^{13}C		ε ^{15}N	
Strain	**mean**	**St dev**	**mean**	**St dev**
Aerobic degradation				
Rhodococcus sp. DN22	-1.0	0.6	-3.0	0.3
Rhodococcus rhodochrous 11Y	0.3	0.9	-2.5	0.3
Rhodococcus sp. Strain A	0.4	1.5	-2.3	0.0
Gordonia sp. KTR9	-0.9	0.6	-2.0	0.5
All Aerobic Strains	**-0.3**	**1.0**	**-2.4**	**0.5**
Anaerobic degradation				
Pseudomonas putida II-B	-3.8	0.2	-13.2	1.8
Pseudomonas fluorescens I-C	-2.8	0.4	-12.8	1.1
Desulfovibrio sp. EFX-DES	-2.1	0.0	-10.6	1.0
Shewanella oneidensis MR-1	-7.1	0.5	-9.7	0.3
Klebsiella pneumoniae SCZ-1	-4.0	1.2	-6.8	0.9
Clostridium acetobutylicum ATCC 824	-4.5	0.6	-10.7	4.1
Clostridium bifermentans HAW-1	--	--	-7.8	NA
All Anaerobic Strains	**-4.0**	**1.7**	**-10.4**	**2.6**

--, no data due to analytical artifacts
NA – not available; only a single replicate was analyzed

3.0 REFERENCES CITED

1. **Adrian, N. R., and C. M. Arnett**. 2004. Anaerobic biodegradation of hexahydro-1,3,5-trinitro-1,3,5-triazine (RDX) by *Acetobacterium malicum* strain HAAP-1 isolated from a methanogenic mixed culture. Current Microbiology **48(5):** 332-340.
2. **Arnett, C., N. Adrian, D. Ringelberg, N. Wesslund, and K. Yenser**. 2009. Sulfate-mediated bacterial population shift in a hexahydro-1,3,5-trinitro-1,3,5-triazine (RDX)-degrading anaerobic enrichment culture. Bioremediation Journal **13(1):** 52-63.
3. **Arnett, C. M., and N. R. Adrian**. 2009. Cosubstrate independent mineralization of hexahydro-1,3,5-trinitro-1,3,5-triazine (RDX) by a *Desulfovibrio* species under anaerobic conditions. Biodegradation **20(1):** 15-26.
4. **Bernstein, A., Z. Ronen, E. Adar, R. Nativ, H. Lowag, W. Stichler, and R. U. Meckenstock**. 2008. Compound-specific isotope analysis of RDX and stable isotope fractionation during aerobic and anaerobic biodegradation. Environmental Science & Technology **42(21):** 7772–7777.
5. **Bernstein, A., Z. Ronen, and F. Gelman**. 2013. Insight on RDX Degradation Mechanism by Rhodococcus Strains Using 13C and 15N Kinetic Isotope Effects. Environmental Science & Technology **47(1):** 479-484.
6. **Bhushan, B., A. Halasz, J. C. Spain, and J. Hawari**. 2002. Diaphorase catalyzed biotransformation of RDX via N-denitration mechanism. Biochemical And Biophysical Research Communications **296(4):** 779-784.
7. **Bhushan, B., A. Halasz, S. Thiboutot, G. Ampleman, and J. Hawari**. 2004. Chemotaxis-mediated biodegradation of cyclic nitramine explosives RDX, HMX, and CL-20 by *Clostridium* sp. EDB2. Biochemical and Biophysical Research Communications **316(3):** 816-821.
8. **Bhushan, B., S. Trott, J. C. Spain, A. Halasz, L. Paquet, and J. Hawari**. 2003. Biotransformation of hexahydro-1,3,5-trinitro-1,3,5-triazine (RDX) by a rabbit liver cytochrome P450: Insight into the mechansism of RDX biodegradation by *Rhodococcus* sp. strain DN22. Applied And Environmental Microbiology **69(3):** 1347-1351.
9. **Blehert, D. S., B. G. Fox, and G. H. Chambliss**. 1999. Cloning and sequence analysis of two *Pseudomonas* flavoprotein xenobiotic reductases. Journal Of Bacteriology **181(20):** 6254-6263.
10. **Boopathy, R., M. Gurgas, J. Ullian, and J. F. Manning**. 1998. Metabolism of explosive compounds by sulfate-reducing bacteria. Current Microbiology **37(2):** 127-131.
11. **Buckley, D. H., V. Huangyutitham, S.-F. Hsu, and T. A. Nelson**. 2007. Stable isotope probing with ^{15}N achieved by disentangling the effects of genome G+C content and isotope enrichment on DNA density. Applied and Environmental Microbiology **73(10):** 3189-3195.
12. **Chen, W., F. Xiang, J. Fu, Q. Wang, W. Wang, Q. Zeng, and L. Yu**. 2009. Identification and phylogenetic analysis of new sulfate-reducing bacteria isolated from oilfield samples. Zeitschrift für Naturforschung C **64c:** 260-269.
13. **Cho, K.-C., D. G. Lee, H. K. Roh, M. E. Fuller, P. B. Hatzinger, and K.-H. Chu**. 2013. Application of ^{13}C-stable isotope probing to identify RDX-degrading microorganisms in groundwater. Environmental Pollution **178:** 350-360.

14. **Coleman, N. V., D. R. Nelson, and T. Duxbury**. 1998. Aerobic biodegradation of hexahydro-1,3,5-trinitro-1,3,5-triazine (RDX) as a nitrogen source by a *Rhodococcus* sp., strain DN22. Soil Biology & Biochemistry **30(8-9):** 1159-1167.
15. **Coleman, N. V., J. C. Spain, and T. Duxbury**. 2002. Evidence that RDX biodegradation by *Rhodococcus* strain DN22 is plasmid-borne and involves a cytochrome p-450. Journal of Applied Microbiology **93(3):** 463-472.
16. **Cummings, D. E., A. W. March, B. Bostick, S. Spring, F. Caccavo, S. Fendorf, and R. F. Rosenzweig**. 2000. Evidence for microbial Fe(III) reduction in anoxic, mining-impacted lake sediments (Lake Coeur d'Alene, Idaho). Applied and Environmental Microbiology **66(1):** 154-162.
17. **DeRito, C. M., G. M. Pumphrey, and E. L. Madsen**. 2005. Use of field-based stable isotope probing to identify adapted populations and track carbon flow through a phenol-degrading soil microbial community. Applied and Environmental Microbiology **71(12):** 7858-7865.
18. **Dionisi, H. M., A. C. Layton, G. Harms, I. R. Gregory, K. G. Robinson, and G. S. Sayler**. 2002. Quantification of *Nitrosomonas* oligotropha-like ammonia-oxidizing bacteria and *Nitrospira* spp. from full-scale wastewater treatment plants by competitive PCR. Applied and Environmental Microbiology **68(1):** 245-253.
19. **Finneran, K. T., C. V. Johnsen, and D. R. Lovley**. 2003. *Rhodoferax ferrireducens* sp. nov., a psychrotolerant, facultatively anaerobic bacterium that oxidizes acetate with the reduction of Fe(III). International Journal of Systematic and Evolutionary Microbiology **53(3):** 669-673.
20. **Fournier, D., A. Halasz, J. Spain, P. Fiurasek, and J. Hawari**. 2002. Determination of key metabolites during biodegradation of hexahydro-1,3,5-trinitro-1,3,5-triazine with *Rhodococcus* sp. strain DN22. Applied and Environmental Microbiology **68(1):** 166-172.
21. **Fournier, D., A. Halasz, J. Spain, R. J. Spanggord, J. C. Bottaro, and J. Hawari**. 2004. Biodegradation of the hexahydro-1,3,5-trinitro-1,3,5-triazine ring cleavage product 4-nitro-2,4-diazabutanal by *Phanerochaete chrysosporium*. Applied and Environmental Micrbiology **70(2):** 1123-1128.
22. **Fournier, D., S. Trott, J. Hawari, and J. Spain**. 2005. Metabolism of the aliphatic nitramine 4-nitro-2,4-diazabutanal by Methylobacterium sp. strain JS178. Applied and Environmental Micrbiology **71(8):** 4199-4202.
23. **Freedman, D. L., and K. W. Sutherland**. 1998. Biodegradation of hexahydro-1,3,5-trinitro-1,3,5-triazine (RDX) under nitrate-reducing conditions. Water Science And Technology **38(7):** 33-40.
24. **Fuller, M. E., J. Hawari, and N. Perreault**. 2010. Microaerophilic degradation of hexahydro-1,3,5-trinitro-1,3,5-triazine (RDX) by three *Rhodococcus* strains. Letters In Applied Microbiology **51(3):** 313-318.
25. **Fuller, M. E., K. McClay, J. Hawari, L. Paquet, T. E. Malone, B. G. Fox, and R. J. Steffan**. 2009. Transformation of RDX and other energetic compounds by xenobiotic reductases XenA and XenB. Applied Microbiology And Biotechnology **84(3):** 535-544.
26. **Fuller, M. E., K. McClay, M. Higham, P. B. Hatzinger, and R. J. Steffan**. 2010. Hexahydro-1,3,5-trinitro-1,3,5-triazine (RDX) bioremediation in groundwater: Are known RDX-degrading bacteria the dominant players? Bioremediation Journal **14(3):** 121-134.

27. **Gieg, L. M., K. E. Duncan, and J. M. Suflita**. 2008. Bioenergy production via microbial conversion of residual oil to natural gas. Applied and Environmental Microbiology **74(10):** 3022-3029.
28. **Ginige, M. P., J. Keller, and L. L. Blackall**. 2005. Investigation of an acetate-fed denitrifying microbial community by stable isotope probing, full-cycle rRNA analysis, and fluorescent in situ hybridization-microautoradiography. Applied and Environmental Microbiology **71(12):** 8683-8691.
29. **Gregory, K. B., P. Larese-Casanova, G. F. Parkin, and M. M. Scherer**. 2004. Abiotic transformation of hexahydro-1,3,5-trinitro-1,3,5-triazine by Fe^{II} bound to magnetite. Environmental Science & Technology **38(5):** 1408-1414.
30. **Halasz, A., D. Manno, S. E. Strand, N. C. Bruce, and J. Hawari**. 2010. Biodegradation of RDX and MNX with Rhodococcus sp. Strain DN22: New Insights into the Degradation Pathway. Environmental Science & Technology **44(24):** 9330-9336.
31. **Halasz, A., J. Spain, L. Paquet, C. Beaulieu, and J. Hawari**. 2002. Insights into the formation and degradation mechanisms of methylenedinitramine during the incubation of RDX with anaerobic sludge. Environmental Science & Technology **36(4):** 633-638.
32. **Hareland, W. A., R. L. Crawford, P. J. Chapman, and S. Dagley**. 1975. Metabolic function and properties of 4-hydroxyphenylacetic acid 1-hydroxylase from *Pseudomonas acidovorans*. Journal of Bacteriology **121(1):** 272-285.
33. **Harms, G., A. C. Layton, H. M. Dionisi, I. R. Gregory, V. M. Garrett, S. A. Hawkins, K. G. Robinson, and G. S. Sayler**. 2002. Real-time PCR quantification of nitrifying bacteria in a municipal wastewater treatment plant. Environmental Science & Technology **37(2):** 343-351.
34. **Hawari, J., A. Halasz, T. Sheremata, S. Beaudet, C. Groom, L. Paquet, C. Rhofir, G. Ampleman, and S. Thiboutot**. 2000. Characterization of metabolites during biodegradation of hexahydro-1,3,5-trinitro-1,3,5-triazine (RDX) with municipal anaerobic sludge. Applied And Environmental Microbiology **66(6):** 2652-2657.
35. **Just, C. L., and J. L. Schnoor**. 2003. Phytophotolysis of hexahydro-1,3,5-trinitro-1,3,5-triazine (RDX) in leaves of reed canary grass. Environmental Science & Technology **38(1):** 290-295.
36. **Kutty, R., and G. N. Bennett**. 2005. Biochemical characterization of trinitrotoluene transforming oxygen-insensitive nitroreductases from *Clostridium acetobutylicum* ATCC 824. Archives Of Microbiology **184(3):** 158-167.
37. **Kwon, M. J., E. J. O'Loughlin, D. A. Antonopoulos, and K. T. Finneran**. 2011. Geochemical and microbiological processes contributing to the transformation of hexahydro-1,3,5-trinitro-1,3,5-triazine (RDX) in contaminated aquifer material. Chemosphere **84(9):** 1223-1230.
38. **Liu, A., E. Garcia-Dominguez, E. D. Rhine, and L. Y. Young**. 2004. A novel arsenate respiring isolate that can utilize aromatic substrates. FEMS Microbiology Ecology **48(3):** 323-332.
39. **Liu, J.-R., R. S. Tanner, P. Schumann, N. Weiss, C. A. McKenzie, P. H. Janssen, E. M. Seviour, P. A. Lawson, T. D. Allen, and R. J. Seviour**. 2002. Emended description of the genus *Trichococcus*, description of *Trichococcus collinsii* sp. nov., and reclassification of *Lactosphaera pasteurii* as *Trichococcus pasteurii* comb. nov. and of *Ruminococcus palustris* as *Trichococcus palustris* comb. nov. in the low-G+C gram-

positive bacteria. International Journal of Systematic and Evolutionary Microbiology **52(4):** 1113-1126.

40. **Livermore, J. A., Y. O. Jin, R. W. Arnseth, M. LePuil, and T. E. Mattes**. 2013. Microbial community dynamics during acetate biostimulation of RDX-contaminated groundwater. Environmental Science & Technology **47(14):** 7672-7678.
41. **Lu, Y., T. Lueders, M. W. Friedrich, and R. Conrad**. 2005. Detecting active methanogenic populations on rice roots using stable isotope probing. Environmental Microbiology **7(3):** 326-336.
42. **Lueders, T., B. Wagner, P. Claus, and M. W. Friedrich**. 2004. Stable isotope probing of rRNA and DNA reveals a dynamic methylotroph community and trophic interactions with fungi and protozoa in oxic rice field soil. Environmental Microbiology **6(1):** 60-72.
43. **Martineau, C., L. G. Whyte, and C. W. Greer**. 2008. Development of a SYBR safe™ technique for the sensitive detection of DNA in cesium chloride density gradients for stable isotope probing assays. Journal of Microbiological Methods **73(2):** 199-202.
44. **Meyer, D., B. Witholt, and A. Schmid**. 2005. Suitability of recombinant *Escherichia coli* and *Pseudomonas putida* strains for selective biotransformation of m-nitrotoluene by xylene monooxygenase. Applied and Environmental Micrbiology **71(11):** 6624-6632.
45. **Monteil-Rivera, F., L. Paquet, A. Halasz, M. T. Montgomery, and J. Hawari**. 2005. Reduction of octahydro-1,3,5,7- tetranitro-1,3,5,7-tetrazocine by zerovalent iron: Product distribution. Environmental Science & Technology **39(24):** 9725-9731.
46. **Motta, A. S., and A. Brandelli**. 2003. Influence of growth conditions on bacteriocin production by Brevibacterium linens. Applied Microbiology and Biotechnology **62:** 163-167.
47. **Oh, B.-T., C. L. Just, and P. J. J. Alvarez**. 2001. Hexahydro-1,3,5-trinitro-1,3,5-triazine mineralization by zerovalent iron and mixed anaerobic cultures. Environmental Science & Technology **35(21):** 4341-4346.
48. **Oladimeji, A. T.** 2011. Kinetics of microbial production of 2, 3-butanediol from cheese whey using *Klebsiella pneumonia*. International Journal of Bioscience, Biochemistry and Bioinformatics **1:** 177-183.
49. **Pak, J. W., K. L. Knoke, D. R. Noguera, B. G. Fox, and G. H. Chambliss**. 2000. Transformation of 2,4,6-trinitrotoluene by purified xenobiotic reductase B from *Pseudomonas fluorescens* I-C. Applied And Environmental Microbiology **66(11):** 4742-4750.
50. **Park, H. S., I. Chatterjee, X. Dong, S.-H. Wang, C. W. Sensen, S. M. Caffrey, T. R. Jack, J. Boivin, and G. Voordouw**. 2011. Effect of sodium bisulfite injection on the microbial community composition in a brackish-water-transporting pipeline. Applied and Environmental Microbiology **77(19):** 6908-6917.
51. **Perreault, N. N., F. H. Crocker, K. J. Indest, and J. Hawari**. 2012. Involvement of cytochrome c CymA in the anaerobic metabolism of RDX by *Shewanella oneidensis* MR-1. Canadian Journal of Microbiology **58(2):** 124-131.
52. **Perreault, N. N., A. Halasz, D. Manno, S. Thiboutot, G. Ampleman, and J. Hawari**. 2012. Aerobic mineralization of nitroguanidine by *Variovorax* strain VC1 isolated from soil. Environmental Science & Technology **46(11):** 6035-6040.
53. **Pester, M., E. Brambilla, D. Alazard, T. Rattei, T. Weinmaier, J. Han, S. Lucas, A. Lapidus, J.-F. Cheng, L. Goodwin, S. Pitluck, L. Peters, G. Ovchinnikova, H. Teshima, J. C. Detter, C. S. Han, R. Tapia, M. L. Land, L. Hauser, N. C. Kyrpides,**

N. N. Ivanova, I. Pagani, M. Huntmann, C.-L. Wei, K. W. Davenport, H. Daligault, P. S. G. Chain, A. Chen, K. Mavromatis, V. Markowitz, E. Szeto, N. Mikhailova, A. Pati, M. Wagner, T. Woyke, B. Ollivier, H.-P. Klenk, S. Spring, and A. Loy. 2012. Complete Genome Sequences of *Desulfosporosinus orientis* DSM765T, *Desulfosporosinus youngiae* DSM17734T, *Desulfosporosinus meridiei* DSM13257T, and *Desulfosporosinus acidiphilus* DSM22704T. Journal of Bacteriology **194(22):** 6300-6301.

54. **Raynal-Gutierrez, M. E.** 2007. Bacterial Dynamics During Aerobic and Anoxic Biodegradation of MTBE at Bench and Pilot-scale. Doctor of Philosophy. Colorado State University,
55. **Robertson, W. J., J. P. Bowman, P. D. Franzmann, and B. J. Mee**. 2001. *Desulfosporosinus meridiei* sp. nov., a spore-forming sulfate-reducing bacterium isolated from gasolene-contaminated groundwater. International Journal of Systematic and Evolutionary Microbiology **51(1):** 133-40.
56. **Roh, H., C.-P. Yu, M. E. Fuller, and K.-H. Chu**. 2009. Identification of hexahydro-1,3,5-trinitro-1,3,5-triazine (RDX)-degrading microorganisms via ^{15}N-stable isotope probing. Environmental Science and Technology **43(7):** 2505–2511.
57. **Senko, J. M., G. Zhang, J. T. McDonough, M. A. Bruns, and W. D. Burgos**. 2009. Metal reduction at low pH by a *Desulfosporosinus* species: Implications for the biological treatment of acidic mine drainage. Geomicrobiology Journal **26(2):** 71-82.
58. **Seth-Smith, H. M. B., J. Edwards, S. J. Rosser, D. A. Rathbone, and N. C. Bruce**. 2008. The explosive-degrading cytochrome P450 system is highly conserved among strains of *Rhodococcus* spp. Applied And Environmental Microbiology **74(14):** 4550-4552.
59. **Seth-Smith, H. M. B., S. J. Rosser, A. Basran, E. R. Travis, E. R. Dabbs, S. Nicklin, and N. C. Bruce**. 2002. Cloning, sequencing, and characterization of the hexahydro-1,3,5-trinitro-1,3,5-triazine degradation gene cluster from *Rhodococcus rhodochrous*. Applied and Environmental Microbiology **68(10):** 4764-4771.
60. **Setlow, P.** 2003. Spore germination. Current Opinion in Microbiology **6:** 550-556.
61. **Shelton, D. R., and J. M. Tiedje**. 1984. General method for determining anaerobic biodegradation potential. Applied and Environmental Microbiology **47(4):** 850-857.
62. **Sherburne, L. A., J. D. Shrout, and P. J. J. Alvarez**. 2005. Hexahydro-1,3,5-trinitro-1,3,5-triazine (RDX) degradation by *Acetobacterium paludosum*. Biodegradation **16(6):** 539-547.
63. **Sheremata, T. W., A. Halasz, L. Paquet, S. Thiboutot, G. Ampleman, and J. Hawari**. 2001. The fate of the cyclic nitramine explosive RDX in natural soil. Environmental Science & Technology **35(6):** 1037-1040.
64. **Song, D. L., M. E. Conrad, K. S. Sorenson, and L. Alvarez-Cohen**. 2002. Stable carbon isotope fractionation during enhanced in situ bioremediation of trichloroethene. Environmental Science & Technology **36(10):** 2262-2268.
65. **Sturchio, N. C., J. K. Böhlke, A. D. Beloso, S. H. Streger, L. J. Heraty, and P. B. Hatzinger**. 2007. Oxygen and chlorine isotopic fractionation during perchlorate biodegradation: Laboratory results and implications for forensics and natural attenuation studies. Environmental Science & Technology **41(8):** 2796-2802.

66. **Sturchio, N. C., J. L. Clausen, L. J. Heraty, L. Huang, B. D. Holt, and T. A. Abrajano**. 1998. Chlorine isotope investigation of natural attenuation of trichloroethene in an aerobic aquifer. Environmental Science & Technology **32(20):** 3037-3042.
67. **Sturchio, N. C., P. B. Hatzinger, M. D. Arkins, C. Suh, and L. J. Heraty**. 2003. Chlorine isotope fractionation during microbial reduction of perchlorate. Environmental Science & Technology **37(17):** 3859-3863.
68. **Thompson, J. D., T. J. Gibson, F. Plewniak, F. Jeanmougin, and D. G. Higgins**. 1997. The CLUSTAL_X Windows interface: Flexible strategies for multiple sequence alignment aided by quality analysis tools. Nucleic Acids Research **25(24):** 4876-4882.
69. **Thompson, K. T., F. H. Crocker, and H. L. Fredrickson**. 2005. Mineralization of the cyclic nitramine explosive hexahydro-1,3,5-trinitro-1,3,5-triazine by *Gordonia* and *Williamsia* spp. Applied And Environmental Microbiology **71(12):** 8265-8272.
70. **Urbanski, T.** 1967. Chemistry and Technology of Explosives. Vol III. **III**: 729.
71. **Valverde, A., E. Velázquez, C. Gutiérrez, E. Cervantes, A. Ventosa, and J.-M. Igual**. 2003. *Herbaspirillum lusitanum* sp. nov., a novel nitrogen-fixing bacterium associated with root nodules of *Phaseolus vulgaris*. International Journal of Systematic and Evolutionary Microbiology **53(6):** 1979-1983.
72. **Winderl, C., H. Penning, F. von Netzer, R. U. Meckenstock, and T. Lueders**. 2010. DNA-SIP identifies sulfate-reducing *Clostridia* as important toluene degraders in tar-oil-contaminated aquifer sediment. ISME J **4(10):** 1314-1325.
73. **Yu, C.-P., R. Ahuja, G. Sayler, and K.-H. Chu**. 2005. Quantitative molecular assay for fingerprinting microbial communities of wastewater and estrogen-degrading consortia. Applied and Environmental Microbiology **71(3):** 1433-1444.
74. **Yu, C.-P., and K.-H. Chu**. 2005. A quantitative assay for linking microbial community function and structure of a naphthalene-degrading microbial consortium. Environmental Science & Technology **39(24):** 9611-9619.
75. **Zhang, C., and J. B. Hughes**. 2003. Biodegradation pathways of hexahydro-1,3,5-trinitro-1,3,5-triazine (RDX) by *Clostridium acetobutylicum* cell-free extract. Chemosphere **50(5):** 665-671.
76. **Zhang, S. Y., Q. F. Wang, and S. G. Xie**. 2012. Molecular characterization of phenanthrene-degrading methanogenic communities in leachate-contaminated aquifer sediment. International Journal of Environmental Science and Technology **9(4):** 705-712.
77. **Zhao, J.-S., C. W. Greer, S. Thiboutot, G. Ampleman, and J. Hawari**. 2004. Biodegradation of the nitramine explosives hexahydro-1,3,5-trinitro-1,3,5-triazine and octahydro-1,3,5,7-tetranitro-1,3,5,7-tetrazocine in cold marine sediment under anaerobic and oligotrophic conditions. Canadian Journal Of Microbiology **50(2):** 91-96.
78. **Zhao, J.-S., A. Halasz, L. Paquet, C. Beaulieu, and J. Hawari**. 2002. Biodegradation of hexahydro-1,3,5-trinitro-1,3,5-triazine and its mononitroso derivative hexahydro-1-nitroso-3,5-dinitro-1,3,5-triazine by *Klebsiella pneumoniae* strain SCZ-1 isolated from an anaerobic sludge. Applied And Environmental Microbiology **68(11):** 5336-5341.
79. **Zhao, J.-S., D. Manno, C. Beaulieu, L. Paquet, and J. Hawari**. 2005. *Shewanella sediminis* sp. nov., a novel Na^+-requiring and hexahydro-1,3,5-trinitro-1,3,5-triazine-degrading bacterium from marine sediment. International Journal of Systematic and Evolutionary Microbiology **55:** 1511-1520.

80. **Zhao, J.-S., L. Paquet, A. Halasz, and J. Hawari**. 2003. Metabolism of hexahydro-1,3,5-trinitro-1,3,5-triazine through initial reduction to hexahydro-1-nitroso-3,5-dinitro-1,3,5-triazine followed by denitration in *Clostridium bifermentans* HAW-1. Applied Microbiology and Biotechnology **63(2):** 187-193.
81. **Zhao, J.-S., L. Paquet, A. Halasz, D. Manno, and J. Hawari**. 2004. Metabolism of octahydro-1,3,5,7-tetranitro-1,3,5,7-tetrazocine by *Clostridium bifermentans* strain HAW-1 and several other H_2-producing fermentative anaerobic bacteria. FEMS Microbiology Letters **237(1):** 65-72.
82. **Zhao, J.-S., J. Spain, and J. Hawari**. 2003. Phylogenetic and metabolic diversity of hexahydro-1,3,5-trinitro-1,3,5-triazine (RDX)-transforming bacteria in strictly anaerobic mixed cultures enriched on RDX as a nitrogen source. Fems Microbiology Ecology **46(2):** 189-196.
83. **Zheng, X., Y. Su, X. Li, N. Xiao, D. Wang, and Y. Chen**. 2013. Pyrosequencing reveals the key microorganisms involved in sludge alkaline fermentation for efficient short-chain fatty acids production. Environmental Science & Technology **47(9):** 4262-4268.